Donor-Acceptor Systems Based on 'Axially' and 'Peripherally' Substituted Metallo- and Metalloid Porphyrins

A Thesis
Submitted for the Degree of
DOCTOR OF PHILOSOPHY

By
T. Anita Rao

School of Chemistry
University of Hyderabad
Hyderabad - 500 046
India

July 1997

CONTENTS

STATEMENT

I hereby declare that the matter embodied in this Thesis is the result of investigations carried out by me in the School of Chemistry, University of Hyderabad, Hyderabad, India under the supervision of Dr. Bhaskar G. Maiya.

In keeping with the general practice of reporting scientific observations, due acknowledgements have been made wherever the work described is based on the findings of other investigators.

T. Anita Rao.
9/7/97

T. Anita Rao

CERTIFICATE

Certified that the work contained in this thesis entitled "**Donor-Acceptor Systems Based on 'Axially' and 'Peripherally' Substituted Metallo- and Metalloid Porphyrins**" has been carried out by **T. Anita Rao** under my supervision and that the same has not been submitted elsewhere for a degree.

Dean

School of Chemistry

Bhaskar G. Maiya

Thesis Supervisor

ACKNOWLEDGEMENTS

I acknowledge Dr. Bhaskar G. Maiya, my supervisor with utmost gratitude. I owe it to him for introducing me to this field of research and teaching me so many techniques and principles. He has always been approachable, helpful and above all, extremely patient in his guidance throughout my research tenure.

I thank the Dean, Professor P. S. Zacharias and all the faculty members of the school, for their help and guidance.

I thank Professor P. S. Zacharias for permitting me to use the facilities for cyclic voltammetry.

I am grateful to Prof. C. K. Mitra for the timely help with laser printing.

I am grateful to Dr. K. C. Kumaraswamy for his helpful suggestions and kind cooperation.

I thank my labmates Dr. M. Sirish, S.Arounaguiri and L.Giribabu for all their help and valuable suggestions. I also thank my colleagues Dr. Satya Prasanna, Dr. Murali, Dr. Nachimuthu, Prasad, Kiran and Ravi.

I am thankful to my friends and colleagues Sreelatha, Prabhavathi, Prasuna, Soujanya, Manjula, Chandrakala, Sindhu, Nisha, Anuradha, Jyotsna, Aneetha, Vijjulatha, Saroja, Sudha, Ramalakshmi, Madhavi and Mangayarkarasi. They have made the atmosphere in the school warm and friendly and my research tenure an unforgettable one.

I am grateful to Dr. K. V. Reddy, and Mrs. Nirmala, CIL, for their cooperation. I thank Mrs. Vijayalakshmi. Mr. Bhaskar Rao, Mr. Satyanarayana and Mr. Venkataramana for their technical help. I acknowledge Mr. Shetty, Mr. Santosh, Mr. Ananta Rao and all other non-teaching staff.

Financial assistance from the University Grants Commission is gratefully acknowledged.

RSIC, Central Drug Research Institute, Lucknow is acknowledged for the mass spectral data.

I take this opportunity to express my deepest sense of gratitude to my parents who, with their love and constant encouragement, have been the guiding light throughout my education, and to my brother who has been my friend and moral support.

Words are very difficult to express my feelings for all my family members and above all, my husband. Without his patience, encouragement and cooperation over the last three years, this thesis would have been but a remote possibility.

SYNOPSIS

This thesis entitled **"Donor-Acceptor Systems Based on 'Axially' and 'Peripherally' Substituted Metallo- and Metalloid Porphyrins"** deals with the design, synthesis, spectroscopy and photoredox properties of metallo- and metalloid porphyrins that have been substituted at their axial or peripheral positions with either electron acceptor or electron donor subunits. Emphasis has been laid on studies with the metalloid-porphyrin based, "vertically-linked" D-A compounds and multi-chromophoric arrays.

Porphyrins and their metal/metalloid derivatives are a versatile class of compounds having applications in various research areas such as biomimetic photosynthesis, molecular electronics, molecular catalysis, photodynamic therapy etc. A variety of donor-acceptor (D-A) type porphyrin systems have been built for use in many of these applications which generally involve photoinduced electron transfer (PET) and electronic energy transfer (EET) as the key principles. While a majority of the D-A systems have been constructed by linking the donor/acceptor subunits at the porphyrin peripheral (i.e. β-pyrrole and *meso*) positions, relatively few such systems have been synthesized by utilizing the axial site (central metal/non-metal ion) of a porphyrin. Thus, extensive investigations have been carried out on the PET and EET reactions of porphyrins substituted at their periphery but,

research on the axially substituted D-A type porphyrins is limited. Moreover, chemistry of the main-group element containing porphyrins has not been sufficiently exploited in this area.

A chapter in this thesis (Chapter 3) deals with studies on D-A systems in which the porphyrin *meso*- and β-pyrrole positions have been utilized for linking the donor/acceptor groups. The major part of the thesis is, however, concerned with the synthesis and spectral, redox and photophysical properties of axially substituted phosphorus(V) (P(V)) porphyrins. Detailed studies on the chemistry, electrochemistry and photochemistry of P(V) porphyrins endowed with various organic donor/acceptor axial ligands have been carried out first. Next, the idea of axial-bonding capability of P(V) porphyrins has been extended to construct multi-porphyrin arrays. A series of 'axial-bonding' type hybrid porphyrin trimers and also a heptameric array have been constructed based on a P(V) porphyrin platform. PET and EET reactions occurring in these novel arrays have also been investigated.

The work embodied in this thesis has been divided into six chapters and a brief, chapter-wise account of the results is presented below.

Chapter 1. ***Introduction***

Recent literature on various peripherally- and axially substituted porphyrin-based D-A systems highlighting their PET and

EET reactions has been reviewed in this chapter. A survey of the oligomeric porphyrin systems is also presented here.

Chapter 2. ***Materials and Methods***

This chapter presents a listing of the chemicals, a general description of the synthetic procedures and the details of spectroscopic and other physical techniques employed during the research work.

Chapter 3. ***Spectroscopic, Redox and Emission Properties of 2-Nitro-Substituted Tetraaryl Porphyrins***

This chapter deals with porphyrins substituted at their β-pyrrole and *meso*- positions with donor-acceptor subunits. Free-base, copper(II) and zinc(II) derivatives of 2-nitro substituted 5,10,15,20-tetraaryl porphyrins (aryl = phenyl, 2-naphthyl or diphenylpyrazolyl) have been synthesized and investigated by absorption, ^{1}H NMR, ESR, cyclic voltammetric and fluorescence methods.

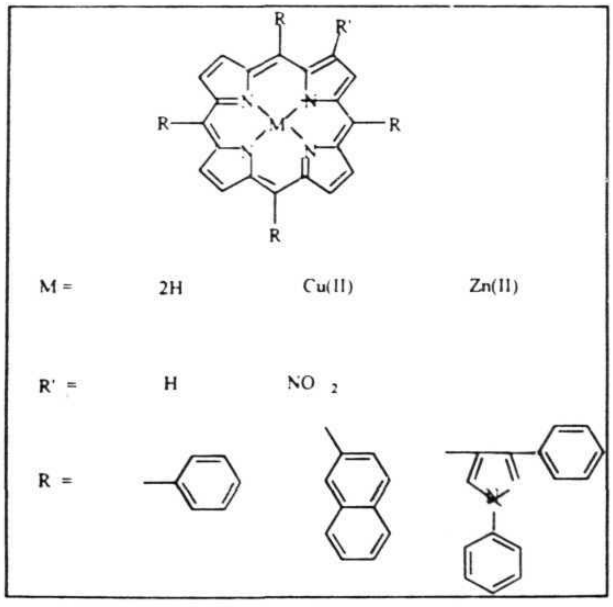

Red shifts and broadening of the optical absorption bands, downfield shifts of both the β-pyrrole and imino proton NMR peaks and

decrements in the reduction potentials have been observed for these nitroporphyrins in comparison with the corresponding spectral or electrochemical parameters for the unsubstituted parent porphyrins. However, the ESR spectral data of the copper(II) derivatives of the nitroporphyrins are indistinguishable from those for the unsubstituted analogues. All of these features have been interpreted in terms of a perturbation of the frontier orbitals of the porphyrin π-ring system by the directly attached nitro group. Solvent-dependent fluorescence spectral data of the free-base and zinc(II) derivatives of the nitroporphyrins have been analyzed in terms of an intramolecular PET involving the β-nitro group. Thus, while the β-pyrrole substituent drastically affects the spectral, redox and photophysical properties of the various *meso*-aryl substituted porphyrins, as such, the *meso*-aryl substituents themselves do not seem to have any major effect on the properties of the nitro- or the unsubstituted porphyrins. (*Polyhedron*, **1994**, 13, 1863-1873)

Chapter 4. ***Synthesis, Spectroscopy, Electrochemistry and Singlet State Properties of Aryloxo Derivatives of Phosphorus(V) Porphyrins***

Aryloxo derivatives of phosphorus(V) porphyrins of the type $[(TTP)P(OR)_2]OH$ where TTP is the dianion of 5,10,15,20 tetratolyl porphyrin and OR represents an axial aryloxo (2,4-dimethylphenoxo, 4-methyl phenoxo, phenoxo, 4-(4-nitrophenoxy) phenoxo, 4-(2,4-dinitrophenoxy) phenoxo, or 4-nitrophenoxo) ligand have been synthesized by reacting together (5,10,15,20-tetratolylporphyrinato) dichlorophosphorus(V) hydroxide and the corresponding phenols. These new, 'vertically-linked' D-A systems have been fully characterized by FAB-mass, UV-visible, fluorescence, IR, and NMR (^1H and ^{31}P) spectroscopies and also by the electrochemical methods. Each porphyrin shows a typical 'normal UV-visible absorption spectrum' indicating the presence of a P(V) ion within the porphyrin cavity. The proton decoupled ^{31}P NMR signal observed for these compounds between -194 and -200 ppm suggests that there exists an octahedral coordination around the phosphorus atom. This supposition is further substantiated by the porphyrin ring-current-induced upfield shifts observed for protons on the two axial

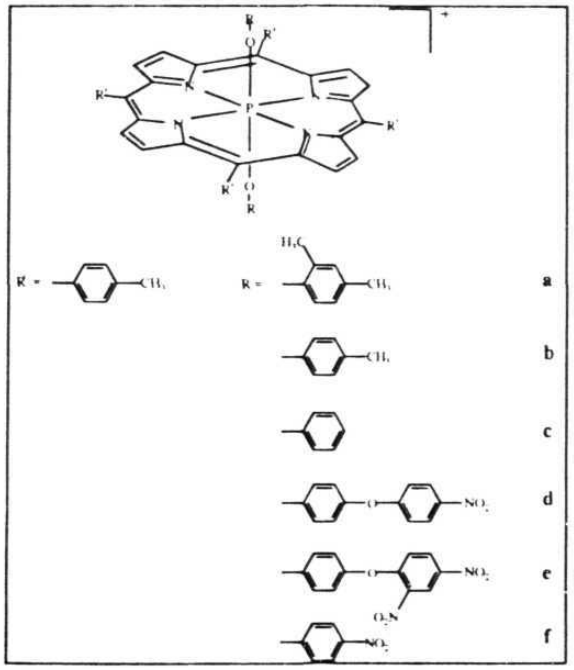

aryloxo ligands in the ^{1}H NMR spectra. Cyclic voltammetric studies reveal that each porphyrin undergoes two successive one-electron reductions with the site of electron transfer being the porphyrin ring. The fluorescence quantum yield values of these porphyrins are found to be sensitive to the nature of the aryloxo ligand and also to the solvent polarity. The singlet state properties of these systems have been discussed in light of both the fluorescence and the redox potential data. Specifically, it has been proposed that a PET reaction from the axial aryloxo "donor" ligands to the singlet P(V) porphyrin is a prominent process and that it accounts for the low fluorescence quantum yields observed for these systems. (*Inorg. Chem.*, **1996**, 35, 4829-4836)

Chapter 5. ***'Axial-Bonding Type', Vertically-Linked Hybrid Porphyrin Arrays: Design, Synthesis and Modulation of Redox and Photophysical Properties***

The axial bonding capability of P(V) porphyrin has been utilized for the design and synthesis of hybrid porphyrin trimers in which the central phosphorus atom of the 'basal' porphyrin unit is axially linked to two ligands which are free-base (**a**), vanadyl (**b**), cobalt (**c**), nickel (**d**), copper (**e**), zinc (**f**) or phosphorus (**g**) porphyrins. Trimer **a** has been synthesized by reacting 5-(4-hydroxyphenyl)-10,15,20-tritolyl porphyrin with an excess of (5,10,15,20-tetratolylporphy-rinato)dichlorophosphorus(V) hydroxide. Further

metallation of this 'free-base-phosphorus' trimer accomplishes compounds **b-f**.

The molecular structures of these trimers have been ascertained by FAB-mass and ^{1}H- and ^{31}P NMR spectroscopies. Their UV-visible spectra are similar to the spectra of 2:1 (mole/mole) mixtures of the corresponding precursors. Cyclic voltammetric data reveal that the peak potentials corresponding to the oxidation and reduction of these trimeric systems are unaltered with respect to those of the corresponding porphyrin monomers. Similarly, the ESR spectral parameters of paramagnetic trimers **b**, **c** and **e** are also similar to those of the corresponding monomeric metallo-porphyrins. All of these observations indicate a minimum ring-ring interaction between the porphyrin subunits in these vertically-linked trimeric systems.

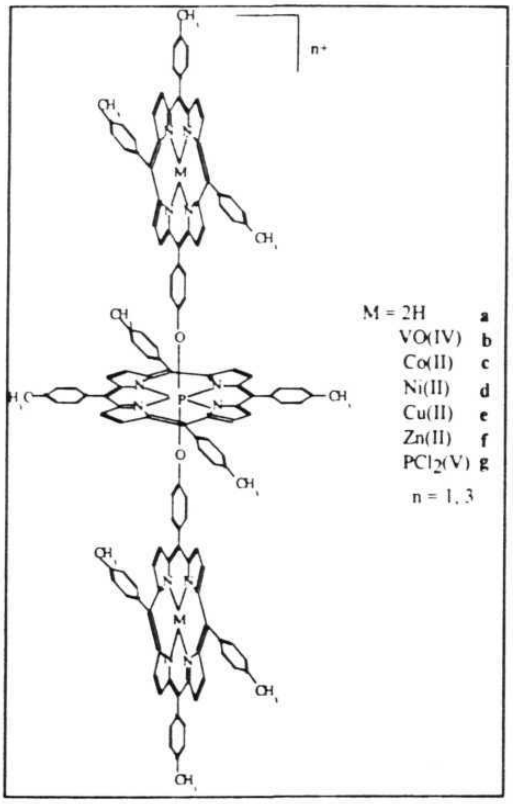

Steady state fluorescence studies on **a**, **f** and **g** show a quenching of emission when these trimers are excited at wavelengths

corresponding to absorption by the central phosphorus porphyrin (445 nm) and by the axial porphyrin (405 nm) subunits. Excitation spectral data reveal that the EET efficiency from the central- to the axial porphyrin subunit is poor in these hybrid trimers. On the other hand, thermodynamic criteria indicate the possibility of a PET from the axial porphyrins to the central porphyrin by the following two pathways.

(i) ^{1}(axial porphyrin)* $\rightarrow$ central porphyrin

(ii) axial porphyrin $\rightarrow$ ^{1}(central porphyrin)*

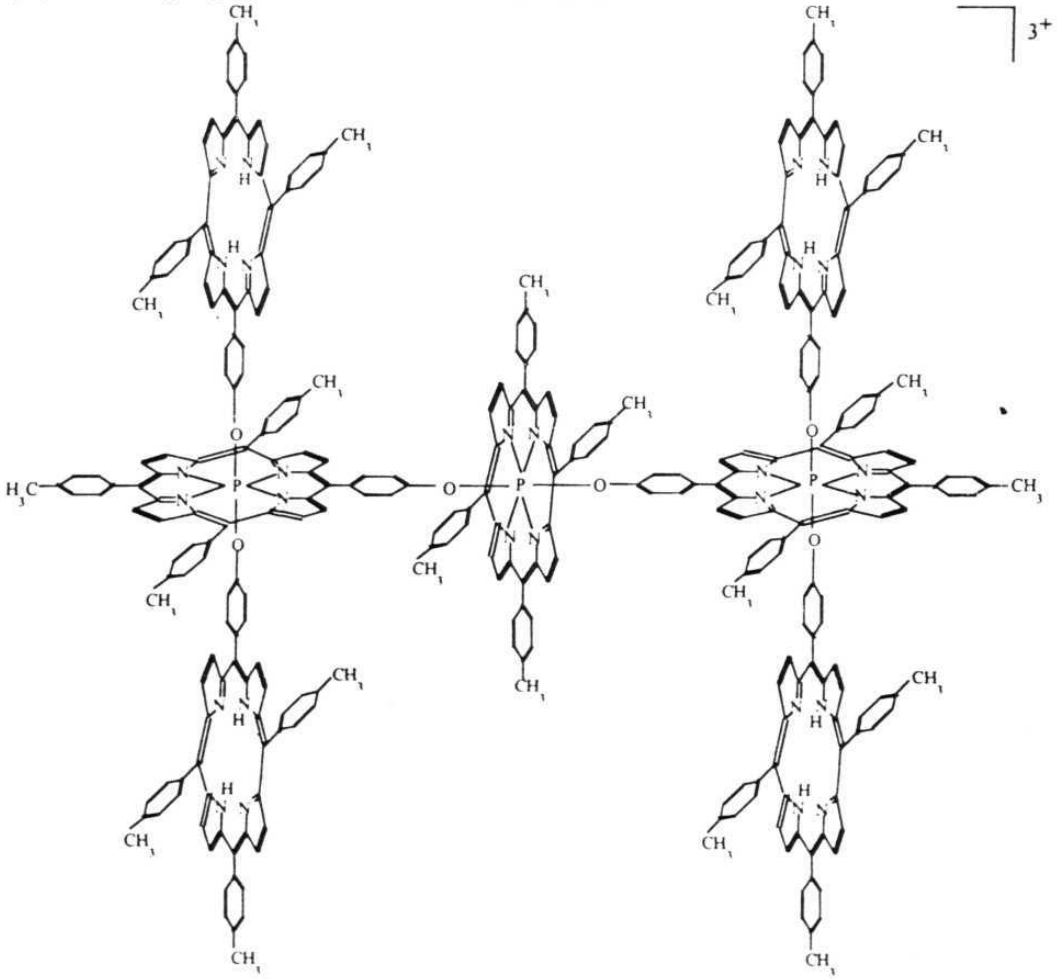

In addition to the results obtained on the above trimers, this chapter also reports on the design, synthesis and photochemical properties of a novel branched chain heptameric porphyrin array. This heptamer has been constructed in two steps. Starting from (5,10,15,20-tetratolylporphyrinato)phosphorus(V) hydroxide and 5,10,15,20-tetratolyl porphyrin, hybrid trimer **a** was obtained first. Next, phosphorus was inserted into the two free-bases of **a** to obtain the 'all-phosphorus' trimer **g,** the reaction of which with excess of 5,10,15,20-tetratolyl porphyrin furnished the heptamer.

The fragmentation pattern observed in the FAB-mass spectrum and the chemical shifts and coupling patterns observed for the various protons of the compound provide sufficient evidence for the symmetric nature of the heptamer. The UV-visible, redox potential and fluorescence data of the heptamer were found to be essentially similar to those of trimer **a** thus suggesting that the ground- and excited state chemistry of these two arrays are also similar. (*J. Chem. Soc., Chem. Commun.*, **1995**, 939-940)

Chapter 6. ***Conclusions***

This chapter presents general conclusions based on the investigations carried out in this work.

CHAPTER 1

Introduction

The chemistry of porphyrins and their metal- as well as metalloid-derivatives has been an attractive subject of investigation over the past few decades because of its relevance to applications such as biomimetic photosynthesis, molecular electronics, supramolecular catalysis, organic synthesis, magnetic resonance imaging, photodynamic therapy, cytochrome P-450 function, etc. Photochemically active donor-acceptor (D-A) systems based on variously substituted monomeric- and oligomeric porphyrin species are of immense utility in many of these applications. The key photochemical reactions associated with these applications are usually photoinduced electron transfer (PET) and excitation energy transfer (EET). This thesis deals with the design, synthesis and photochemical properties of D-A systems derived from 'axial' and/or 'peripheral' site substitution of free-base, metallo- and metalloid porphyrins. Specifically, monomeric free-base, zinc(II) and phosphorus(V) porphyrin complexes substituted at their *meso*-, β-pyrrole, or axial positions with organic donor/acceptor subunits and also phosphorus(V) porphyrin based "axial-bonding" type oligomeric porphyrin arrays have been investigated in this study .

1.1 Basic theory of photoinduced electron transfer (PET) and excitation energy transfer (EET)

Marcus theory of electron transfer process provides a convenient way of discussing certain key aspects involved in the PET reactions.[1] According to this theory, the electronic states of a system consisting of a donor (D; D* is the corresponding excited state) and an acceptor (A) are represented by parabolic functions. Fig. 1.1 shows the energy surfaces for electron transfer (ET) reactions. Here, the potential energy (E) of *D-A is shown as a function of the nuclear coordinate *q*. Allowed transitions can occur only when the parabolas cross, that is, when the nuclear coordinates of both the D-A complex and the environment are reorganized to such an extent that the energy of the precursor state (before ET) and the energy of the successor state (after ET) are equal. $\Delta G^{\varnothing'}$ is the standard free energy for the overall ET reaction and includes a correction term ΔG_{corr} to take care of any specific interaction between D and A. $\Delta G^{\#}$ is the free energy of activation, and is related to $\Delta G^{\varnothing'}$ and λ, the reorganization energy by the expression

$$\Delta G^{\#} = (\lambda + \Delta G^{\varnothing'})^2/4\lambda \qquad (1.1).$$

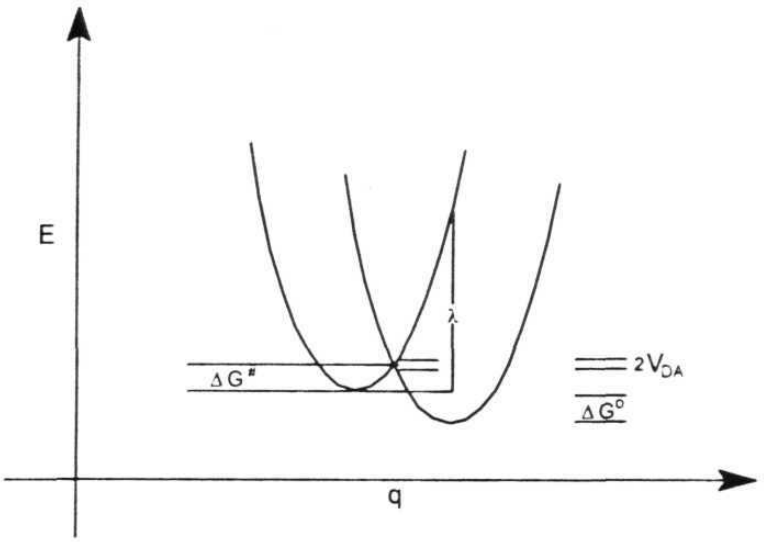

Fig. 1.1

For exergonic reactions, when $-\Delta G^{\varnothing'} < 0$, the ET rate ($k_{ET}$) increases with increasing exergonicity. It reaches a maximum at $-\Delta G^{\varnothing'} = \lambda$ and decreases again when $-\Delta G^{\varnothing'} > \lambda$. This region of decrease of k_{ET} with respect to increasing exergonicity $\Delta G^{\varnothing'}$ is termed as the "Marcus inverted region". According to the Marcus theory, k_{ET} is given by the expression

$$k_{ET} = k_{el}\, \nu_n \exp-(\Delta G^{\varnothing'} + \lambda)/4k_BT \qquad (1.2)$$

Here, k_{el} is the electronic transmission coefficient, ν_n is the frequency of nuclear motion through the transition state, $\Delta G^{\varnothing'}$ is the standard Gibb's free energy change for the overall ET reaction, λ is the reorganization energy needed to orient the initial complex to have a suitable

configuration for ET, k_B is the Boltzmann's constant, and T, the absolute temperature.

The quantum mechanical derivation of the rate of an electron transfer process results in the following expression for k_{ET}.

$$k_{ET} = 2\pi/h V^2_{DA} (4\pi\lambda k_B T)^{-1/2} \exp\text{-}(\Delta G^{\varnothing} + \lambda)^2/4\lambda k_B T \qquad (1.3).$$

Here, V_{DA}, the electronic matrix element is related to the splitting of the energy surfaces in the transition region (see Fig, 1.1).

Electronic energy transfer reactions can, in principle, operate by two mechanisms:

(i) Dipole-dipole mechanism which involves mutual Coulombic interaction of electrons (based on Forster's theory)

(ii) Exchange mechanism which involves mutual exchange of electrons (based on Dexter's theory).

Forster has utilized experimentally obtainable parameters to derive an expression for the rate of electronic energy transfer by mechanism (i).[2] This theory postulates the rate constant for energy transfer, $k_{Forster}$, to be

$$k_{Forster} = \frac{8.8 \times 10^{-25} \kappa^2 \phi_D}{n^4 \tau_D R^6} \int F_D(\nu) \varepsilon_A(\nu) \nu^{-4} d\nu \qquad (1.4)$$

where ν is the wave number, $F_D(\nu)$ is the spectral distribution of the donor emission in quanta normalized to unity, $\varepsilon_A(\nu)$ is the molar extinction coefficient for the acceptor absorption and n is the refractive index of the solvent. κ^2 is a function of relative orientation of transition dipole moments of the donor and the acceptor. ϕ_D is the quantum yield of donor emission, τ_D is the donor emission lifetime (in seconds) and R is the distance between the donor and acceptor molecules (in centimetres). Energy transfer by this mechanism can occur over long distances. As seen in equn. 1.4, among the other things, $k_{Forster}$ depends on (a) the distance and orientation between the donor and the acceptor and (b) the extent of overlap of the donor emission and the acceptor absorption. It is inversely proportional to the sixth power of R.

Dexter has derived an expression for the rate of energy transfer of type (ii) and here, the initial and the final states are coupled through exchange interaction.[3]

$$k_{Dexter} = (2\pi/\hbar)\, K \exp(-2R/L) \int \bar{F}_D(\nu)\, \bar{\varepsilon}_A(\nu)\, d\nu \qquad (1.5)$$

where K is related to specific orbital interactions, R is the distance between the donor and the acceptor molecules, L is an effective average Bohr radius and $\bar{F}_D(\nu)$ and $\bar{\varepsilon}_A(\nu)$ are the spectral distributions of the donor emission and the acceptor absorption normalized to unity on a wavenumber scale. According to this mechanism, k_{Dexter} depends on (a) orbital interactions of the donor and the acceptor, (b) the distance between

the donor and the acceptor molecules, and (c) the spectral contributions of the donor emission and the acceptor absorption.

To summarize, rates of electron transfer and energy transfer depend, mainly, on the following factors.

(i) The mutual geometric relation, that is, the distance and orientation, between the donor and the acceptor.

(ii) the chemical nature of the donor and the acceptor as expressed in the spectral overlap and driving force.

(iii) the nuclear reorganization of donor, acceptor and the surrounding medium accompanying the reaction.

1.2 EET and PET in biological and abiological systems

Many applications of the porphyrin compounds rely on their photochemical characteristics. In recent years, considerable developments taken place in research areas such as photosynthesis, photodynamic therapy and molecule-based optoelectronics have provided greater impetus to research related to photochemistry of porphyrins. The following subsections provide a brief introduction to these biological and abiological issues as applied to the theme of this thesis.

1.2.1 Photosynthesis

Investigations on the PET and EET reactions of porphyrin-based D-A systems are generally inspired by their possible application in biomimetic photosynthesis.[4] The initial events of photosynthesis involve both PET

and EET reactions and the main pigment involved, *i.e.* chlorophyll, is known to bear structural and electronic similarity with porphyrins. Salient features of this aspect are briefly alluded to below.

Green plants and photosynthetic bacteria utilize antenna pigments to harvest sunlight and channel photons to the reaction centre where chemical reactions originate. Depending on the organism or plant and its environmental conditions, there exist a variety of antenna systems. These systems contain chlorophylls of various types, carotenoid polyenes and other polypyrroles. Upto three hundred antenna chlorophyll molecules are utilized by the photosynthetic plant cells to relay the trapped photon to the reaction centre.[8]

The features of a typical photosynthetic reaction centre, for example *Rhodobacter spheroides* , (Fig 1.2)[5,6] are as follows. Two pairs of bacteriochlorophyll molecules are present along with a pair each of bacteriopheophytin, carotene and quinone molecules. A pair of these bacteriochlorophyll molecules (called the "special pair", P) absorbs energy, that is funnelled to it by the antenna pigments, to go to the singlet photoexcited P* state. The P* transfers an electron to one of the bacteriopheophytin molecules, *via* the intermediacy of the bacteriochlorophyll monomer, within two to four picoseconds of excitation. This bacteriopheophytin molecule in turn transfers an electron to one of the quinone molecules. These multistep electron transfer processes occur over a distance of ~30 A° with a quantum

yield of unity, leading to a transmembrane charge-separated state consisting of the oxidized "special

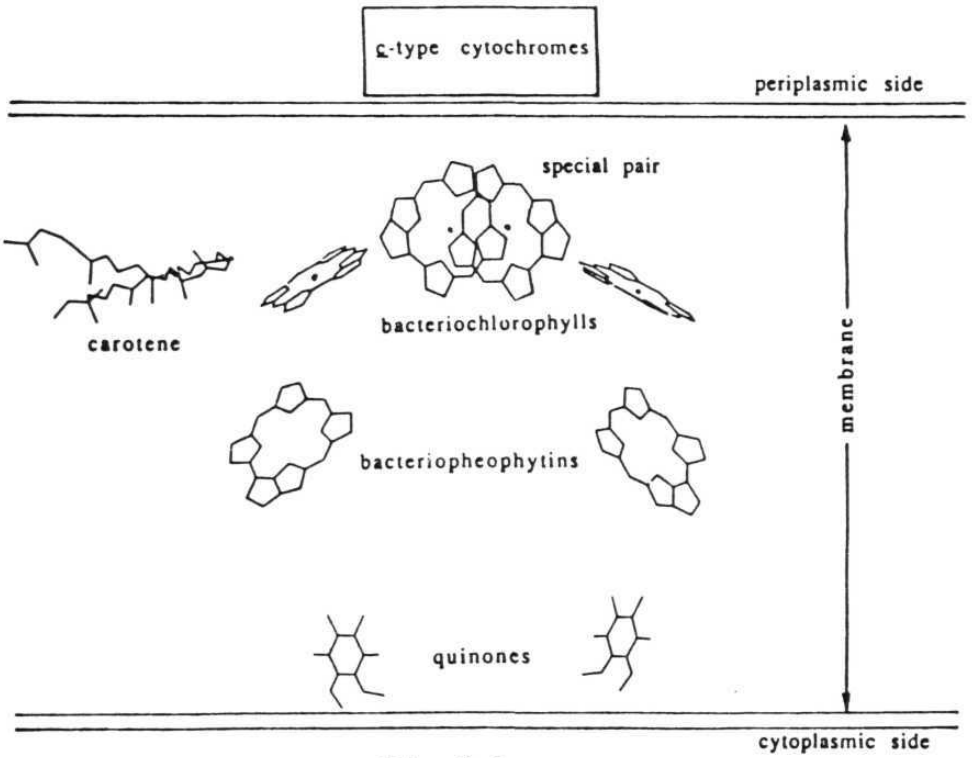

Fig. 1.2

pair" and the reduced quinone.

Thus, the donor and the acceptor moieties participating in the initial stages of photosynthesis are involved in mainly three basic processes: (i) singlet-singlet energy transfer, (ii) triplet-triplet energy transfer and (iii) photoinitiated electron transfer. Singlet-singlet energy transfer occurs when antenna pigments collect photons and relay them to the reaction centre. Carotenoids provide photoprotection through triplet-triplet energy

transfer by quenching the triplet chlorophyll which can produce the highly reactive and, therefore, destructive singlet oxygen. A series of photoinduced electron transfer reactions takes place in the photosynthetic reaction centre. Besides the number of molecules involved in these energy migration and charge separation processes, the donor-acceptor distance and relative orientation are also of important consequence in deciding the efficiencies of these processes.

Considerable progress has been achieved in this field through X-ray crystallography, and visible and magnetic spectroscopies.[7] Further understanding of the natural systems has been achieved through model studies. A great number of substituted porphyrins and metalloporphyrins have been synthesized as photosynthetic model systems and a number of reviews monographs are available. [9a, 10-22]

1.2.2 Molecular electronics

Currently, molecular electronics is receiving world-wide attention. Molecular rectifiers, transistors, wires, photodiodes etc. are being designed by utilizing the chemistry of the excited- and charge transfer states of both inorganic and organic molecules.[9b]

The design of a 'molecular wire' is one among the many important aspects of research in this subject. Many 'molecular wires' have been designed by adhering to the following criteria: (i) the system must exhibit electron conduction and should have a defined length capable of spanning a supporting element, (ii) it must also have a terminus that can be

connected to its functional components and (iii) it must be insulated from the surrounding environment to prevent indiscriminate electron transfer. Attempts have been made to build molecular wires based on porphyrin-arrays.[31-33]

Another aspect that is relevant to the subject matter of this thesis and which merits mention here is concerned with the so-called light-conversion molecular device. A light-conversion molecular device basically consists of two components - a light collector (or antenna) formed by an array of absorbing units and an emitter which would allow separate optimization of absorption and emission. Efficient energy transfer is a criterion for proper functioning of these systems. Fig. 1.3 illustrates a hypothetical light- conversion molecular device. The rectangular blocks represent antennae which receive and absorb light (A). Electronic energy transfer (EET) from the antenna to the emitter (represented by the circle) results in emission (E).

The following sections deal with a survey of recent literature on porphyrin-based photosynthetic model systems and molecular devices. Specific emphasis is placed on oligomeric porphyrins as well as on porphyrins substituted with electron accepting/donating functional groups at various sites on the macrocycle.

1.3 Covalently-linked porphyrin oligomers

A great variety of porphyrin dimers and higher oligomers have been reported in the literature and multistep energy- and electron transfe

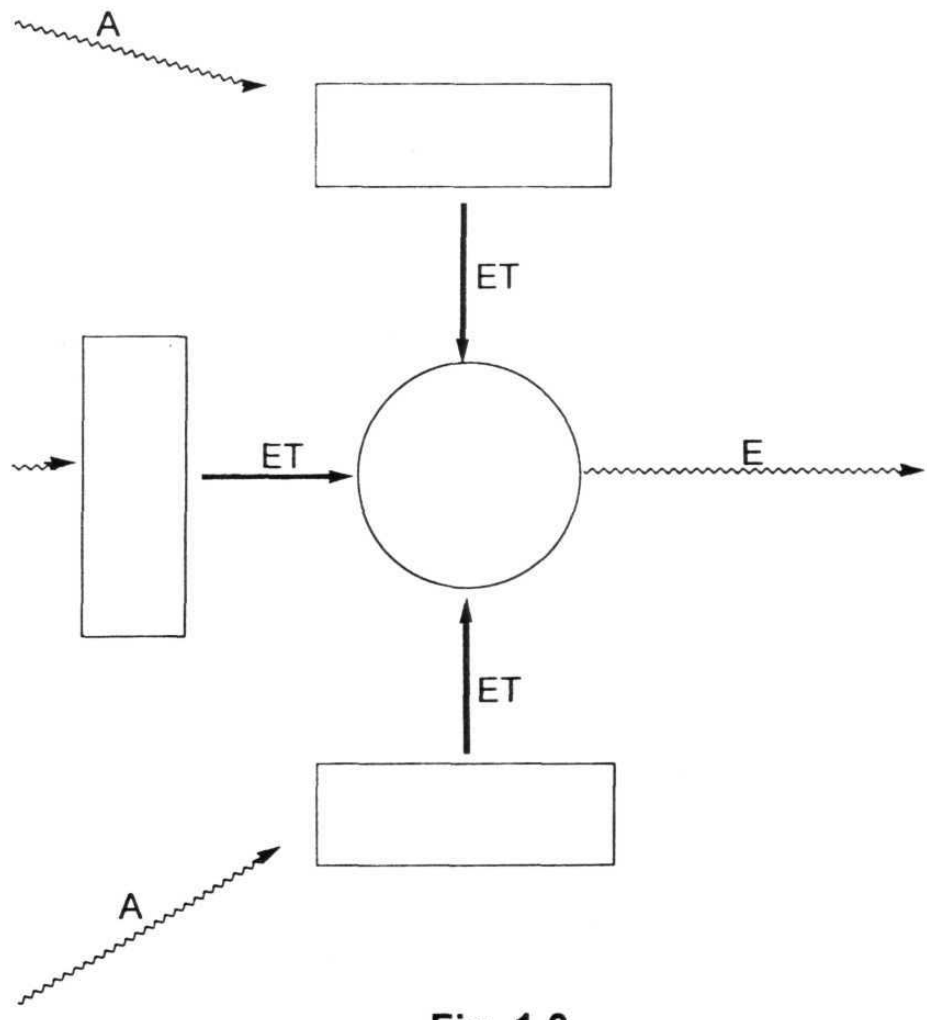

Fig. 1.3

reactions have been elucidated in some of these systems. Recently-reported systems are discussed below.

1.3.1 Linear oligomers

Among the first examples of linear arrays are the systems developed by Kong and Loach and also by Boxer and Bucks.[68]

Linear porphyrin oligomers formed by conjugated bridging of porphyrin subunits have been the focus of current interest for their potential application in non-linear optics, organic semiconductors and light harvesting antenna systems.[28-39] Therien and co-workers have synthesized an acetylenyl bridged porphyrin trimer **1** in an effort to maximize mutual electronic and excitonic interactions between individual porphyrin units.[28] They have demonstrated efficient electronic interactions in these systems by fluorescence and absorption spectroscopies and electrochemistry. It has been suggested, by comparing the visible absorption spectrum of the compound with those of naturally occurring photosynthetic pigments, that a suitably designed single array of the type **1** may be able to mimic the chloroplast's essential light harvesting spectral characteristics. Utilizing the "extended conjugation" principle, Burrell *et al.* have synthesized linear trimers with aldehyde-appended porphyrin units.[30a] The utility of aldehyde appended porphyrin unit as an ideal building block for construction of larger linear arrays has been demonstrated in this study. Similar etheno-bridged systems have also been synthesized..[30b]

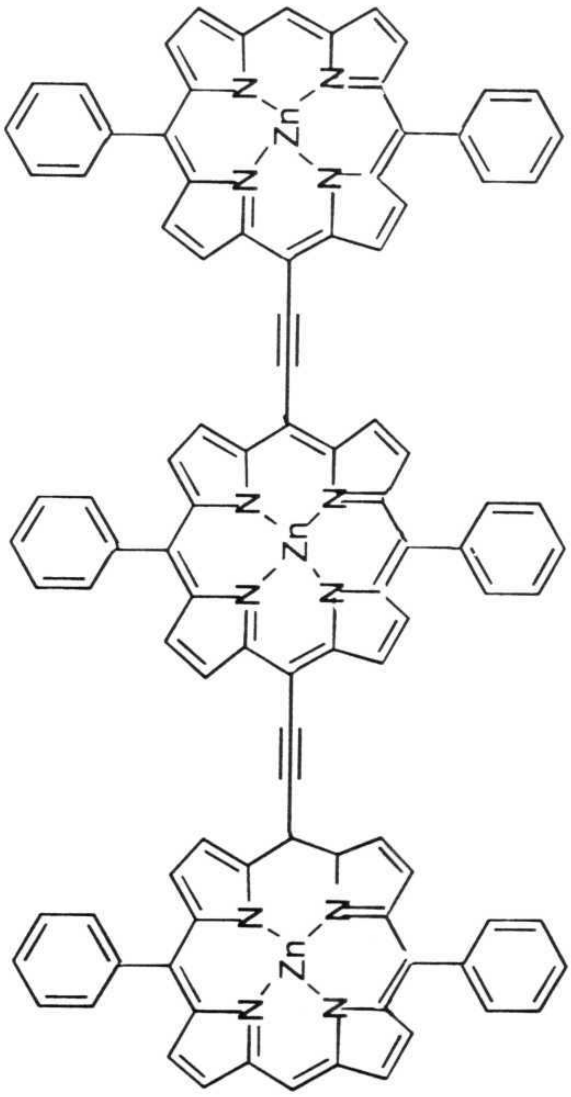

1

Anderson has reported a *meso*- butadiyne-linked zinc porphyrin dimer which forms a self-assembled "ladder" by non-covalent linkage *via* the central zinc atoms[31]. Evidence for the ladder complex has been provided by NMR spectra and UV-vis titration method. It has been further suggested that a similar polymeric ladder would be a good candidate as a low-band-gap material.

Crossley and co-workers.[32] and also Reimers *et al.*[33] have synthesized linear and bent porphyrin arrays by fusing individual porphyrin units through rigid aromatic units as models for "molecular wires". Compound **2** is an illustrative example. Reimers *et al.* have also discussed the relationship between the inter-ring coupling responsible for electron or hole conduction and the oligomer size in these types of arrays.[33] The advantage of this system is that it is completely rigid, spans large distances and possesses a sizeable, switchable electronic coupling between its ends.

Osuka *et al.* have constructed linear porphyrin arrays of upto nine porphyrin units **3**.[34] They have observed that with an increase in the number of porphyrins, the fluorescence spectra become broader and more red-shifted without any significant decrease in fluorescence quantum yields showing that these systems possess stretched conformations which do not allow the formation of a singlet-excited-energy trapping site.

The first quinone substituted trimer was synthesized by Sessler and Capuano.[29] Porphyrin ---> quinone electron transfer in this system is over a distance comparable to that found in the natural photosynthetic reaction

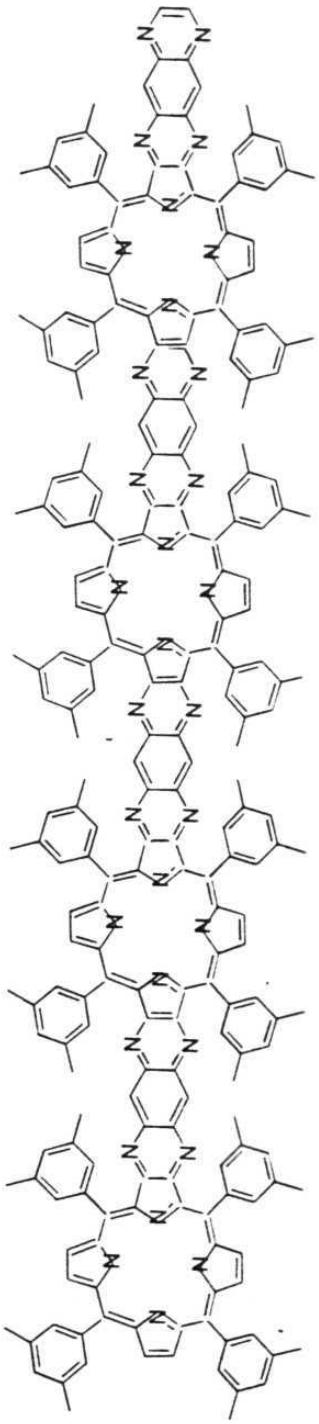

2

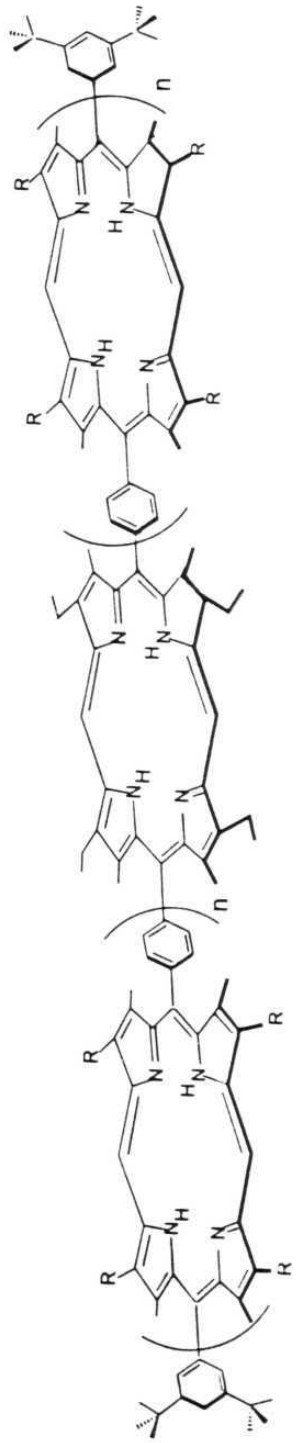

n = 1, 2, 3, 4 R = C_2H_5 or C_6H_{13}

3

centres and has been shown to be efficient enough to use this system as a model for studying long range electron transfer mechanisms.

1.3.2 Branched oligomeric porphyrin arrays

Based on the architecture of antenna chlorophyll systems, porphyrin oligomers have been fashioned to generate the so-called "light-harvesting arrays". A number of conformationally restricted porphyrins such as face-to-face porphyrins, stacked porphyrins and other similarly rigidly linked systems have been studied.[46-52]

Pentameric porphyrins comprising a central porphyrin that is covalently linked to four others are among the interesting examples of the branched oligomeric arrays. These have been designed to serve as light harvesting models and photovoltaic cells. The ether-bridged pentameric arrays **4a** were first reported by Milgrom.[40] Harriman and co-workers have demonstrated an efficient Forster-type EET from the antenna zinc porphyrins to the central free-base porphyrin in this system.[41] The central porphyrin unit has been shown to retain long-lived singlet- and triplet excited states.

Wennerstrom *et al.* have further modified the architecture of **4a** and designed a more rigid pentamer **4b** using phenyl bridges.[42] Similarly, with a view to increase conjugation between the porphyrin subunits, a diarylethyne bridged pentameric array was synthesized.[43] This array has been tailored such that the centre-to-centre inter-porphyrin distances are ~20 A° making the porphyrin units close enough for rapid energy transfer

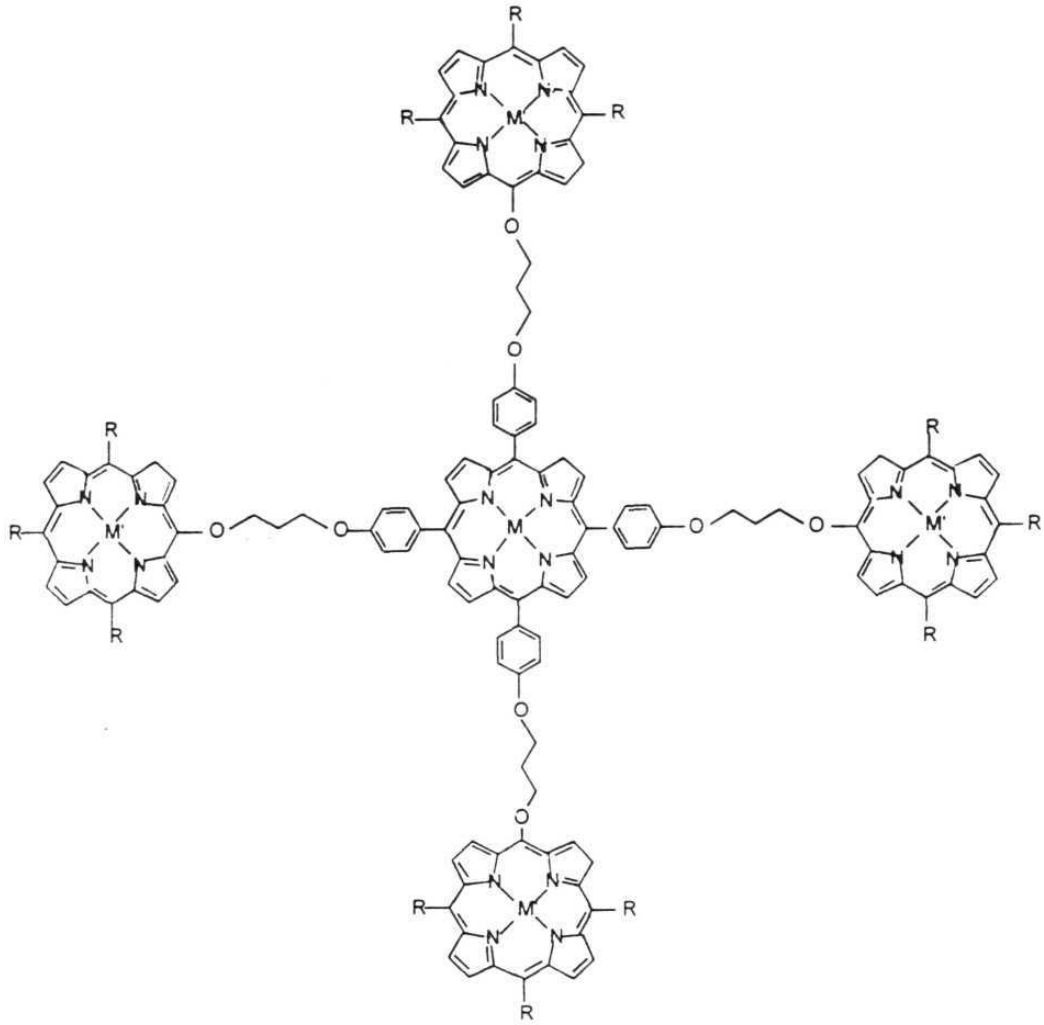

M = M' = Zn

M = 2H M' = Zn

M = Zn M' = 2H

R = C_6H_5

4a

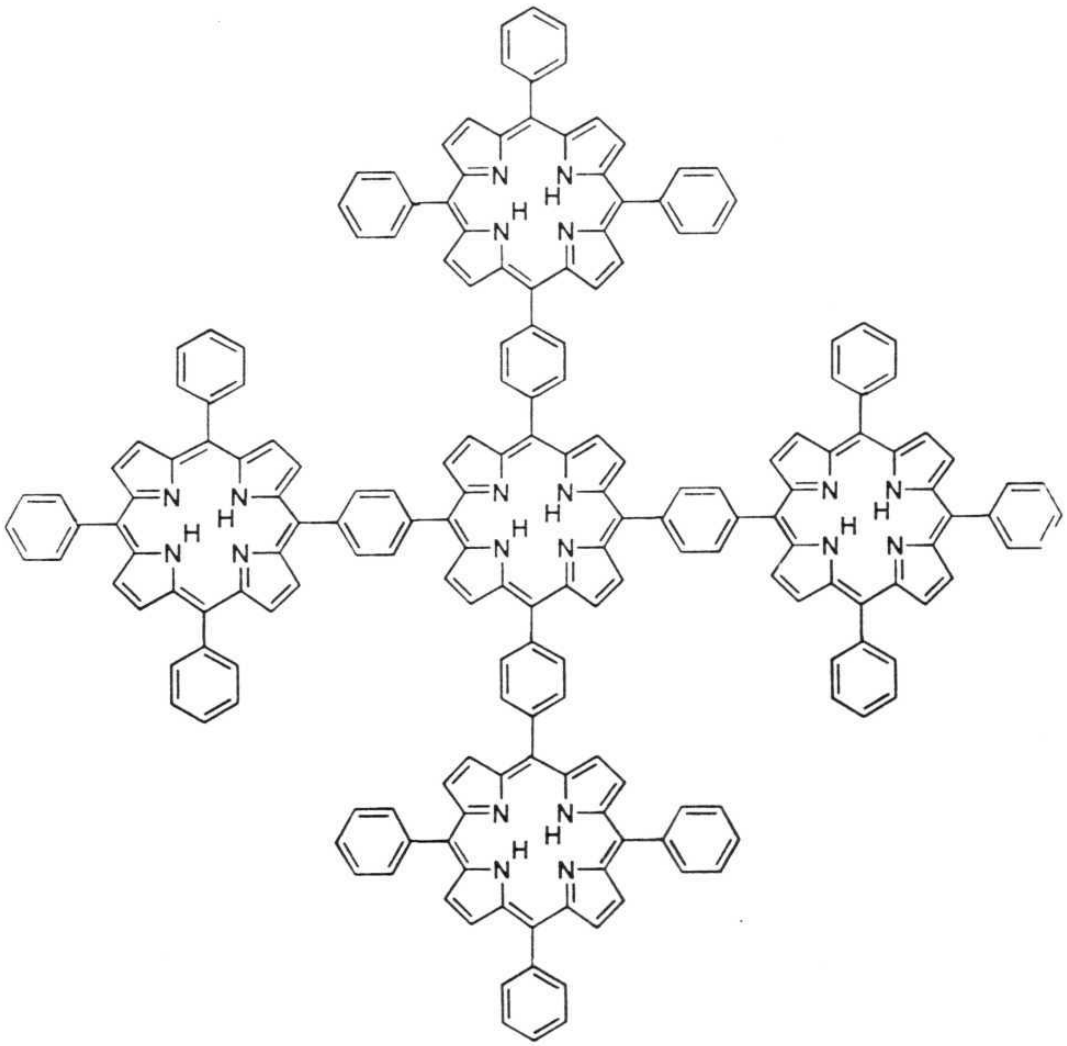

4b

but far enough to preclude any competing electron-transfer quenching reactions. It is possible to remove five electrons from these arrays indicating their possible application as 'controlled-potential' electron reservoirs. Detailed spectral and electrochemical studies have been carried out on the zinc- and free-base analogues of this latter system.[44]

Recent examples of branched arrays include pentamers and a novel nonamer **5**. Officer *et al.* have achieved a single step construction of two geometrically different pentamers and a nonamer starting from a porphyrin phosphonium salt building block.[45]

Cyclic oligomers have been synthesized in an effort towards mimicking the conformation of the photosynthetic reaction centre as well as enzymatic catalysis.[53] During their elegant studies on supramolecular catalysis using macrocyclic systems, Sanders and co-workers have developed an 'extended conjugation' approach to synthesize various oligomeric porphyrins.[54] In an effort to create a system in which convergent binding sites are positioned in such a way that substrate molecules can be held in close proximity, they have synthesized a cyclic porphyrin system **6** in which three zinc porphyrins have been covalently linked by extended conjugation.[54c54e] This cyclic porphyrin has been identified to be a host for binding substrate molecules. The transition state between the two reacting substrates is stabilized because it is doubly bound to the porphyrin host. A cyclic zinc porphyrin tetramer fitted with a zinc tetrapyridyl porphyrin guest molecule has also been reported by the same group.[54f] This supramolecular D-A compound showed fluorescence

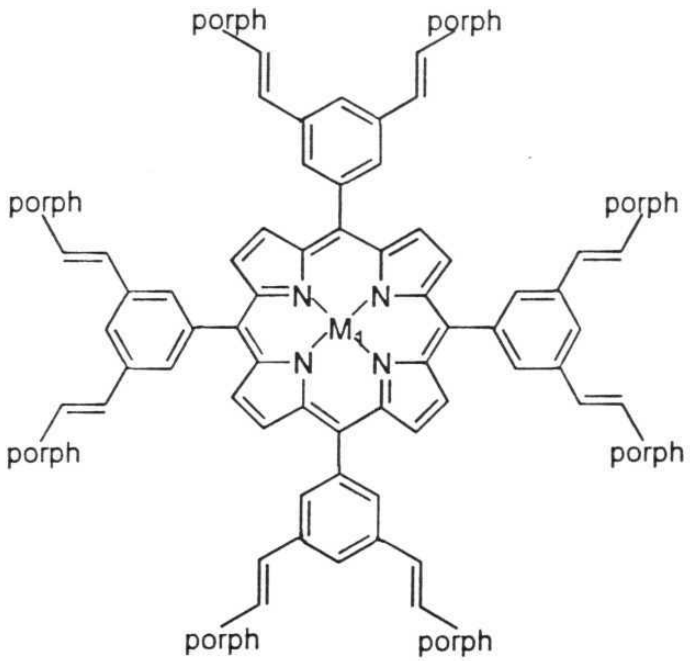

porph =

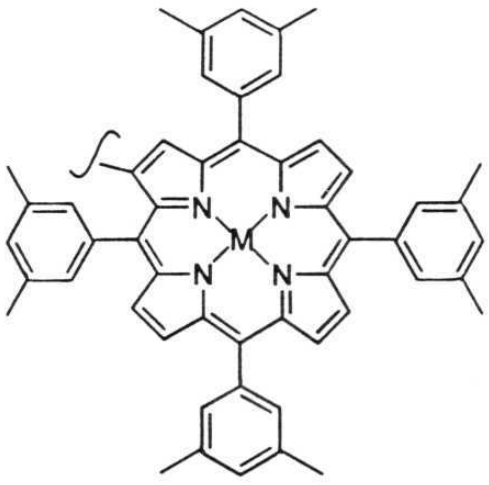

5a: M = Ni, M_1 = 2H

5b: M = Ni, M_1 = Zn

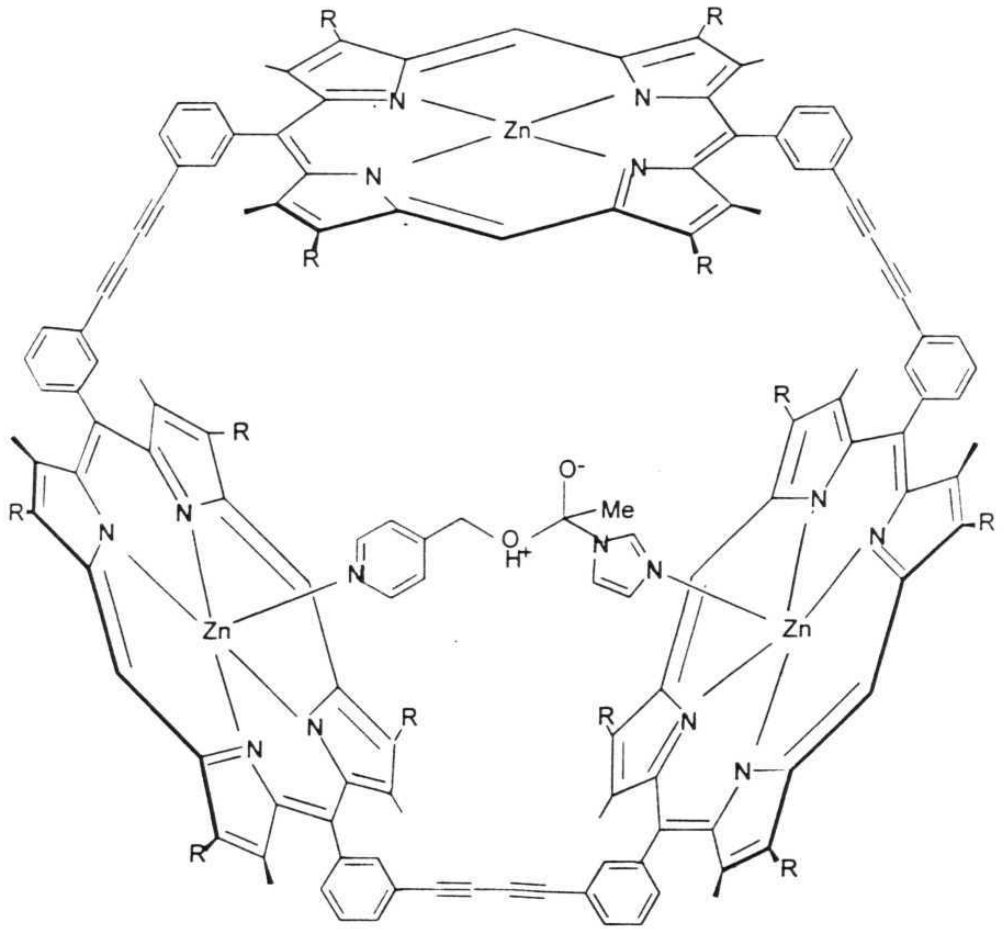

R = CH_2CH_2COY Y = OMe or 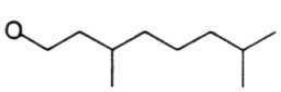

6

which is *ca.* thousand times less compared to the individual components. This observation has been explained by invoking photoinduced electron transfer followed by non-radiative decay of the charge separated state.

1.3.3 Porphyrin oligomers linked by metal/nonmetal coordination

Ordered supramolecular arrays formed by self-assembly of porphyrin units *via* metal ion coordination have been studied.[55-59] For example, Drain and Lehn have utilized the pyridine nitrogen coordination of cis- or trans- substituted *meso*-dipyridyl porphyrins with cis- or trans- substituted Pd(II) or Pt(II) ions to construct arrays **7** and **8** which show 'square' architecture.[55]

Ruthenium porphyrins linked axially, *via* pyridine bridges, to other porphyrin subunits further illustrate the utility of coordinate-covalent bond formation reactions in porphyrin array building process.[67b] Alessio *et al.* have constructed an "open-box shaped pentamer" **9** consisting of four ruthenium(II) porphyrins linked non-covalently to a central tetrapyridyl porphyrin.[67a] This pentamer has been shown to selectively recognize S-bonded DMSO complexes.

Self assembly of oligomers in solution has been reported by Hunter and co-workers where coordination of zinc porphyrins by pyridine ligands is used to construct di- tri- or tetrameric assemblies.[56] Sanders and McCallien have utilized 5,15-dioxoporphyrins as supramolecular building blocks and synthesized a pentameric assembly.[57] Here, four zinc

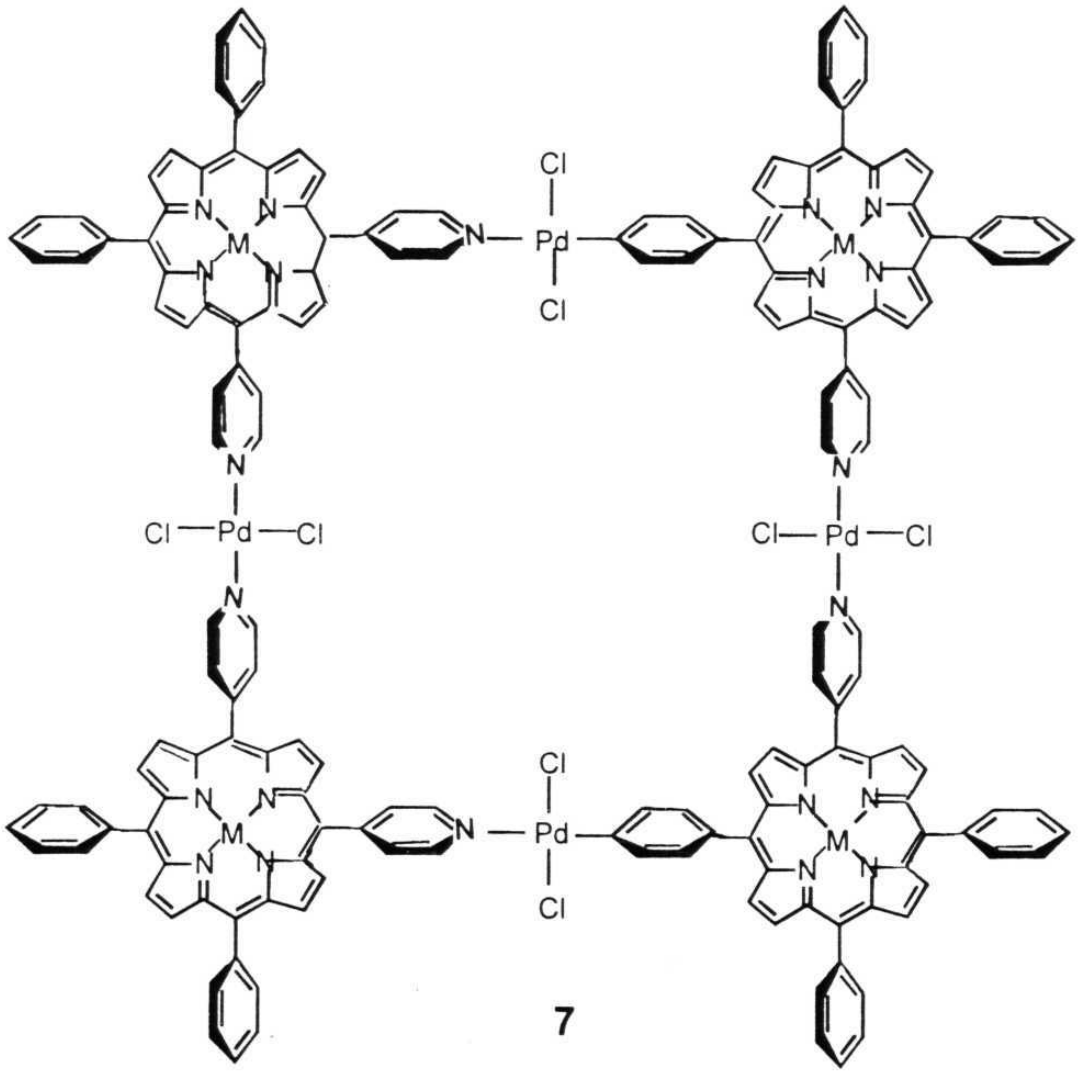

7

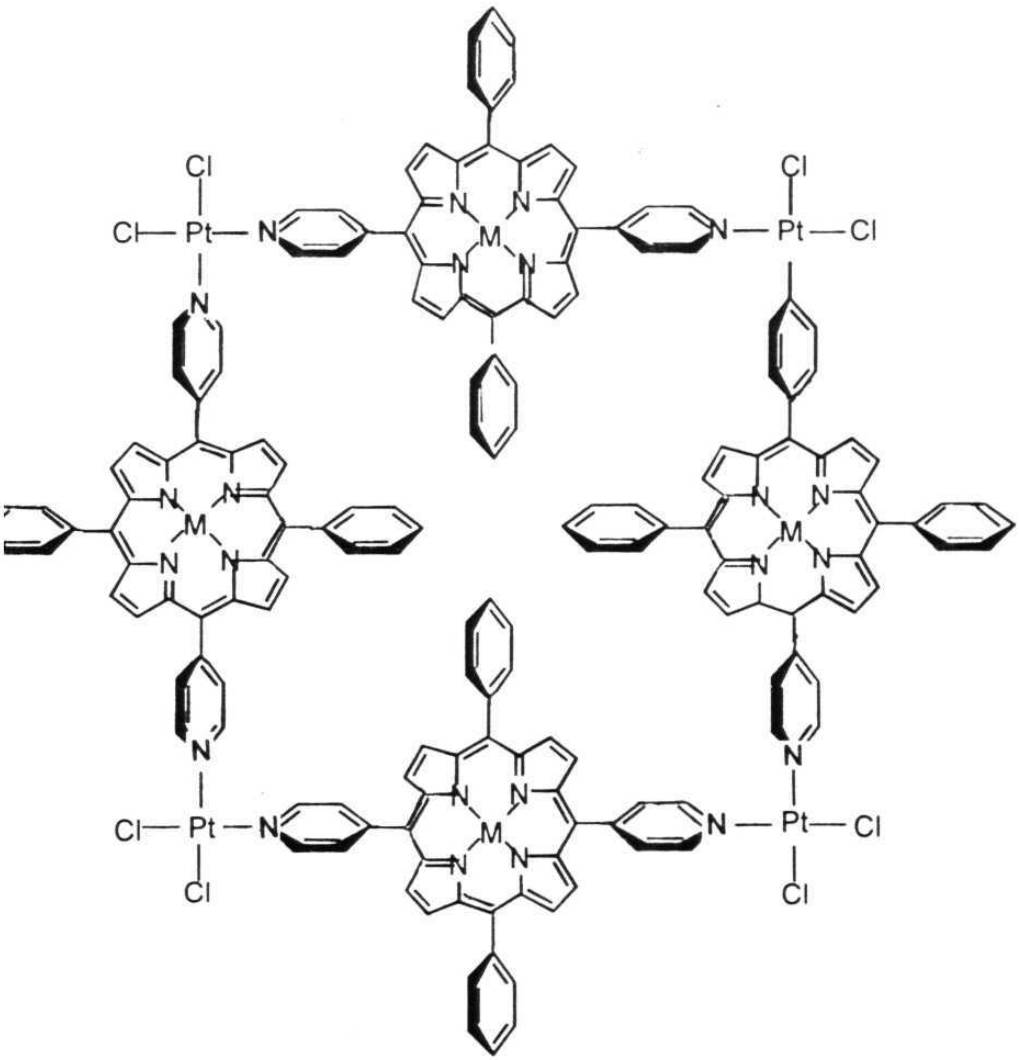

8

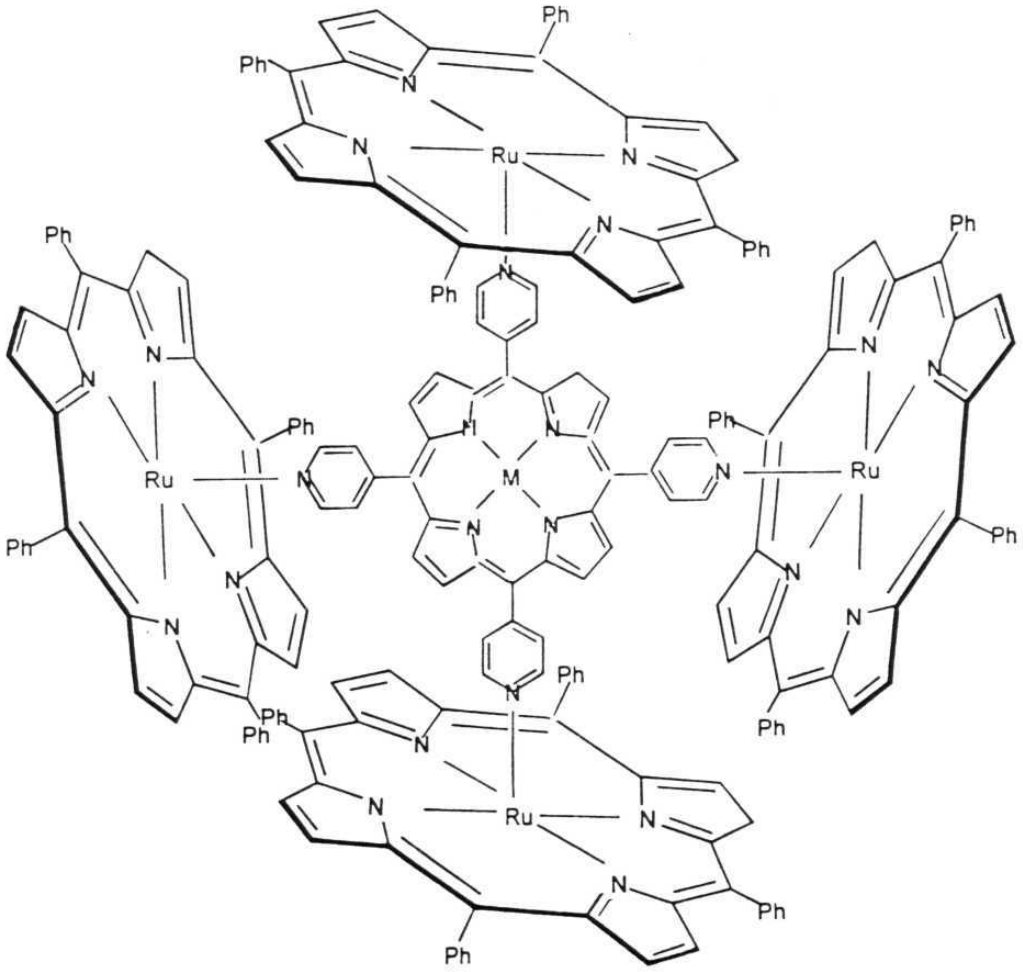

M =2H, Zn

9

dioxoporphyrin molecules are linked to a central tetrapyridyl porphyrin by zinc-pyridyl bonding.

Recently, Wojaczynski and Latos-Grazynski synthesized novel porphyrin trimers formed by a "head-to-tail" arrangement.[63] The oligomerization of an iron(III) porphyrins by axial linkage *via* the central iron atom of one porphyrin to the β-position of another yielded a "cyclic" iron porphyrin trimer.[63a] Similar structures have been architectured using Ga(III)[63b] and Mn(III)[63c] as the metal centers.

Porphyrin oligomers have also been synthesized using the covalent bond formation ability of the resident central metal/non-metal ion in the porphyrin cavity.[60-63] For example, a series of "wheel and axle" type phosphorus porphyrin arrays in which porphyrin units are linked to each other *via* the central phosphorus atoms has been recently reported.[60a] The dimer in this series was investigated for charge transfer in its excited state.[60b] Shimidzu's group has studied photochemical properties of a triad composed of three phosphorus porphyrin units and it has been suggested that the excited state decay of this system involves a charge transfer state.[60c] In another report, electrochemically synthesized donor-acceptor polymers containing oligothiophenes and phosphorus porphyrins have been reported.[60d]

1.4 D-A Systems having peripheral and axial substitution of porphyrins

Porphyrins substituted at their peripheral (*i.e.*, β-pyrrole or *meso*-positions) and/or axial have been extensively investigated over the last few decades. Porphyrins substituted with donor or acceptor groups at these sites are of interest for the present study.

1.4.1 D-A Systems involving linkage at the porphyrin *meso*-position

A number of D-A type hybrid porphyrin dimers have been synthesized and studied.[9-20,23-36] Gust et al have observed quenching of fluorescence in amide-linked 'zinc porphyrin-free-base porphyrin' diads and have attributed it to energy transfer and electron transfer reactions.[25] A final charge separated state that lives for 8 ps has been spectroscopically detected. In an elegant study, Therein and co-workers have designed three types of porphyrin dimers, illustrated by compounds **10a-c** in order to evaluate the relative magnitudes of electronic coupling in these systems.[24] Using laser flash excitation studies to measure the PET rate constants, they have concluded that the most efficient electronic coupling is observed in the hydrogen-bond dimer **10a**, thus depicting the importance of hydrogen bonds in biological electron transfer processes.

Kong and Loach have synthesized the ester-linked porphyrin-quinone (P-Q) diad in 1978[68a] and the corresponding amide linked diad was reported in 1979 by Tabushi and co-workers.[69] Since then, a great variety of P-Q diads have been reported; a few recent examples follow.

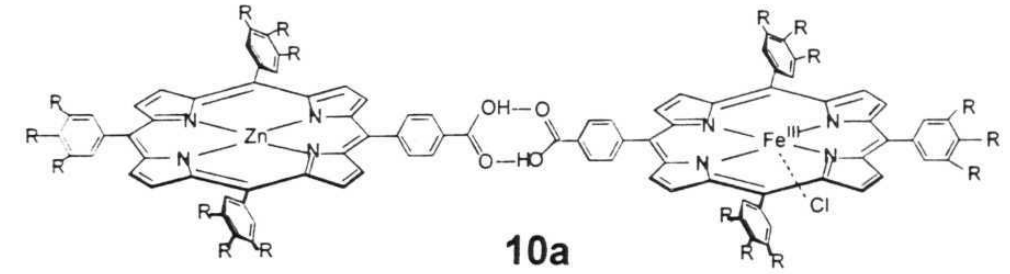

10a

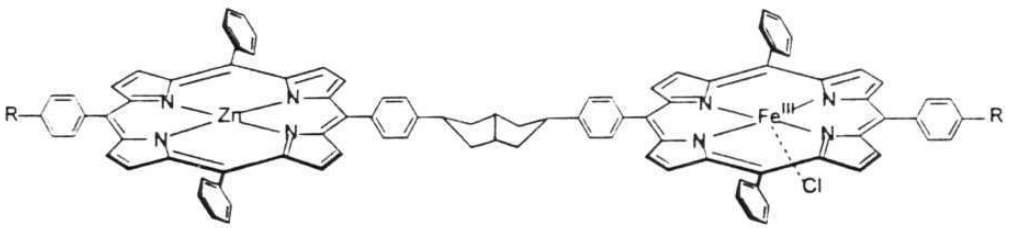

10b

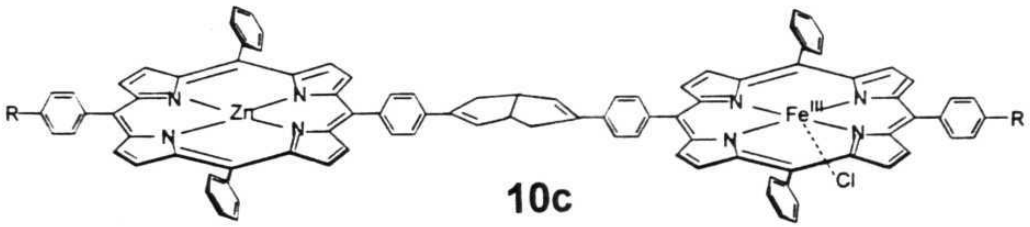

10c

R = OMe

Availability of a D-A system, having a rigid structure and a well defined distance and relative orientation between the donor and the acceptor, is one of the important criteria for the investigation of electron transfer process.[9-22,70-72] This idea has been much exploited in work in this area. For example, systems with quinones at different orientations with respect to the plane of the porphyrin have been developed by Mobius and co-workers in order to study the D-A orientation effect on the charge separation.[70] They have observed that for efficient charge separation in porphyrin-quinone systems, the MO coefficient in the HOMO of the porphyrin at the site of coupling should be as small as possible and that the quinone moiety should be in a maximal orthogonal orientation with respect to the bridge between the porphyrin and the quinone groups.

Porphyrin-quinone systems have been designed with variations in spacers to control the D-A distance and orientation.[73-76] Rigidly-linked porphyrin-quinone compounds synthesized by Sakata and co-workers are illustrative examples.[76a-d] In a more recent interesting study, the same group has shown that 'spacer-dependent' PET can take place by both 'through-bond' and 'through-space' mechanisms in rigidly linked porphyrin-spacer-quinone systems **11** with the same D-A distance and orientation.[76d]

Sessler and co-workers have synthesized and studied a number of quinone substituted monomers and dimers.[72b] Time-resolved studies were carried out in order to observe the charge separation and recombination in these complexes. In a more recent study, Sakata and co-workers have

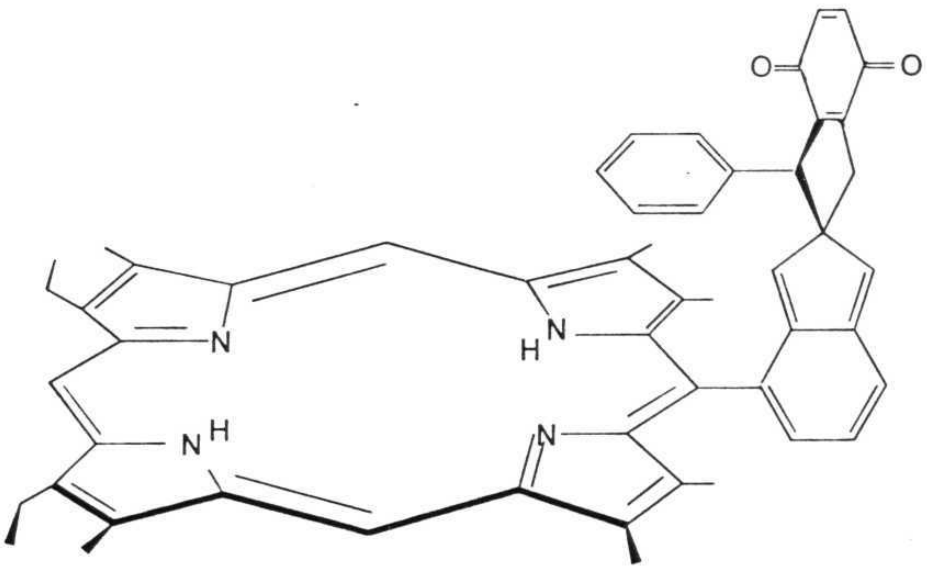

11a

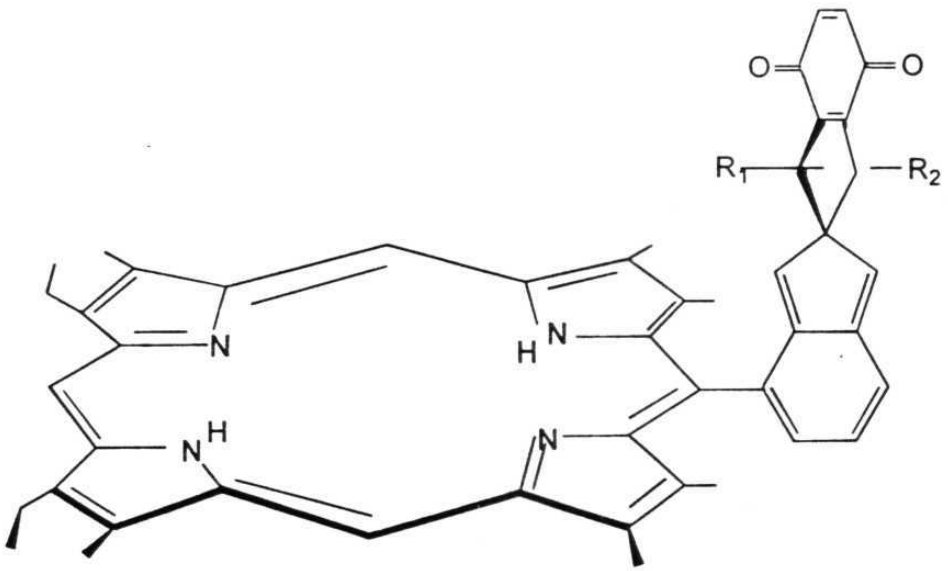

11b: $R_1 = H$, $R_2 = C_6H_5$

11c: $R_1 = R_2 = H$

elegantly established PET between a quinone moiety and a zinc porphyrin dimer through coordination bonds **12**.[76e]

In order to more closely mimic certain finer mechanistic features involved in the natural photosynthetic electron transfer, several triad, tetrad and pentad systems having various combinations of donors and acceptors have been developed.[14,16,20,25,80-83,89] The biomimetic triads of the type D-D-A were first reported by Gust, Moore and their co-workers.[14,77] One example is system **13** which comprises of a porphyrin linked covalently to a carotenoid polyene on one side and a quinone on the other. The carotenoid serves as the secondary donor in this system. It also performs the additional tasks of acting as an antenna by absorbing light in spectral regions where the porphyrin does not absorb strongly and transfers singlet excitation to the porphyrin. Similar synthetic triads have also been prepared from chlorophylls.[78]

Gust *et al.* have also demonstrated three sequential electron transfer steps to stabilize charge separation in a tetrad consisting of a carotenoid polyene, a porphyrin and two quinones. More recently, molecular triads **14a-f** were designed in order to slow down the charge recombination of the carotenoid-porphyrin-quinone (C^{+}-P-Q^{-}) species that is formed by photoexcitation followed by subsequent forward electron transfer.[83a] These triads have been shown to demonstrate coordinated photoinduced electron and proton transfer. Further improvisation on these photosynthetic model systems has resulted in a pentad which includes a carotenoid polyene, two porphyrins, and two quinones in a single

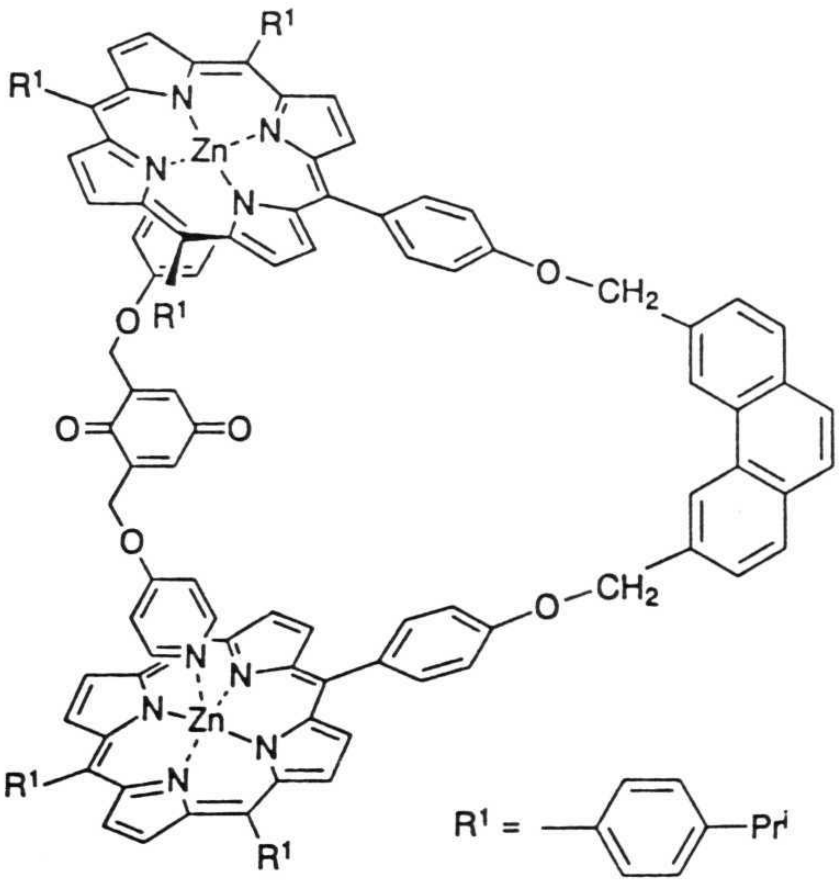

12

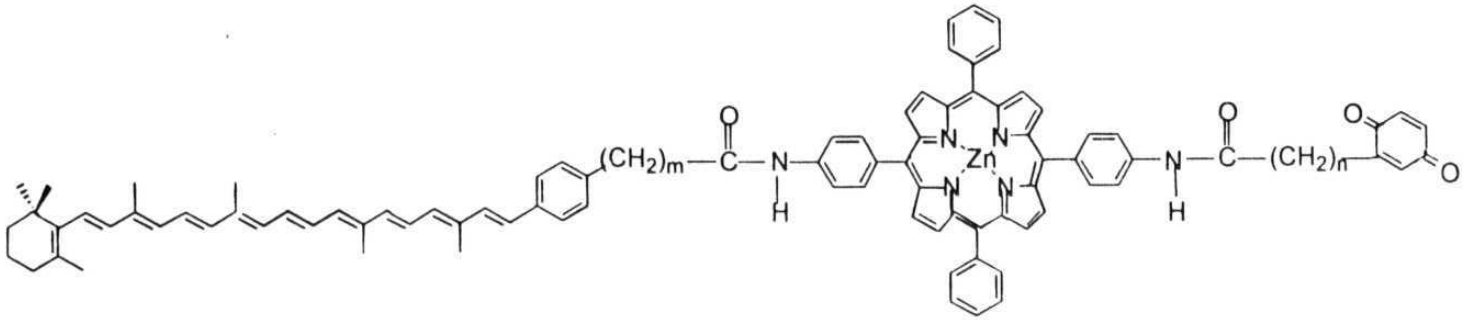

13a: n = 1, m = 0
13b: n = 2, m = 0
13c: n = 3, m = 0
13d: n = 4, m = 0
13e: n = 1, m = 1

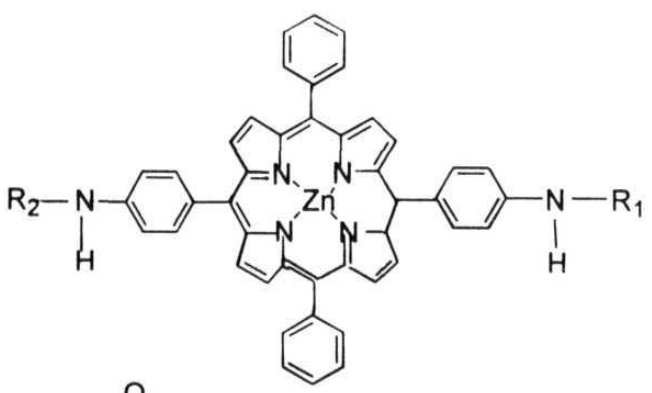

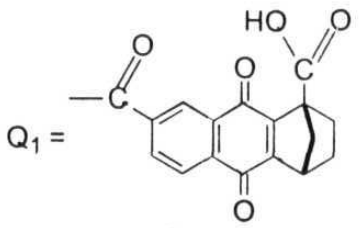

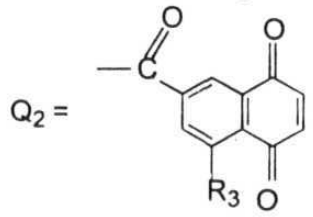

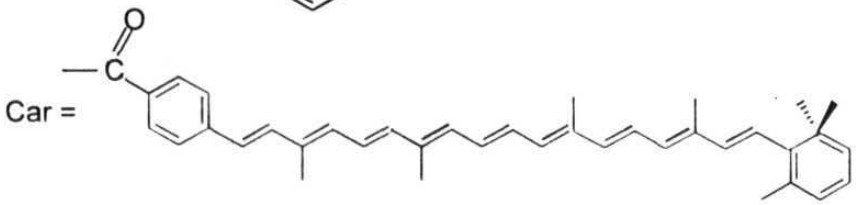

14a: $R_1 = Q_1$ $R_2 =$ Car

14b: $R_1 = Q_2$ $R_2 =$ Car $R_3 =$ Cl

14c: $R_1 = Q_2$ $R_2 =$ Car $R_3 = H$

14d: $R_1 = Q_1$ $R_2 = H$

14e: $R_1 = Q_2$ $R_2 = H$ $R_3 =$ Cl

14f: $R_1 = Q_2$ $R_2 = H$ $R_3 = H$

supramolecular complex.[83b] A long lived charge separated state (340μs) has been observed in the complex.

Porphyrins substituted with multiple crown ether voids have been investigated in great detail.[87] A recent study has investigated a porphyrin substituted with a redox active crown ether (**15**) as a biomimetic model.[88] Folding of the crown-ether-quinone moiety towards the porphyrin and the 'intramolecular' PET has been demonstrated in this system at the room temperature. At low temperatures, however, PET has been shown to be absent.

Besides quinones, other acceptors have also been linked to porphyrins in order to cover a wide range of free-energy changes and PET mechanisms. These acceptors include methyl viologen, pyromellitimide and nitroaromatic groups.[9-19] More recently, fullerenes have been linked to porphyrins and the resulting diads have been investigated for PET from porphyrin to fullerene.[84-86]

1.4.2 D-A Systems with directly attached donor/acceptor groups at the porphyrin β-pyrrole- or *meso*-position/s

Tuning the electronic structure and redox potentials of the porphyrin macrocycle is more facile in systems where the donor/acceptor groups are substituted directly on the porphyrin π-frame compared to that in systems wherein such groups are linked to the aryl rings at the *meso*-positions. Thus, porphyrins substituted with electron acceptors or donors directly at their *meso*- or β-pyrrole positions have been investigated in detail.

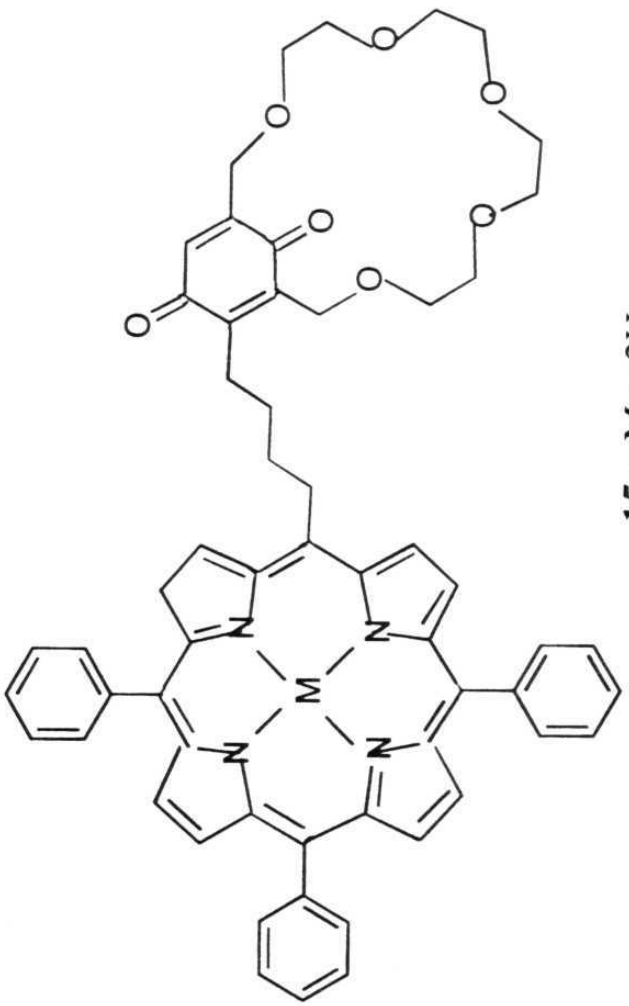

15a: M = 2H
15b: M = Zn

Examples of such species which are of consequence to this thesis are briefly discussed below.

Octaethyl- and octamethylporphyrins were among the first β-substituted porphyrins to be synthesized.[89] Padilla *et al* have synthesized β-substituted porphyrins *via* the corresponding zinc π-cation radical species.[90] Smith and co-workers have studied the effect on the planarity of porphyrins upon extensive substitution at β-pyrrole and/or meso positions.[91] A variety of polyhalogenated porphyrins with substituents on their β- positions have been synthesized and their catalytic activities have been investigated with reference to biological monooxygenation and catalytic organic functional group transformation.[92]

An extensive study has been carried out on porphyrins substituted at their β-positions with various strong electron-withdrawing groups. Giraudeau *et al* have demonstrated that these porphyrins are easier to reduce compared to the corresponding unsubstituted analogues and have, in addition, provided a criterion to distinguish between electron transfer reactions implicating the central cation and the porphyrin ligand.[93] Modulation of the electronic properties of metalloporphyrins by β-substitution was studied by Binstead *et al*..[95] A new approach for obtaining information about the relative ordering of the frontier orbitals in metalloporphyrins has been suggested. The role of pyrrolic β-substituents in the fine-tuning of energy levels in porphyrin-based molecular-electronic logic and memory devices has also been suggested. Gust, Moore and their and co-workers have studied the photophysical properties

of β-nitro-substituted porphyrins.[94a] They have observed that these systems have short singlet lifetimes and anomalous temperature and solvent dependant emission spectra suggesting the formation of an intramolecular charge transfer state in these systems. Fluorescence spectra of zinc porphyrins substituted with various electron-withdrawing groups were studied by Takahashi *et al.*[94b]

Recently, a novel β-pyrrole substituted anthrylporphyrin, viz: 9-anthrylporphyrin, has been synthesized.[96] This system, upon protonation, has been observed to form a dication which, upon photoexcitation, accepts an electron from the anthryl moiety to yield an emissive charge transfer state. More recently, β-pyrrole substituted porphyrin-quinone systems has been synthesized by Sen and Krishnan.[97] Energy of the charge transfer state in these systems is higher than that in the corresponding *meso*- substituted analogues. PET in the zinc porphyrin **16b** is more exergonic by 350 mV relative to the free-base analogue, **16a**.

In comparison with the availability of a vast body of literature on PET or EET reactions of porphyrins with appended electron acceptors, reports on donor-appended porphyrin systems are only a few. Porphyrins systems, as energy acceptors, have been covalently linked to carotenoid,[98] cyanine dye,[99] and molecular-wire-anthracene[100] subunits. In addition, naphthalene,[101a,b] anthracene,[101b,c] phenanthrene,[101d] pyrene[101d] and pyrazole[101e] groups have been linked directly to the four *meso*-carbon positions of a porphyrin. In certain cases, steady state fluorescence spectroscopic investigations have indicated intramolecular

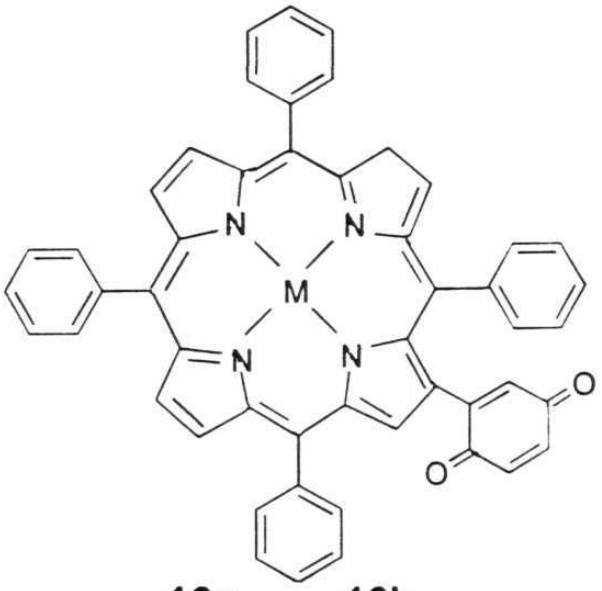

16a M = 2H, **16b** Zn

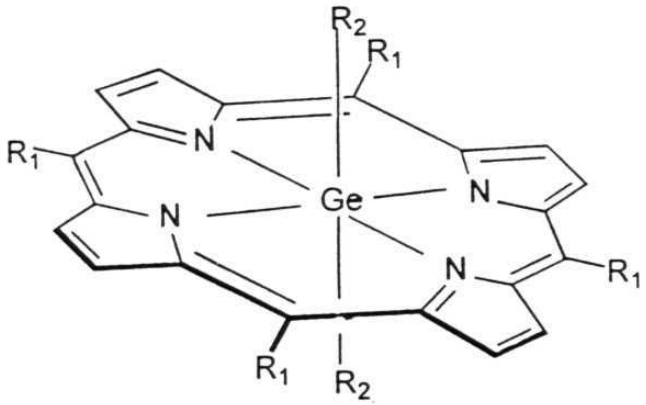

$R_1 = C_6H_5$

17a $R_2 = C_6H_5$

17b $R_2 = CH_2C_6H_5$

17c C_6H_5, R' = Ferrocene

energy/electron transfer from the attached hydrocarbon units to the central porphyrin.

1.4.3 D-A Systems involving axial substitution of porphyrins

Although a large amount of work has been carried out with regard to the synthesis and spectral studies of porphyrins containing almost every element of the periodic table, reports dealing with investigations on PET or EET reactions involving metallo/metalloid porphyrin excited states and the axially ligated electron donors or acceptors are scarce. This contrasts with the innumerable studies carried out on the PET and EET reactions of metallo/metalloid porphyrins linked at their peripheral positions with donor/acceptor subunits. A few important ones among the available examples of D-A systems involving axial substitution of porphyrins are discussed below.

Hoshino *et al.* have studied ligand assisted-photoinduced electron transfer from metalloporphyrins to methyl viologen.[102] Detailed electrochemical and photochemical investigations have been carried on σ-bonded indium and gallium porphyrins by Kadish and co-workers.[103] Generation of zwitterionic species upon laser-flash excitation of these systems has been noticed. Photoreactivity of σ-bonded alkyl, aryl and ferrocenyl germanium porphyrins (**17**) have been compared in another study.[104] Whereas the alkyl- and aryl--metal bonded porphyrins are observed to be photoreactive, in contrast, ferrocenyl bonded germanium porphyrins have been shown to be stable. The photostability of these

complexes has been explained in terms of an energy transfer from the porphyrin triplet state to the axially bound ferrocene.

Photoactivation of the porphyrin macrocycle has been shown to be affected by the axial coordination of azaferrocene to transition metal porphyrins.[105] Kinetics of charge transfer from a zinc porphyrin to an axially bound pyridine has been investigated. [106] It has been observed that irradiation of the complex gives rise to a charge transfer state.

Summary

The basic principles involved in electron- and energy transfer and relevance of these in biological and abiological systems as applicable to the subject matter of this thesis are presented in this chapter.

This thesis is divided into six chapters and a brief chapter-wise account follows.

Chapter 1 gives a general introduction to the basic principles involved in electron- and energy transfer. It also includes a survey of the recent literature on oligomeric porphyrins and various peripherally- and axially substituted porphyrin-based D-A systems highlighting their PET and EET reactions.

Chapter 2 presents a listing of the chemicals, a general description of the synthetic procedures and the details of the spectroscopic techniques employed during the research work.

Chapter 3 deals with the spectroscopic, redox and emission properties of free-base, copper(II) and zinc(II) derivatives of 2-nitro substituted 5,10,15,20-tetraaryl porphyrins (aryl = phenyl, 2-naphthyl or dipheylpyrazolyl).

Chapter 4 describes the synthesis of aryloxo derivatives of phosphorus(V) porphyrins wherein the aryloxo substituents have been linked to the porphyrin *via* the central phosphorus atom. Spectroscopy, electrochemistry and singlet state properties of these systems have been studied.

Chapter 5 presents the design, synthesis, spectroscopy and electrochemistry of a series of 'axial-bonding type' vertically-linked porphyrin arrays. These arrays comprise of a central phosphorus(V) porphyrin linked axially to two free-base or metallo-/metalloid porphyrins. Similar studies on a novel heptameric array are also presented in this chapter.

Chapter 6 presents general conclusions based on the results obtained during this research work.

References

1. Marcus, R.A.; *J. Chem. Phys.* **1956**, 24, 966. (b) Marcus, R.A.; *J. Chem. Phys.* **1965**, 43, 679. (c) Marcus, R.A. In *Light Induced Charge Separation in Biology and Chemistry*; Gerischer, H.; Katz, J.J. Eds.; Verlag Chemie: Berlin, 1979, p 15. (d) Marcus, R.A. *Angew. Chem., Int. Ed. Engl.* **1993**, 32, 1111 and references therein.
2. Forster, T. *Discuss. Faraday Soc.* **1959**, 27, 7. (b) Forster, T. *Ann. Phys.(Leipzig)* **1948**, 2, 55.
3. Dexter, D.L. *J. Chem. Phys.* **1953**, 21, 836.
4. *Photosynthesis* Amesz, J. Ed.; Elsevier : Amsterdam, 1987.
5. Chang, C.-H.; Tiede, D.M.; Tang, J.; Smith, U.; Norris, J.R.; Schiffer, M. *FEBS Lett.* **1986**, 205, 82.
6. (a) Allen, J.P.; Feher, G.; Yeates, T.O.; Komiya, H.; Rees, D.C. *Proc. Natl. Acad. Sci. U.S.A.* **1987**, 84, 5730. (b) Yeates, T.O.; Komiya, H.; Chirino, A.; Rees, D.C.; Allen, J.P.; Feher, G. *Proc. Natl. Acad. Sci., U.S.A.* **1988**, 85, 7993.
7. (a) Larkum, A.W.D.; Barrett, J. *Adv. Bot. Res.* **1983**, 10, 1. (b) *Photosynthetic Light Harvesting Systems*; Scheer, H.; Schneider, S. Eds.; W. deGruyter : Berlin, 1988. (c) Mauzerall, D.C.; Greenbaum, N.L. *Biophys. Biochim. Acta* **1989**, 974, 119.
8. (a) Sundstrom, V.; van Grondelle, R.; In *The Chlorophylls*; Scheer, H. Ed.; CRC Press : Boca Raton, FL, 1991; p1097. (b) Holzwarth, A.R.; *ibid.* p.1125.

9. (a)Connolly, J.S. In *Photochemical Conversion and Storage of Solar Energy*; Rabani, J. Ed.; The Weizman Science Press : Jerusalem, 1982, Part A, p.175. (b) Yamamoto, M.; Ito, S.; Ohmori, S. In *Photochemical Processes in Organized Molecular Systems*; Honda, K., Ed.; Elsevier: Amsterdam, 1991; p 329.

10. *Photochemistry of Polypyridine and Porphyrin Complexes*; Kalyanasundaram, K.; Academic Press : London, 1992.

11. Harriman, A. In *Supramolecular Photochemistry*; Balzani, V.; D. Reidel : Boston, 1987, p.207.

12. Connolly, J.S.; Bolton, J.R. In *Photoinduced Electron Transfer Part A*, Fox, M.A.; Channon, M. Eds.; Elsevier : Amsterdam, 1988, Chapter 6.2.

13. Wasielewski, M.R. In *Photoinduced Electron Transfer, Part D*, Fox, M.A.; Channon, M. Eds.; Elsevier : Amsterdam, 1988, Chapter 1.4.

14. Gust, D.; Moore, T.A. *Science*, **1989**, 244, 35.

15. *The Porphyrins*, Dolphin, D.; Ed.; Academic Press: New York, 1979, Vols. 1-7.

16. Gust, D.; Moore, T.A. *Top. Curr. Chem.* **1991**, 159, 103.

17. Wasielewski, M.R. *Chem. Rev.* **1992**, 92, 435.

18. (a) Fox, M.A. *Chem. Rev.* **1992**, 92, 365. (b) Fox, M.A. *Photochem. Photobiol.* **1990**, 52, 617.

19. Kurreck, H.; Huber, M. *Angew. Chem., Int. Ed. Engl.* **1995**, 34, 849.

20. Gust, D.; Moore, T.A.; Moore, A.L. *Acc. Chem. Res.* **1993**, 26, 198.

21. Morgan, B.; Dolphin, D. *Structure and Bonding* **1987**, 64, 115.

22. Baldwin, J.E.; Perlmutter, P. *Top. Curr. Chem.* **1984**, 121, 181.

23. Boxer, S.G. *Biochim. Biophys. Acta* **1983**, 726, 265.

24. de Rege, P.J.F.; Williams, S.A.; Therien, M.J. *Science* **1995**, 269, 1409.

25. Gust, D.; Moore, T.A.; Moore, A.L.; Leggett, L.; Sin, S.; DeGraziano, J.M.; Hermant, R.M.; Nicodem, D.; Craig, P.; Seely, G.R.; Nieman, R.A. *J. Phys. Chem.* **1993**, 97, 7926.

26. Tabushi, I.; Kugimiya, S.-i.; Kinnaird, M.G.; Sasaki, T. *J. Am. Chem. Soc.* **1985**, 107, 4192.

27. Brun, A.M.; Harriman, A.; Heitz, V.; Sauvage, J.-P. *J. Am. Chem. Soc.* **1991**, 113; 8657.

28. Lin, V.S.-Y.; DiMagno, S.G.; Therien, M.J. *Science* **1994**, 264, 1105.

29. Sessler, J.L.; Capuano, V.L. *Angew. Chem., Int. Ed. Engl.* **1990**, 29, 1134.

30. (a) Burrell, A.K.; Officer, D.L.; Reid, D.C.W. *Angew. Chem., Int. Ed. Engl.* **1995**, 34, 900. (b) Higuchi H.; Shimizu, K.; Ojima, J.; Sugiura, K.-i.; Sakata, Y. *Tetrahedron Lett.* **1995**, 36, 5359.

31. Anderson, H.L. *Inorg. Chem.* **1994**, 33, 972.

32. (a) Crossley, M.J.; Burn, P.L. *J. Chem. Soc., Chem. Commun.* **1987**, 39. (b) Crossley, M.J.; Burn, P.L. *J. Cem. Soc., Chem. Soc.* **1991**, 1569. (c) Crossley, M.J.; Govenlock, L.J.; Prashar, J. *J. Chem. Soc., Chem. Commun.* **1995**, 2379. (d) Crossley, M.J.; Burn, P.L.; Langford, S.J.; Prashar, J.K. *J. Chem. Soc., Chem. Commun.* **1995**, 1921.

33. Reimers, J.R.; Lu, T.X.; Crossley, M.J.; Hush, N.S. *Chem. Phys. Lett.* **1996**, 256, 353.

34. Osuka, A.; Tanabe, N.; Nakajima, S.;Maruyama, K. *J. Chem. Soc., Perkin Trans. 2* **1996**, 199.

35. Sessler, J.L.; Capuano, V.L.; Harriman, A. *J. Am. Chem. Soc.* **1993**, 115, 4618.

36. Sessler, J.L.; Capuano, V.L. *Tetrahedron Lett.* **1993**, 34, 2287.

37. Wagner, R.W.; Lindsey, J.S. *J. Am. Chem. Soc.* **1994**, 116, 9759.

38. Higuchi, H.; Shimizu, K.; Ojima, J.; Sugiura, K.-i.; Sakata, Y. *Tetrahedron Lett.* **1995**, 36, 5359.

39. Ichihara, K.; Naruta, Y. *Chem. Lett.* **1995**, 631.

40. Milgrom, L.R. *J. Chem. Soc., Perkin Trans.2* **1983**, 2535.

41. Davila, J.; Harriman, A.; Milgrom, L.R. *Chem. Phys. Lett.* **1987**, 136, 427.

42. Wennerstrom, O.; Ericsson, H.; Raston, I.; Svensson, S.; Pimlott, W. *Tetrahedron Lett.* **1989**, 30, 1129.

43. Prathapan, S.; Johnson, T.E.; Lindsey, J.S. *J. Am. Chem. Soc.* **1993**, 115, 7519.

44. Seth, J.; Palaniappan, V.; Johnson, T.E.; Prathapan, S.; Lindsey, J.S.; Bocian, D.F. *J. Am. Chem. Soc.* **1994**, 116, 10578.

45. Officer, D.L.; Burrell, A.K.; Reid, D.C.W. *J. Chem. Soc., Chem. Commun.* **1996**, 1657.

46. Tran-Thi, T.H.; Lipskier, J.F.; Maillard, P.; Momenteau, M.; Lopez-Castillo, J.-M.; Jay-Gerrin, J.-P. *J. Phys. Chem.* **1992**, 96, 1073.

47. Wasielewski, M.R.; Niemczyk, M.P.; Svec, W.A. *Tetrahedron Lett.* **1982**, 23, 3215.

48. Nagata, T.; Osuka, A.; Maruyama, K. *J. Am. Chem. Soc.* **1990**, 112, 3054.

49. Abdalmuhdi, I.; Chang, C.K. *J. Org. Chem.* **1985**, 50, 411.

50. Osuka, A.; Ida, K.; Maruyama, K. *Chem. Lett.* **1989**, 741.

51. (a) Osuka A.; Nagata, T.; Maruyama, K. *Chem. Lett.* **1991**, 481. (b) Osuka, A.; Nakajima, S.; Maruyama, K.; Mataga, N.; Asahi, T.; Yamazaki, I.; Nishimura, Y.; Ohino, T.; Nozaki, K. *J. Am. Chem. Soc.* **1993**, 115, 4577. (c) Osuka, A.; Yamada, H.; Maruyama, K.; Ohno, T.; Nozaki, K.; Okada, T.; Tanaka, Y.; Mataga, N. *Chem. Lett.* **1995**, 591. (d) Osuka, A.; Okada, T.; Taniguchi, S.; Nozaki, K.; Ohno, T.; Mataga, N. *Tetrahedron Lett.* **1995**, 36, 5781.

52. Osuka, A.; Lin, B.-l.;Maruyama,K. *Chem. Lett.* **1993**, 949.

53. (a) Dubowchik, G.M.; Hamilton, A.D. *J. Chem. Soc., Chem. Commun.* **1986**, 1391. (b) Dubowchik, G.M.; Hamilton, A.D. *J. Chem. Soc., Chem. Commun.* **1986**, 665. (c) Dubowchik, G.M.; Hamilton, A.D. *J. Chem. Soc., Chem. Commun.* **1987**, 293.

54. (a) Anderson, H.L.; Hunter, C.A.; Sanders, J.K.M. *J. Chem. Soc., Chem. Commun.* **1989**, 226. (b) Anderson, H.L.; Hunter, C.A.; Meah,

M.N.; Sanders, J.K.M. *J. Am. Chem. Soc.* **1990**, 112, 5780. (c) Anderson, S.; Anderson, H.L.; Sanders, J.K.M. *Acc. Chem. Res.* **1993**, 26, 469. (d) Vidal-Ferran, A.; Muuler, C.M.; Sanders, J.K.M. *J. Chem. Soc., Chem. Commun.* **1994**, 2657. (e) Mackay, L.G.; Wylie, R.S.; Sanders, J.K.M. *J. Am. Chem. Soc.* **1994**, 116, 3141. (f) Anderson, S.; Anderson, H.L.; Bashall, A.; McPartlin, M.; Sanders, J.K.M. *Angew. Chem., Int. Ed. Engl.* **1995**, 34, 1096.

55. Drain, C.M.; Lehn, J.-M. *J. Chem. Soc., Chem. Commun.* **1994**, 2313.

56. Chi, X.; Guerin, A.J.; Haycock, R.A.; Hunter, C.A.; Sarson, L.D. *J. Chem. Soc., Chem. Commun.* **1995**, 2567.

57. McCallien, D.W.J.; Sanders, J.K.M. *J. Am. Chem. Soc.* **1995**, 117, 6611.

58. Chernook, A.V.; Rempel, U.; von Borczyskowski, C.; Shulga, A.M.; Zenkevich, E.I. *Chem. Phys. Lett.* **1996**, 254, 229.

59. Funatsu, K.; Kimura, A.; Imamura, T.; Sasaki, Y. *Chemistry Lett.* **1995**, 765.

60. (a) Segawa, H.; Kunimoto, K.; Susumu, K.; Taniguchi, M.; Shimidzu, T. *J. Am. Chem. Soc.* **1994**, 116, 11193. (b) Susumu, K.; Kunomoto, K.; Segawa, H.; Shimidzu, T. *J. Phys. Chem.* **1995**, 99, 29. (c) Susumu, K.; Segawa, H.; Shimidzu, T. *Chem. Lett.* **1995**, 929.

(d) Segawa, H.; Nakayama, N.; Shimidzu, T. *J. Chem. Soc., Chem. Commun.* **1992**, 784.

61. Susumu, K.; Segawa, H.; Shimidzu, T. *Chemistry Lett.* **1995**, 929.

62. Kimura, A.; Funatsu, K.; Imamura, T.; Kido, H., Sasaki, Y. *Chemistry Lett.* **1995**, 207.

63. (a) Wojaczynski, J.; Latos-Grazynski, L. *Inorg. Chem.* **1995,** 34, 1044. (b) Wojaczynski, J.; Latos-Grazynski, L. *Inorg. Chem.* **1995**, 34, 1054. (c) Wojaczynski, J.; Latos-Grazynski, L. *Inorg. Chem.* **1996**, 35, 4812.

64. Segawa, H.; Nakayama, N.; Shimidzu, T. *J. Chem. Soc., Chem. Commun.* **1992**, 784.

65. Fleischer, E.B.; Shachter, A.M. *Inorg. Chem.* **1991**, 30, 3763.

66. Marvaud, V.; Launay, J.-P. *Inorg. Chem.* **1993**, 32, 1376.

67. (a) Alessio, E.; Macchi, M.; Heath, S.; Marzilli, L.G. *J. Chem. Soc., Chem. Commun.* **1996**, 1411. (b) Kimura, A.; Funatsu, K.; Imamura, T.; Kido, H.; Sasaki, Y. *Chem. Lett.* **1995**, 207.

68. (a) Kong, J.; Loach, P.A. In *Frontiers of Biological Energetics : From Electrons to Tissues* Dutton, P.L.; Leigh, J.S.; Scarpa, S. Eds.; Academic : New York, Vol.1, p.73. (b) Anton, J.A.; Kong, J.A.;

Loach, P.A. *J. Heterocycl. Chem.* **1976**, 13, 717. (c) Boxer, S.G.; Bucks, R.R. *J. Am. Chem. Soc.* **1979**, 101, 1883.

69. Tabushi, I.; Koga, N.; Yanagita, M. *Tetrahedron Lett.* **1979**, 20, 257.

70. von Gersdorff, J.; Huber, M.; Schubert, H.; Niethammer, D.; Kirste, B.; Plato, M.; Mobius, K.; Kurreck, H.; Eichberger, R.; Kietzmann, R.; Willig, F. *Angew. Chem., Int. Ed. Engl.* **1990**, 29, 670.

71. Antolovich, M.; Keyte, P.J.; Oliver, A.M.; Paddon-Row, M.N.; Kroon, J.; Verhoeven, J.W.; Jonker, S.A.; Warman, J.M. *J. Phys. Chem.* **1991**, 95, 1933.

72. (a)Gaines, G.L.; O'Neil, M.P.; Svec, W.A.; Niemczyk, M.P.; Wasielewski, M.R. *J. Am. Chem. Soc.* **1991**, 113, 719. (b) Rodriguez, J.; Kirmaier, C.; Johnson, M. R.; Friesner, R. A.; Holten, D.; Sessler, J. L. *J. Am. Chem. Soc.* **1991**, 113, 1652.

73. (a) Wasielewski, M.R.; Niemczyk, M.P.; Johnson, D.G.; Svec, W.A.; Minsek, D.W. *Tetrahedron* **1989**, 45, 4785. (b) Wasielewski, M.R.; Johnson, D.G.; Niemczyk, M.P.; Gaines, G.L.; O'Neil, M.P.; Svec, W.A. *J. Am. Chem. Soc.* **1990**, 112, 6482. (c) Hayashi, T.; Takimura, T.; Hitomi, Y.; Ohara, T.; Ogoshi, H. *J. Chem. Soc., Chem. Commun.* **1995**, 545.

74. Cave, R.; Marcus, R.A.; Siders, P. *J. Phys. Chem.* **1986**, 90, 1486.

75. (a) Oliver, A.M.; Craig, D.C.; Paddon-Row, M.N.; Kroon, J.; Verhoeven, J.W. *Chem. Phys. Lett.* **1988**, 150, 366. (b) Oevering, H.; Verhoeven, J.W.; Paddon-Row, M.N.; Warman, J.M. *Tetrahedron* **1989**, 45, 4751.

76. (a) Sakata, Y.; Tsue, H.; Goto, S.; Misumi, T.; Asahi, S.; Nishikawa, T.; Okada, T.; Mataga, N. *Chemistry Lett.* **1991**, 1307. (b) Sakata, Y.; Tsue, H. O'Neil, M.P.; Wiederrecht, P.; Wasielewski, M.R. *J. Am. Chem. Soc.* **1994**, 116, 6904. (c) Higashida, Y.; Tsue, H.; Sugiura, K.; Kaneda, T.; Tanaka, Y.; Taniguchi, S.; Okada, T.; Sakata, Y. *Chemistry Lett.* **1995**, 515. (d) Higashida, S.; Tsue, H.; Kaneda, T.; Sakat, Y.; Tanaka, Y.; Taniguchi, S.; Okada, T. *Bull. Chem. Soc. Jpn.* **1996**, 69, 1329. (e) Imahori, H.; Yoshizawa, E.; Yamada, K.; Hagiwara, K.; Sakata, Y. *J. Chem. Soc., Chem. Commun.* **1995**,1133.

77. (a) Gust, D.; Mathis, P.; Moore, A.L.; Liddell, P.A.; Nemeth, G.A.; Lehman, W.R.; Moore, T.A.; Bensasson, R.V.; Land, E.J.; Chachaty, C. *Photochem. Photobiol.* **1983**, 37S, S46. (b) Moore, T.A.; Mathis, P.; Gust, D.; Moore, A.L.; Liddell, P.A.; Nemeth, G.A.; Lehman, W.R.; Bensasson, R.V.; Land, E.J.; Chachaty, C. In *Advances in Photosynthesis Research*, Sybesma, E.; Ed.; Nijhoff/Junk : The Hague, p729.

78. Liddell, P.A.; Barrett, D.; Makings, L.R.; Pessiki, P.J.; Gust, D.; Moore, T.A. *J. Am. Chem. Soc.* **1986**, 108, 5350.

79. Hung, S.-C.; MacPherson, A.N.; Lin, S.; Liddell, P.A.; Seely, G.R.; Moore, A.L.; Moore, T.A.; Gust, D. *J. Am. Chem. Soc.* **1995**, 117, 1657.

80. Moore, T.A.; Gust, D.; Mathis, P.; Mialocq, J.C.; Chachaty, C. Bensasson, R.V.; Land, E.J.; Doizi, D.; Liddell, P.A. Lehman, W.R.; Nemeth, G.A.; Moore, A.L. *Nature* **1984**, 307, 63.

81. Gust, D.; Moore, T.A.; Moore, A.L.; Gao, F.; Luttrull, D.; DeGraziano, J.M.; Ma, C.X.; Makings, L.R.; Lee, S.-J.; Trier, T.T.; Bittersmann, E.; Seely, G.R.; Woodward, S.; Bensasson, R.V.; Rougee, M.; deSchryver, F.C.; Vander, M. *J. Am. Chem. Soc.* **1991**, 113, 3638.

82. Gosztola, D.; Yamad, H.; Wasielewski, M.R. *J. Am. Chem. Soc.* **1995**, 117, 2041.

83. (a) Gust, D.; Moore, T.A.; Moore, A.L.; Makings, L.R.; Seely, G.R.; Ma, C.X.; Trier, T.T.; Gao, F. *J. Am. Chem. Soc.* **1988**, 110, 7567. (b) Gust, D.; Moore, T.A.; Moore, A.L.; Lee, S.-J.; Bittersmann, E.; Luttrull, D.K.; Rehms, A.A.; DeGraziano, J.M.; Ma, X.C.; Gao, F.; Belford, R.E.; Trier, T.T. *Science* **1990**, 246, 199.

84. Liddell, P.A.; Sumida, J.P.; MacPherson, A.N.; Noss, L.; Seely, G.R.; Clark. K.N.; Moore, A.L.; Moore, T.A.; Gust, D. *Photochem. Photobiol.* **1994**, 60, 537.

85. Imahori, H.; Hagiwara, K.; Aiyama, T.; Taniguchi, S.; Okada, T.; Sakata, Y. *Chemistry Lett.* **1995**, 265.

86. Drovetskaya, T.; Reed, C.A. *Tetrahedron Lett.* **1995**, 36, 7971.

87. (a) Lehn, J.-M. In *Supramolecular Photochemistry*, Balzani, V.; Ed.; NATO ASI Ser. Ser. C, 1987, Vol. 24, p29f. (b) Thanabal, V.; Krishnan, V.; *J. Am. Chem. Soc.* **1982**, 104, 3643. (c) Maiya, G.B.; Krishnan, V. *Inorg. Chem.* **1985**, 24, 3253. (d) Chandrashekhar, T.K.; van Willigen, H.; Ebersole, M.H. *J. Phys. Chem.* **1985**, 89, 3453. (e) van Willigen, H.; Chandrashekhar, T.K. *J. Am. Chem. Soc.* **1986**, 108, 709.

88. Sun, L.; van Gersdorff, J.; Niethammer, D.; Tian, P.; Kurreck, H. *Angew. Chem., Int. Ed. Engl.* **1994**, 33, 2318.

89. (a) Eisner, U.; Linstead, R. P.; Parkes, E. A.; Stephen, E. *J. Chem. Soc.* **1956**, 1655. (b) Eisner, U.; Lichtarowicz, A.; Linstead, R. P. *J. Chem. Soc.* **1957**, 733.

90. Padilla, A. G.; Wu, S. -M.; Shine, H. J. *J. Chem. Soc., Chem. Commun.* **1976**, 236.

91. Medforth, C.J.; Senge, M.O.; Smith, K.M.; Sparks, L.D.; Shelnutt, J.A. *J. Am. Chem. Soc.* **1992**, 114, 9859.

92. (a) Callot, H. J. *Bull. Soc. Chim. Fr.* **1974**, 8, 1492. (b) Callot, H. J. *Tetrahedron Lett.* **1973**, 1487. (c) Traylor, T. G.; Tsuchiya, S. *Inorg. Chem.* **1987**, 26, 1338. (d) Bhyrappa, P; Krishnan, V. *Inorg. Chem.* **1991**, 30, 239. (e) Hariprasad, G.; Dahal, S.; Maiya, B.G. *J. Chem. Soc., Dalton Trans.* **1996**, 3429 and refs, therein.

93. Giraudeau, A. Callot, H.J.; Jordan, J.; Ezhar, I.; Gross, M. *J. Am. Chem. Soc.* **1979**, 101, 3857.

94. (a) Gust, D.; Moore, T.A.; Luttrull, D.K.; Seely, G.R.; Bittersmann, E.; Bensasson, R.V.; Rougee, M.; Land, E.J.; DeSchryver, F.C.; Van der Auweraer, M. *Photochem. Photobiol.* **1990**, 51, 419. (b) Takahashi, K.; Hase, S.; Komura, T.; Imanaga, H.; Ohno, O. *Bull. Chem. Soc., Jpn.* **1992**, 65, 1475.

95. Binstead, R.A.; Crossley, M.J.; Hush, N.S. *Inorg. Chem.* **1991**, 30, 1259.

96. Nakajima, S. and Osuka, A. *Tetrahedron Lett.* **1996**, 37, 8457.

97. Sen, A. and Krishnan, V. *Tetrahedron Lett.*, **1996**, 37, 8437.

98. (a) Gust, D.; Moore, T. A.; Bensasson, R. V.; Mathis, P.; Land, E. J.;Chachaty, C.; Moore, A. L.; Liddell. P. A. and Nemeth, G. A. I. *J. Am. Chem. Soc.*, **1985**, 107, 3631. (b) Gust, D.; Moore, T. A.; Moore, A. L.; Devadoss, C.; Liddell, P. A.; Hermant, R.; Nieman, R. A.; Demanche, L. J.; DeGraziano, J. M. and Gouni, I. *J. Am. Chem. Soc.*

1992, 114, 3590. (c) Osuka, A.; Yamada, H.; Maruyama, K.; Mataga, N.; Asahi, T.; Ohkouchi, M.; Okada, T.; Yamazaki, I. and Nishimura, Y. *J. Am. Chem. Soc.* **1993**, 115, 9439.

99. Lindsey, J. S.; Brown, J. S. and Siesel, D. A. *Tetrahedron* **1989**, 45, 4845.

100. Effenberger, F.; Schlosser, H.; Bauerle, P.; Maier, S.; Port, H. Wolf, H. C. *Angew. Chem., Int. Ed. Engl.* **1988**, 27, 281.

101. (a) Abraham, R. J.; Hawkes, G. E.; Hudson, M. F.; Smith, K. M. *J. Chem. Soc., Perkin Trans. II* **1975**, 204. (b) Fonda, H. N.; Gilbert, J. V.; Cormier, R. A.; Sprague, J. R.; Kamioka, K.; Connolly, J. S. *J. Phys. Chem.* **1993**, 97, 7024. (c) Cense, J. M.; Le Quax, R. M. *Tetrahedron Lett.* **1979**, 39, 3725. (d) Toeibs, A.; Haeberle, N. *Justus. Leibigs Ann. Chem.* **1968**, 718, 183. (e) Suriyanarayanan, P.; Krishnan, V. *Photochem. Photobiol.* **1983**, 38, 533.

102. Hoshino, M.; Ida, H.; Yasufuku, K.; Tanaka, K. *J. Phys. Chem.* **1986**, 90, 3984.

103. Kadish, K. M.; Maiya, B. G.; Xu, Q. Y. *Inorg. Chem.* **1989**, 28, 2518.

104. Maiya, G. B.; Barbe, J.-M.; Kadish, K. M. *Inorg. Chem.* **1989**, 28, 2524.

105. Zakrzewski, J.; Giannotti, C. *Coord. Chem. Rev.* **1995**, 140, 169.

106. Crouch, A. M.; Sharma, D. K.; Langford, C. H. *J. Chem. Soc., Chem. Commun.* **1988**, 307.

CHAPTER 2

Materials and Methods

2.1 Introduction

This chapter presents a listing of all the chemicals and other materials employed at various stages of the research work. Procedures followed for the purification of solvents and chemicals used are given. Further, a brief discussion of the physicochemical techniques employed during the course of investigation is also presented.

2.2 Materials

Pyrrole was obtained from Aldrich Chemicals (U. S. A.). It was distilled (129-131 °C) over KOH before use.

Phenol, 4-methylphenol and 4-nitrophenol were procured from E. Merck (India). 4-nitrophenol was recrystallised from ethanol before use. 2.4 dimethylphenol was procured from Fluka Chemika (Switzerland).

p-hydroxybenzaldehyde and *p*-tolualdehyde were purchased from Sisco-Chem Industries (India). They were distilled under vacuum and then used. 2-naphthaldehyde was purchased from Aldrich Chemicals (U. S. A.). Diphenylpyrazolaldehyde was prepared according to a reported procedure.[1]

Phosphorus oxychloride was procured from Merck (Switzerland). It was fractionally distilled prior to use.

Tetrabutylammonium perchlorate was procured from Aldrich Chemicals (U. S. A.).

The various metal acetates employed in the study were purchased from B. D. H. (India). Vanadyl (IV) acetylacetonate was purchased from Merck (India). These compounds were of AR grade and were used as such.

Calcium hydride was obtained from Spectrochem (India).

The other drying agents used were calcium chloride, sodium sulphate and magnesium sulphate. These were purchased from B.D.H. (India) or from Qualigens (India) and were of LR grade.

The mineral acids such as hydrochloric acid, nitric acid and sulphuric acid were of AR grade and were obtained either from Ranbaxy (India) or from B.D.H. (India).

Trifluoroacetic acid was procured from Aldrich Chemicals (U.S.A.).

Potassium chloride, potassium hydroxide, potassium carbonate and sodium bicarbonate were of LR grade and were obtained from B.D.H. (India).

Aluminium oxide (basic and neutral) and silica gel for column chromatography were procured from Acme Synthetic Chemicals (India) and were used as such.

Nitrogen gas was obtained from Indian Oxygen Limited. It was further purified and dried by passing it through alkaline pyrogallol solution, sulphuric acid, and potassium hydroxide pellets.

2.3 Solvents

The common solvents employed during the research work were purified according to standard procedures.[2,3]

Acetic acid, acetic anhydride and propanoic acid were purchased from Ranbaxy (India).

Pyridine was obtained from Ranbaxy (India). It was dried over KOH pellets and distilled over calcium hydride and under nitrogen before use.

Dimethyl formamide and dimethyl sulphoxide were obtained from E.Merck (India). They were purified by flash vacuum distillation over calcium hydride.

Toluene was of recrystallisable grade from Ranbaxy (India). It was distilled over sodium and stored over sodium wire.

Chloroform, methylene chloride, hexane and methanol were of LR grade from B.D.H. (India) and were used for synthetic or chromatographic purposes. These solvents were extensively purified as described below, for spectroscopic purposes.

The LR grade methylene chloride was washed twice with sulphuric acid, and then with water. This was followed by washing twice with sodium bicarbonate solution and then water. The solvent was then dried over calcium chloride and distilled over phosphorus pentoxide. It was stored over basic alumina before use. Chloroform (LR) was washed with water three or four times, stored over calcium chloride, and distilled over phosphorus pentoxide. It was stored in the dark over basic alumina.

Acetone, ethanol and acetonitrile were purified according to known procedures.[2.3]

$CDCl_3$ (99.8%) was obtained from Aldrich Chemicals (U. S.A.). It was used as such for ^1H NMR measurements.

2.4 Physical methods

The various porphyrins synthesized in this study were characterized and investigated using mass, infrared, electronic absorption and emission, proton- and phosphorus nuclear magnetic resonance, electron paramagnetic resonance spectroscopic methods and electrochemical methods. These methods are briefly alluded to below.

The elemental analyses were done on a Perkin-Elmer model 240C-CHN analyzer.

The infrared spectra were recorded either on a Perkin-Elmer Model 1310 or on a Jasco Model 5300 FT-IR spectrophotometer. The spectra of the solid samples were recorded by dispersing the sample in Nujol mull or as KBr wafers.

The UV-vis spectra were recorded with either a Perkin-Elmer Lambda 3B, a Shimadzu model 160A or a Jasco model 7800 spectrophotometer. A matched pair of quartz cuvettes were employed. The concentration of the porphyrins employed for this purpose ranged from ca. 2×10^{-6} (Soret bands) to 5×10^{-5} M (Q bands).

Steady state fluorescence spectra of the compounds were recorded either on a Hitachi Model F-3010 or a Jasco Model FP 777

spectrofluorometer using 1 cm quartz cell. Right angle detection technique was employed for these measurements. The excitation and emission slit widths usually employed were both either 2 nm or 5 nm. The concentration of the samples was adjusted so that the optical densities at the excitation wavelengths were less than ca. 0.2 for emission spectra and about 1 x 10^{-7} M (or the optical density at the emission wavelength, λ_{em} < 0.02) for excitation spectra. A Rhodamine 6G quantum counter was employed for spectral corrections at wavelengths < 600nm. Fluorescence quantum yields (ϕ) were estimated by integrating the areas under the fluorescence curves using the expression of Austin and Gouterman,[4]

$$\phi_{sample} = \frac{A_{sample} \times O.D._{standard}}{A_{standard} \times O.D._{sample}} \times \phi_{standard} \qquad (2.1)$$

where A is the area under the corrected emission spectral curve, O.D. is the optical density of the compound at the wavelength of the exciting light. The fluorescence standards employed were either *meso*-5,10,15,20-tetraphenyl porphyrin (H_2TPP) or its zinc (II) complex (ZnTPP) (ϕ_{H_2TPP} = 0.13 and ϕ_{ZnTPP} = 0.033)[5a] for excitation into the porphyrin absorption maxima of the free-base and zinc(II) porphyrin derivatives respectively. Dihydroxophosphorus 5,10,15,20-tetratolyl porphyrin hydroxide ([P(TTP)$(OH)_2$]OH) ($\phi_{[P(TTP)(OH)2]OH}$ = 0.036)[5b] was the fluorescence standard employed for excitation into the phosphorus porphyrin

absorption maxima. Refractive index corrections have been employed while estimating the ϕ values in various solvents.[6]

The proton- and phosphorus magnetic resonance (^{1}H NMR and ^{31}P NMR, respectively) were recorded either on a JEOL JNM FX-100 spectrometer or a Bruker NR-200 AF-FT NMR spectrometer using $CDCl_3$ as the solvent. Tetramethylsilane (TMS) was the internal standard employed for ^{1}H NMR and 80% phosphoric acid (H_3PO_4) was the standard for ^{31}P NMR. The sample concentration was $\approx 1.0 \times 10^{-3}$ M.

The electron spin resonance (ESR) spectra were recorded on a JEOL JM-FE3X spectrometer. Diphenylpicrylhydrazide (DPPH) was used as a g-marker. The spectra were recorded for ca.1.0×10^{-3} M solutions of copper (II)- and vanadyl(IV) porphyrins in toluene at 100±3 K.

The FAB mass spectra were recorded on a JEOL SX 102/DA-6000 mass spectrometer/data system using xenon (6kV, 10mA) as the FAB gas. The accelarating voltage was 10kV and the spectra were recorded at room temperature. *m*-nitrobenzyl alcohol (NBA) was used as the matrix.

The cyclic- and differential pulse voltammetric experiments were carried out with a Princeton Applied Research (PAR) model 174A/175 polarographic analyzer/universal programmer, a BAS model CV-27 and a PAR model RE 0074 X-Y recorder or with a Cypress Systems Model CS-1090/Model CS-1087 computer controlled electroanalytical system. Tetrabutylammonium perclorate (TBAP) was used as the supporting

electrolyte in all the cases. The working electrode employed was either platinum or glassy carbon. The auxillary (counter) electrode was always platinum. The reference electrode chosen was either Ag/AgCl or a saturated calomel electrode (SCE). A salt bridge containing the same concentration of base electrolyte as that of the bulk solution was positioned between the nitrogen-purged bulk-test-solution and the reference electrode to reduce the effect due to liquid junction potentials. Half-wave potentials in the cyclic voltammetic experiments were measured as the average of the cathodic and anodic peak potentials for all the reversible processes. Ferrocene was chosen as the standard and could be reversibly oxidized at 0.48 V in CH_2Cl_2, 0.1 M TBAP (*versus* SCE) under these experimental conditions.

2.5 General considerations

At all times, care was taken to avoid the entry of direct, ambient light into the samples in the spectroscopic and electrochemical experiments. Unless otherwise specified, all experiments were carried out at ambient temperature (ca. 293±3K).

All hazardous chemicals were handled with appropriate precautions. Protective gloves, goggles, and safety mask were employed to minimize exposure to obnoxious chemicals, ultraviolet light etc.

The following are the standard error limits involved in various measurements (unless otherwise stated):

λ_{max} (absorption/fluorescence) ±1 nm

logε	±10%
^{1}H NMR chemical shifts	0.01 ppm
ϕ_f	±10%
$E_{1/2}$	±0.03 V

2.6 Summary

This chapter presents a brief account of various solvents and chemicals used in this study. A description of the spectroscopic and other physical methods employed in this study are also given.

2.7 References

1. Suriyanarayanan, P.; Krishnan, V. *Photochem. Photobiol.* **1983**, 38, 533.
2. *Vogel's Textbook of Practical Organic Chemistry*; ELBS: England, 1989.
3. Perrin, D. D.; Armarego, W. L. F.; Perrin, D. R. *Purification of Laboratory Chemicals* Pergamon: Oxford, 1986.
4. Austin, E.; Gouterman, M. *Bioinorg. Chem.* **1978**, 9, 281.
5. Quimby, D.J.; Longo, F. R. *J. Am. Chem. Soc.* **1975**, 19, 5111.
6. Lackowwicz, J. R. *Principles of Fluorescence Spectroscopy*; Plenum: New York, 1983.

CHAPTER 3

Spectroscopic, Redox and Emission Properties of 2-Nitro-Substituted Tetraaryl Porphyrins

3.1 Introduction

This chapter deals with studies on porphyrin-based D-A systems with substituents located at the porphyrin peripheral (*meso*- and β-pyrrole) positions. While a nitro group has been chosen as the β-substituent, phenyl, naphthyl and pyrazolyl groups have been chosen as *meso*-substituents at the porphyrin periphery.

Porphyrins substituted with electron-withdrawing groups have been synthesized and studied for mimicking cytochrome P-450 activity[1], tuning redox and photophysical properties,[2-9] and for further chemical modification of the macrocycle.[10-14] Thus, porphyrins endowed with nitro groups either at the β-pyrrole position(s)[3-5, 9-13] or directly at the *meso* position(s) or on the *meso*-aryl ring(s)[6,7] have been studied for various applications. The interest in probing the effect of the nitro group substituted directly on the porphyrin ring has been a result of studies on nitroaromatic subunit-linked porphyrins as photosynthetic model systems.[14,15] In addition, a survey of the literature suggested that apart from the optical and photophysical properties of 2-nitro-5,10,15,20-tetratolylporphyrin [$H_2TTP(NO_2)$] and its zinc (II) analog, [$ZnTTP(NO_2)$],[4] and the spectral and electrochemical data on free-base,

copper(II) and zinc(II) derivatives of 2-nitro-5,10,15,20-tetraphenylporphyrin ($H_2TPP(NO_2)$, $CuTPP(NO_2)$ and $ZnTPP(NO_2)$),[3a] no other substantial data on the 2-nitro substituted porphyrins are available. Here, syntheses, optical absorption and emission spectra, magnetic resonance data (^1H NMR and ESR) and redox properties of a series of free-base, zinc(II) and copper(II) derivatives of 2-nitro-substituted tetraaryl porphyrins (aryl = phenyl, 2-naphthyl and diphenylpyrazolyl) are described. The molecular structures and nomenclature of the porphyrins investigated in this chapter are given in Fig. 3.1.

3.2 Experimental details

3.2.1 Synthesis of 5,10,15,20-tetraarylporphyrins (aryl = phenyl, 1a; 2-naphthyl, 1b and diphenylpyrazolyl, 1c)

Free base derivatives of 5,10,15,20-tetraarylporphyrins (aryl = phenyl, **1a**,[16] 2-naphthyl, **1b**,[17] and diphenylpyrazolyl, **1c**[18]) were synthesized according to reported procedures starting from the respective aldehydes and pyrrole. A general synthetic method is illustrated in Scheme 3.1.

Briefly, pyrrole was added to an equi-molar ratio of the respective aryl-aldehyde in refluxing propanoic acid. The mixture was refluxed for 45 minutes and left overnight at 10 °C. It was then filtered and the black-violet residue was washed several times with hot water followed by

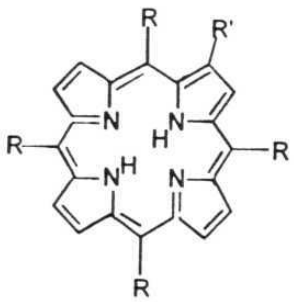

R	R'	M =	2H	Cu(II)	Zn(II)
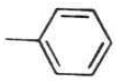	H		**1a**	**3a**	**5a**
	NO_2		**2a**	**4a**	**6a**
	H		**1b**	**3b**	**5b**
	NO_2		**2b**	**4b**	**6b**
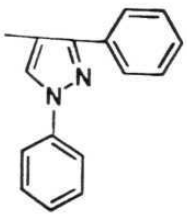	H		**1c**	**3c**	**5c**
	NO_2		**2c**	**4c**	**6c**

Figure 3.1

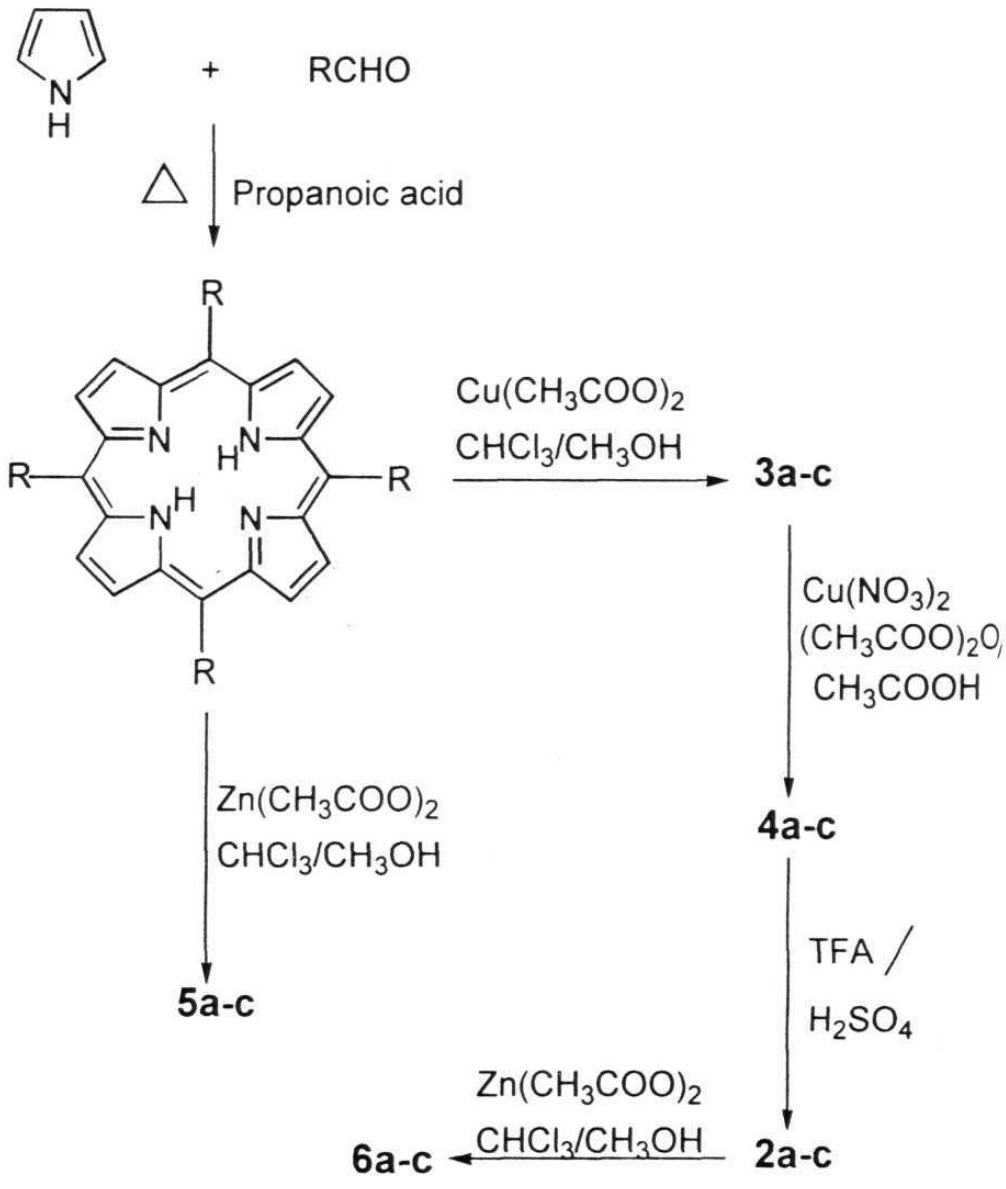
RCHO
Propanoic acid
Cu(CH3COO)2
CHCl3/CH3OH
3a-c
Cu(NO3)2
(CH3COO)2O/
CH3COOH
4a-c
TFA /
H2SO4
2a-c
Zn(CH3COO)2
CHCl3/CH3OH
6a-c
Zn(CH3COO)2
CHCl3/CH3OH
5a-c

Scheme 3.1

methanol. The solid obtained was dried in air and loaded onto a basic alumina (activity 1) column . The desired tetraaryl porphyrin was eluted out with chloroform. Yield : ~30%.

3.2.2 Metallation of 1a-c.

The copper(II) (**3a-c**) and zinc(II) derivatives (**5a-c**) of the above tetraarylporphyrins were synthesized according to the standard procedures.[19] The porphyrin was dissolved in chloroform and was mixed with the corresponding metal acetate (excess) dissolved in methanol. The mixture was refluxed for about 30 minutes. The solvents were evaporated and the crude metalloporphyrins were purified on a basic alumina column using chloroform as the eluent. Yield : >90%.

3.2.3 Syntheses of free-base (2 a-c) and metallo (4 a-c and 6 a-c) 2-nitro-5,10,15,20-tetraarylporphyrins.

These 2-nitroporphyrins were prepared by adopting methods analogous to those employed by Giraudeau *et al.*[3a] and Gust *et al.*[4] for the synthesis of 2-nitro tetratolyl porphyrins. Copper(II) complexes **3a-c** were nitrated using an excess of copper(II) nitrate in an acetic acid-acetic anhydride mixture (1:1) to give the corresponding 2-nitro copper(II) derivatives **4a-c**. The solvents were evaporated under reduced pressure and the product was purified by column chromatography (basic alumina, $CHCl_3$ eluent). Demetallation was carried out using concentrated H_2SO_4 to obtain the corresponding 2- nitro free-base derivatives **2a**, **2b**, or **2c**.

The zinc(II) complexes of the 2-nitroporphyrins, **6a**, **6b** and **6c**, were obtained by metallation of the free-base nitroporphyrins as described above for free-base tetraarylporphyrins.[19]

Each synthesized porphyrin was checked for its purity by TLC, CHN analysis, UV-vis spectra and ^{1}H NMR methods.

Analytical data

2a. Found : C,79.6; H,4.4; N,10.3. Calc. for $C_{44}H_{29}N_5O_2$: C,80.1; H,4.4; N,10.6%.

2b. Found : C,83.3; H,4.2; N,7.9. Calc. for $C_{60}H_{37}N_5O_2$: C,83.8; H,4.3; N,8.1%.

2c. Found : C,77.8; H,4.3; N,14.8. Calc. for $C_{80}H_{53}N_{13}O_2$: C,78.2; H, 4.3; N,14.8%.

3.3 Results and discussion

3.3.1 Ground state properties

The optical absorption spectra of **1b** and **2b** in CH_2Cl_2 are shown in Fig. 3.2 . The λ_{max} and log ε (ε = molar extinction coeffient) values of each porphyrin synthesized in this study are given in Table 3.1. It is clear from these data that substitution by a nitro group alters both the wavelengths of absorption bands and their relative extinction coefficients. Soret bands of the nitroporphyrins are red shifted by 5-10 nm in comparison with those of the unsubstituted porphyrins. Nitro substitution

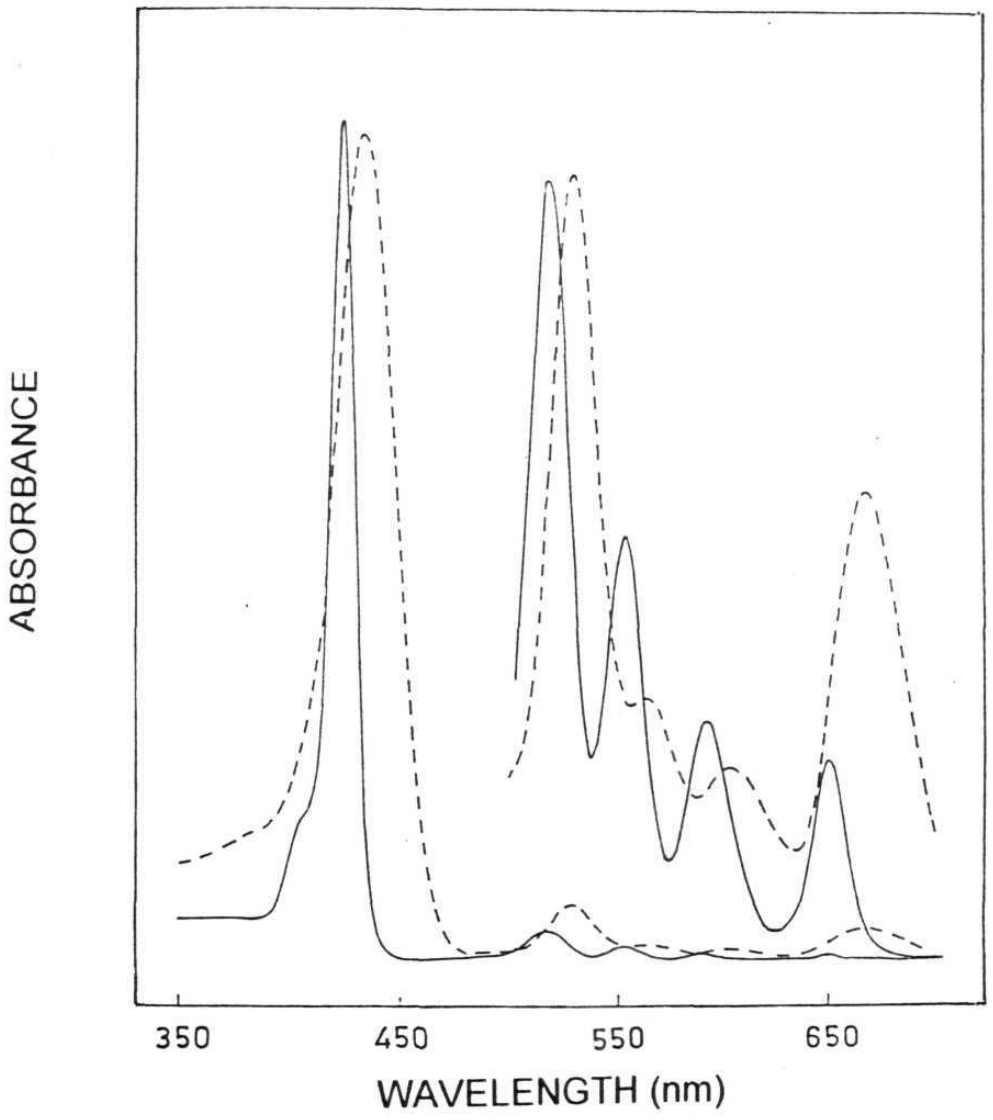

Fig. 3.2. UV-visible spectra of **1b** and **2b** in CH_2Cl_2.

Table 3.1 UV-vis data of unsubstituted- and nitroporphyrins in CH_2Cl_2.

Compound	λ_{max}, nm (log ε)				
	Q-bands				*B*-band
1a	647.5	590.0	550.0	515.0	418.5
	(3.62)	(3.65)	(3.80)	(4.17)	(5.64)
2a	665.0	605.0	562.5	528.0	427.0
	(3.85)	(3.52)	(3.55)	(4.12)	(5.30)
1b	649.0	593.0	554.0	518.0	424.0
	(3.78)	(3.83)	(4.08)	(4.35)	(5.90)
2b	668.0	605.0	566.0	531.0	435.0
	(4.01)	(3.66)	(3.78)	(4.24)	(5.40)
1c	651.8	594.6	555.4	519.0	423.8
	(3.60)	(3.75)	(3.98)	(4.24)	(5.70)
2c	666.7	602.1	568.2	531.3	435.1
	(3.77)	(3.57)	(3.69)	(4.06)	(5.29)
3a		571.3	535.0		415.0
		(3.44)	(4.31)		(5.67)
4a		590.0	545.0		420.0
		(3.92)	(4.10)		(5.25)
3b		574.0	538.2		417.0
		(3.61)	(4.37)		(5.64)
4b		593.0	547.8		427.0
		(4.01)	(4.18)		(5.27)

.....

3c	580.0	545.1	421.3
	(3.52)	(4.35)	(5.58)
4c	594.9	553.0	427.9
	(3.68)	(3.90)	(4.93)
5a	590.8	549.0	421.0
	(3.59)	(4.21)	(5.77)
6a	607.8	561.4	428.9
	(3.98)	(4.08)	(5.26)
5b	588.0	552.5	425.0
	(3.82)	(4.42)	(5.71)
6b	603.0	560.0	435.0
	(4.09)	(4.22)	(5.81)
5c	593.0	552.0	426.0
	(3.62)	(4.28)	(5.53)
6c	605.1	563.3	434.2
	(3.70)	(3.87)	(4.93)

has broadened the Soret bands in each complex and has decreased their maximum intensity. The *Q*-bands are also red-shifted with the largest shifts being seen for the longest wavelength absorption band ($Q_{0\text{-}0}$, 8-19 nm). The increase in intensity of the $Q_{0\text{-}0}$ bands of the nitro porphyrins reflects an increase in oscillator strengths, at the expense of other *Q* bands in all the nitroporphyrins, in comparison with the unsubstituted porphyrins. These observations suggest that nitration of the porphyrin perturbs the frontier orbitals of the π-ring system.[23]

^{1}H NMR spectral data of the free-base nitro-substituted and unsubstituted tetraaryl porphyrins are given in Table 3.2. Spectra of **1a** and **2a** are shown in Fig.3.3. In addition to providing the evidence the molecular structure and integrity of these porphyrins, data given in Table 3.2 also reveal the following.

(i) The β-pyrrole proton resonance which appeared as a singlet in the absence of substitution in the parent porphyrin appears as a downfield shifted complex multiplet in each nitroporphyrin. The β-pyrrole proton adjacent to the nitro group experiences the largest deshielding effect and appears as a separate peak in the complex multiplet. The mean position of the complex multiplet is also shifted downfield relative to the resonance peak position of the singlet in the parent porphyrin.

(ii) The resonance positions of the central imino (-NH) protons of the nitroporphyrins appear broad and are also shifted downfield compared to the resonance positions of the corresponding protons in the parent unsubstituted porphyrins.

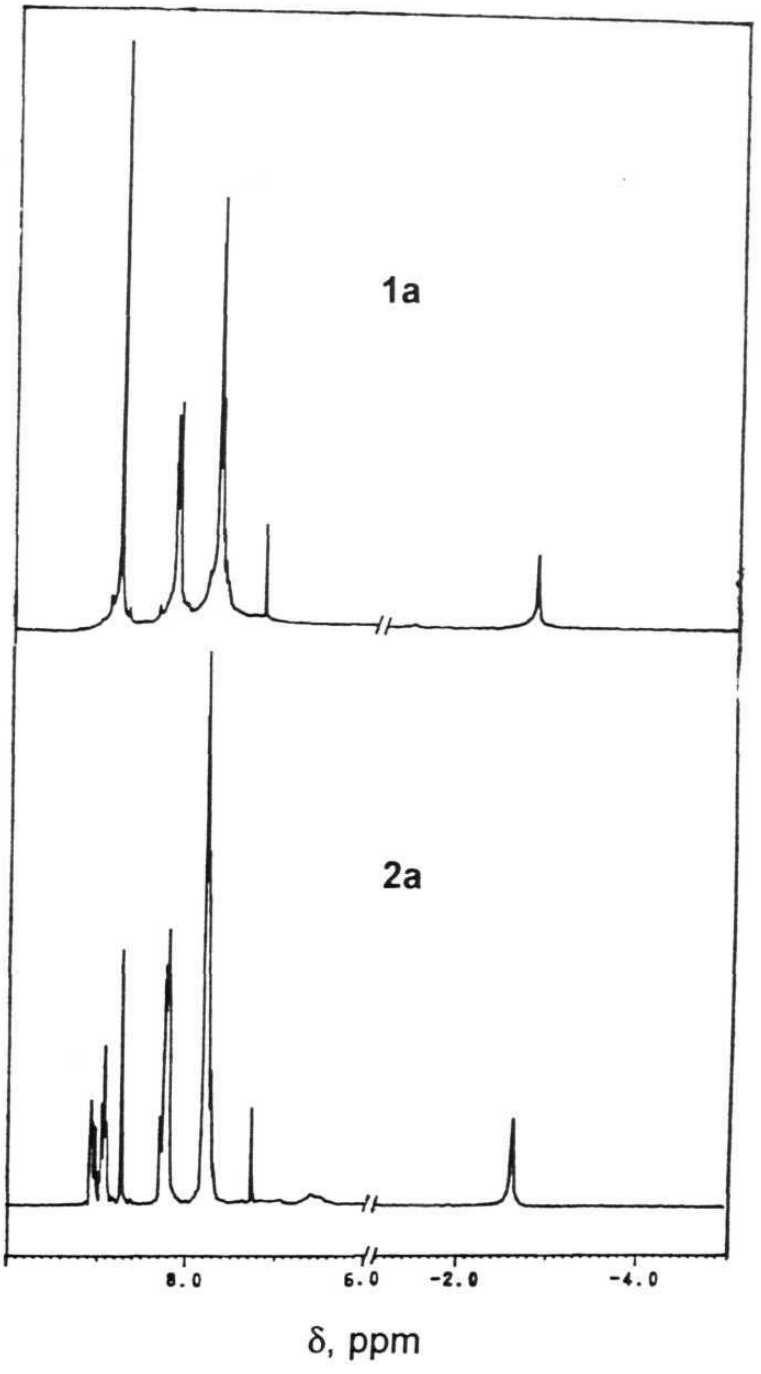

Fig. 3.3. ^{1}H NMR spectra of **1a** and **2a** in $CDCl_3$.

Table 3.2. ^{1}H NMR data of unsubstituted- and nitroporphyrins in $CDCl_3$

.

Compound	(δH, ppm)			
	Pyrrole	Substituents		-NH
1a	8.80(s), 8H	8.20(m), 8H	7.80(m), 12H	-2.80(s), 2H
2a	8.99(m), 3H	8.20(m), 8H	7.75(m), 12H	-2.75(s), 2H
	8.70 (s) 4H			
1b	8.86(s), 8H	8.68(s), 4H	8.40(d), 4H	-2.56(s), 2H
		8.13(m), 12H	7.70(m), 8H	
2b	8.99(m), 7H	8.65(m), 4H	8.38(m), 4H	-2.41(s), 2H
		8.11(m), 12H	7.70(m), 8H	
1c	9.08(s), 8H	8.67(m), 4H	8.08(m), 8H	-2.50(m), 2H
		7.50(m), 20H	6.83(m), 12H	
2c	9.19(m), 7H	8.67(m), 4H	8.08(m), 8H	-2.40(m), 2H
		7.54(m), 20H	6.92(m), 12H	

(iii) In general, the *meso*-aryl proton resonances are marginally affected upon nitration of the porphyrins. Only the resonances of those protons on the meso-substituent that are nearest to the π-framework seem to be perturbed most.

Similar results as those described above have also been obtained for the zinc(II) porphyrin series **5a-c** and **6a-c**. These spectra, however, obviously do not show the imino proton resonances.

Thus, the electron withdrawing nature of the attached nitro group is reflected in the downfield shifts observed for both β-pyrrole and -NH proton resonances of the nitroporphyrins. Interestingly, such downfield shifts are more prominent when the nitro group(s) are on the macrocyclic ring, as reported in this study for β-pyrrole-substituted tetraaryl porphyrins or as reported by Dolphin *et al.* for *meso*-nitro-substituted octaethyl porphyrins,[8] compared to the shifts observed by Quintana *et al.*[1b] for a 5,10,15,20-tetraphenyl porphyrin, endowed with two nitro groups on each of the four phenyl rings.

The copper(II) porphyrins reported in this study gave ESR spectra typical of the spectra observed for copper(II) derivatives of various tetraaryl porphyrins.[20] The spectra were analyzed using a Hamiltonian reported for the interpretation of the ESR spectrum of **3a**,[21]. The corresponding g and A values are summarized in Table 3.3. An inspection of Table 3.3 suggests that , within the experimental error, g and A values of the nitroporphyrins are similar to the values for the corresponding unsubstituted copper(II) porphyrins.

Table 3.3. ESR spectral data of copper(II) derivatives of unsubstituted- and nitroporphyrins in toluene at 100±3K

Compound	g//	g⊥	$A_{//}^{Cu}$	$A_{\perp}^{Cu}$	$A_{//}^{N}$	$A_{\perp}^{N}$
			($\times 10^{4}$ cm^{-1})			
3a	2.190	2.015	199	29.7	14.2	14.8
4a	2.192	2.020	204	29.4	13.5	14.7
3b	2.189	2.011	207	30.2	14.2	15.1
4b	2.194	2.017	202	30.8	13.9	15.4
3c	2.185	2.019	204	33.4	14.7	16.7
4c	2.167	2.015	195	30.3	14.0	15.4

Table 3.4 shows the first oxidation and first reduction potentials of all the 18 porphyrins synthesized in this study as determined by cyclic voltammetric experiments in CH_2Cl_2, 0.1 M TBAP. Representative voltammograms depicting the changes that occur upon nitration of **5b** to give **6b** are shown in Fig. 3.4. Most electrode processes are reversible, one electron transfer reactions as judged by wave analysis[22a] ($i_p/\upsilon^{1/2}$ = constant, E_{pa}-E_{pc} = 60 ± 10 mVs^{-1} and i_{pa}/i_{pc} = 0.9 - 1.0, with scan rate (υ) over the range of 100 - 500 mVs^{-1}) and also by comparing the data to data for the electrochemical oxidation of ferrocene, which was used as an internal standard.[22b] Table 3.4 also gives the difference between the first oxidation and the first reduction potentials (E_{ox} - E_{red}) for each porphyrin.

Each nitroporphyrin is easier to reduce relative to the corresponding parent unsubstituted porphyrin, with the decrement in the first reduction potential ranging from 0.22 (**1b** and **2b**) to 0.42V (**3b** and **4b**). On the other hand, in general, each nitro-substituted porphyrin is marginally difficult to oxidize relative to the parent unsubstituted porphyrin. The maximum increment of oxidation potential noticed upon nitro substitution is 0.12 V (**1a** and **2a**). These data, however, do not indicate the exact site of electron transfer on the nitroporphyrins.[24] In this regard, it must be mentioned that, in their electrochemical study on a series of tetraaryl porphyrins having one or more β-pyrrole substituents, Giraudeau *et al.* have suggested that the addition of an electron was to the conjugated π-system.[3e] They have also suggested that the electron abstraction in those porphyrins is from the lone electron pair found on the

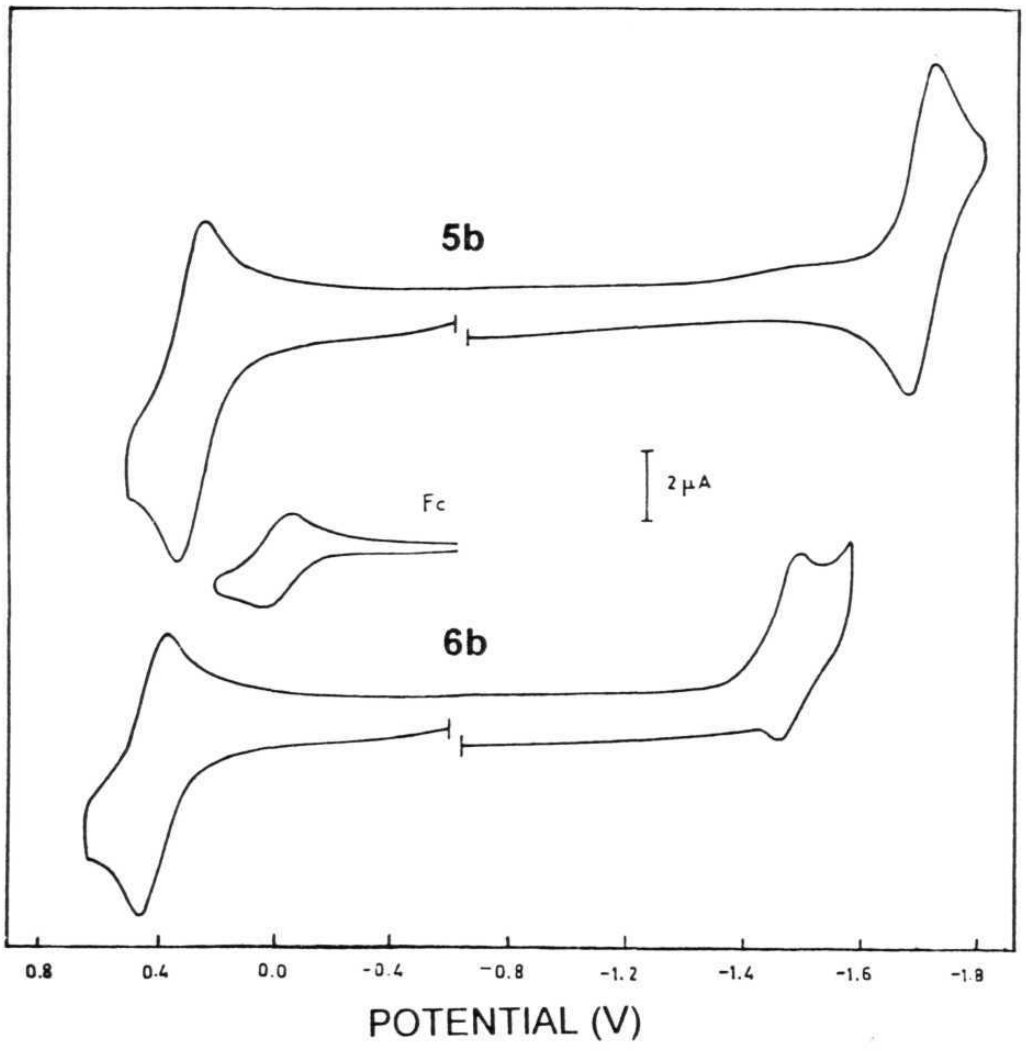

Fig. 3.4. Cyclic voltammograms of **5b** and **6b** in CH_2Cl_2, 0.1M TBAP (scan rate, 100 mVs^{-1})

Table 3.4. Redox potential data in CH_2Cl_2, 0.1M TBAP (with respect to internal Fc^+/Fc)

Compound	$E_{1/2}^{ox}$ (V)	$E_{1/2}^{red}$ (V)	$E^{ox}-E^{red}$ (V)	$-\delta\varepsilon_i$	$-\delta\varepsilon_j$	$-\delta\varepsilon_k$
1a	0.56	-1.48	2.04	0	0	0
2a	0.68	-1.19	1.87	0.35	0.12	0.29
1b	0.59	-1.38	1.97	0	0	0
2b	0.64	-1.16	1.80	0.26	0.05	0.22
1c	0.57	-1.50	2.07	0	0	0
2c	0.58	-1.26	1.84	0.35	0.01	0.24
5a	0.30	-1.75	2.05	0	0	0
6a	0.40	-1.41	1.81	0.47	0.10	0.34
5b	0.34	-1.69	2.03	0	0	0
6b	0.37	-1.46	1.83	0.41	0.03	0.28
5c	0.33	-1.70	2.03	0	0	0
6c	0.40	-1.45	1.85	0.33	0.07	0.25
3a	0.48	-1.84	2.32	0	0	0
4a	0.58	-1.52	2.10	0.44	0.10	0.32
3b	0.53	-1.76	2.29	0	0	0
4b	0.60	-1.34	1.94	0.63	0.07	0.42
3c	0.55	-1.79	2.34	0	0	0
4c	0.57	-1.38	1.95	0.70	0.02	0.41

pyrrole nitrogens. Such an involvement of the π-ring system in the redox reactions of the nitroporphyrins is assumed in the present study as well.

The E_{ox} - E_{red} values given in Table 3.4 span a range of 1.81 - 2.34 V depending on the metal ion and the substituent present (or absent) on the porphyrin, and these values are similar to those reported for several free-base porphyrins and porphyrins containing "inactive" metal ions.[24,25] Furthermore, the E_{ox} - E_{red} values for the nitroporphyrins are lower than those for the respective unsubstituted porphyrins. This observation is consistant with that reported earlier for $CuTPP(NO_2)$[9] and also with the fact that the extent of electron delocalization is higher on the nitroporphyrins relative to that on the unsubstituted analogues. Similar lowering of E_{ox} - E_{red} values has been noted earlier for several of the substituted 22π-electron texaphyrin complexes as well.[26] It was shown that the direct substitution by the nitro group on the macrocyclic periphery renders the maximum lowering of the E_{ox} - E_{red} value compared to the effect shown by all other substituents used on the texaphyrin complex.

An attempt has been made in this study to understand the magnitude of spectral and redox potential shifts observed for the nitroporphyrins relative to the unsubstituted analogues. Binstead *et al.* have reported a new approach for obtaining information about the electronic structure and, in particular, the relative ordering of the frontier orbitals in metalloporphyrin systems using both spectral and redox potential data.[9] Briefly, the method relates the shifts observed in the centre of gravity of *Q*- and *B*-bands in the absorption spectra (δE^{cg}) and

the redox potentials (δE^{red} and δE^{ox}) due to the substituent to the energy shifts of the HOMO (a_{1u} and a_{2u}) and LUMO (e_g). Thus,

$$\delta E^{red} = E^{red}[MTP(NO_2)] - E^{red}[MTP] = - \delta\varepsilon_k \quad (3.1)$$

$$\delta E^{ox} = E^{ox}[MTP(NO_2)] - E^{ox}[MTP] = - \delta\varepsilon_j \quad (3.2)$$

and

$$\delta\varepsilon_i = 2[-\delta E^{cg} + \delta\varepsilon_k - 1/2\delta\varepsilon_j] \quad (3.3)$$

Here, MTP refers to either the free-base, zinc(II) or copper(II) derivative of a tetraaryl porphyrin and $MTP(NO_2)$ to the corresponding nitroporphyrin. The values of $\delta\varepsilon_i$, $\delta\varepsilon_k$, and $\delta\varepsilon_j$ so obtained are given in Table 3.4.

An inspection of Table 3.4 reveals that the shifts at levels *i* and *k* are quite similar, whereas those for level *j* are significantly smaller. This trend is similar to that observed by Binstead *et al.* for several 2-substituted porphyrins and can be rationalized if *i* and *j* are identified respectively with the a_{1u} and a_{2u} levels and *k* with the e_g levels.[9] However, data given in Table 3.4 are apparently insensitive to changes in the type of metal ion and to the *meso*-substituent present on the porphyrin. Possibly, while the β-substitution markedly affects the porphyrin HOMO and LUMO levels through a strong resonance interaction, further modulation

by the metal ion and/or the *meso*-substituent could involve several stabilizing or destabilizing effects, which can involve steric, conjugative and inductive interactions.

Thus, all these observations collectively suggest that the HOMO and LUMO of the nitroporphyrins reported in this study involve the porphyrin π-ring system and that they possess maximum coefficients on the macrocyclic π-ring atoms, as is the case with their parent unsubstituted porphyrins.[9,23] This suggestion is also consistent with the ESR data of the nitroporphyrins, which suggest minimal influence on the electronic structure of the central metal ion upon substitution.

3.3.2 Excited state properties

Fluorescence spectra of **1a**, **1b** and **1c**, as well as those of the corresponding nitro analogues dissolved in CH_3CN, are given in Fig. 3.5. Wavelengths of major emission bands of the free-base and zinc(II) derivatives of each tetraaryl porphyrin are given in Table 3.5. Also given in Table 3.5 are the fluorescence quantum yields (ϕ) of these porphyrins in terms of the ratio $\phi_{nitro}/\phi_{non\text{-}nitro}$. As seen from the spectra given in Fig. 3.5, compounds **1a**, **1b** and **1c** show prominent bands at 649, 651 and 655 nm respectively. There is also a less intense band with its maximum appearing in the wavelength region 710-718 nm for these porphyrins. Fluorescence spectra of the corresponding nitroporphyrins in the same solvent show red-shifted broad bands, and the maxima appear at 678, 680 and 680 nm for **2a**, **2b** and **2c** respectively. In addition to the shifts in the

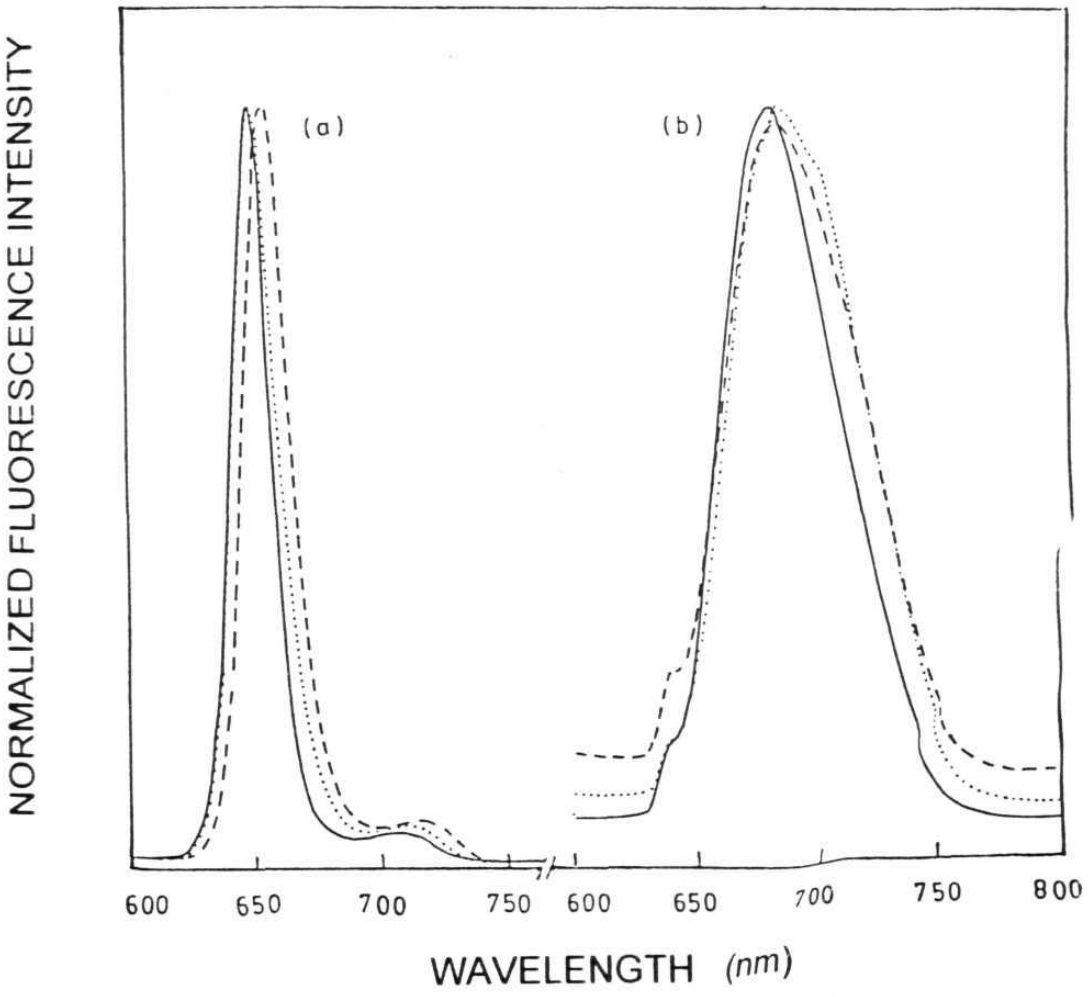

Fig.3.5. Steady state fluorescence spectra of (a) **1a** (——), **1b** (.....) and **1c** (----); (b) **2a** (—), **2b** (.....) and **2c** (----) in CH_3CN.

Table 3. 5. Fluorescence maxima (nm) and quantum yield (ϕ) data of unsubstituted- and nitroporphyrins in various solvents.

	λ_{em}, nm			
	toluene	CH_2Cl_2	CH_3CN	DMSO
1a	651, 710	652, 710	649, 710	649, 710
2a	676	682	676	680
ϕ(**2a**)/ϕ(**1a**)	0.26	0.12	0.08	0.04
1b	654, 718	657, 715	651, 713	653, 715
2b	676	690	680	680
ϕ(**2b**)/ϕ(**1b**)	0.22	0.10	0.08	0.04
1c	656, 720	660, 715	655, 716	656, 718
2c	678	690	680	680
ϕ(**2c**)/ϕ(**1c**)	0.28	0.14	0.14	0.10
5a	596, 642	597, 640	602, 650	605, 655
6a	630	635	654	660
ϕ(**6a**)/ϕ(**5a**)	0.51	0.12	0.04	0.05
5b	601, 645	600, 644	606, 654	611, 661
6b	640	644	654	664
ϕ(**6b**)/ϕ(**5b**)	0.38	0.11	0.05	0.05
5c	602, 648	602, 648	608, 656	611, 662
6c	633	641	650	652
ϕ(**6c**)/ϕ(**5c**)	0.47	0.17	0.08	0.06

band-positions, the ϕ values of the nitroporphyrins also are reduced compared to those for the corresponding unsubstituted analogues; the $\phi_{nitro}/\phi_{non\text{-}nitro}$ values are <1.0 in each case.

As seen from the data in Table 3.5, similar spectral shifts and reduction in quantum yields have been noticed for each nitroporphyrin in comparison with the corresponding parent unsubstituted porphyrin in CH_3CN.

Fig. 3.6 shows the fluorescence spectra of **6b** in three solvents of different polarities. As the solvent is changed from toluene to dichloromethane and to acetonitrile, the emission wavelength changes from 640 to 644 and to 654 nm. There is also a concomitant reduction of the ϕ values as seen from Table 3.5. The case is similar with all other nitroporphyrins in that each shows a red-shifted broad band with considerable quenching of fluorescence in comparison with the parent tetraaryl porphyrin. It is to be noted that the unsubstituted porphyrin in each case does not show any major change with respect to a change of solvent.

The excited state properties of the nitroporphyrins merit further discussion owing to their interesting fluorescence behaviour. The decreased quantum yields, the shape of the fluorescence spectra and the solvent depedence of both that are observed here for the free-base and the zinc(II) derivatives of the nitroporphyrins are similar to the results obtained earlier for **2a** and **6a** in various solvents. In their studies on photophysical properties of the latter two porphyrins (P-NO_2), Gust *et al.*[4]

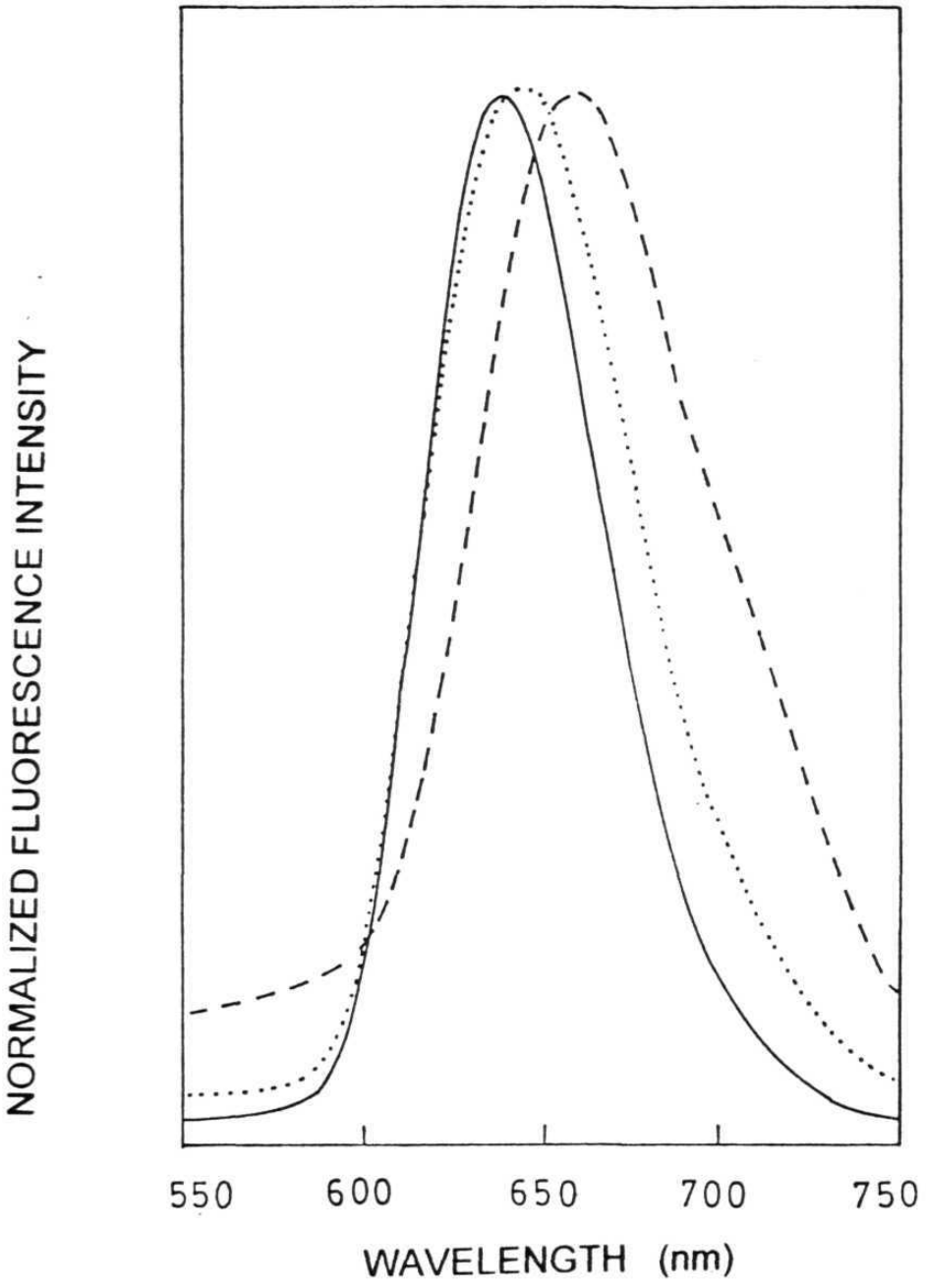

Fig. 3.6. Steady state fluorescence spectra of **6b** in toluene (——), CH_2Cl_2 (.....) and CH_3CN (-----).

have observed short lifetimes and anomolous temperature- and solvent-dependent emission spectra which are consistent with the formation of an intramolecular charge transfer of the type P^{+}-NO_2^{-}. It was suggested that in the charge transfer state the nitro group is twisted about its bond to the porphyrin, relative to the ground state geometry, and that twisted intramolecular charge transfer (TICT) is possible in those porphyrins. Based on similarities in the results obtained for **2a** and **6a** and for the six nitro-substituted tetraaryl porphyrins for which the data is given in Table 3.5, a TICT is apparently operative in the latter cases as well. However, the influence of steric and electronic effects exerted by the meso-aryl substituents on the TICT process is not discernible from the data presented in Table 3.5. Possibly, the nitro group is already twisted in the ground state and further twisting of it in the excited state would be insensitive to the nature of the *meso*-aryl substituent on the porphyrin.

3.4 Summary

Free-base, copper(II) and zinc(II) derivatives of 2-nitro-substituted 5,10,15,20-tetraarylporphyrins (aryl = phenyl, 2-naphthyl or diphenylpyrazolyl) have been synthesized and investigated by optical absorption and emission, ^{1}H NMR, ESR and cyclic voltammetric methods. Red shifts and broadening of the optical absorption bands, downfield shifts of both the β-pyrrole and imino proton NMR peaks and decrements in the reduction potentials have been observed for these nitroporphyrins, in comparison with the corresponding spectral or

electrochemical parameters for the unsubstituted parent porphyrins. Solvent-dependent fluorescence spectral data of the free-base (**2a-c**) and zinc(II) derivatives (**6a-c**) of the nitroporphyrins have been analyzed in terms of twisted intramolecular charge transfer in these complexes. However, the ESR spectral data of copper(II) derivatives of the nitroporphyrins (**4a-c**) are indistinguishable from the data for the unsubstituted analogues. All these features of the nitroporphyrins have been interpreted in terms of a perturbation of the frontier orbitals of the porphyrin π-ring system by the directly attached nitro group.

References

1. (a) Gunter, M. J.; Turner, P. *Coord. Chem. Rev.* **1991**, 108, 115 (b) Quintana, C. A.; Assink, R. A.; Shelnutt, J.A. *Inorg. Chem.* **1989**, 28, 3421.
2. Bhyrappa, P.; Krishnan, V. *Inorg. Chem.* **1991**, 30, 239.
3. (a) Giraudeau, A.; Callot, H. J.; Jordan, J.; Ezhar, I.; Gross, M. *J. Am. Chem. Soc.* **1979**, 101, 3857. (b) Callot, H. J.; Giraudeau, A.;Gross, M. *J. Chem. Soc., Perkin Trans.2* **1975**, 1321. (c) Callot, H. J.; *Tetrahedron Lett.* **1973**, 4987. (d) Giraudeau, A.; Ezhar, I.; Gross, M.; Callot, H. J.; Jordan, J. *Bioelectrochem. Bioenerg.* **1976**, 3, 519. (e) Giraudeau, A.; Callot, H. J.; Gross, M. *Inorg. Chem.* **1979**, 18, 201.

4. Gust, D.; Moore, T. A.; Luttrull, D. K.; Seely, G. H.; Bittersmann, E.; Bensasson, R. V.; Rougee, M.; Land, E. J.; DeSchryver, F. C.; Van der Auweraer, M.; *Photochem. Photobiol.* **1990**, 41, 419.

5. Cowan, J. A.; Sanders, J. K. M. *J. Chem. Soc., Chem. Commun.* **1985**, 1214.

6. (a) Harriman, A.; Hosie, R. J. *J. Chem. Soc., Faraday Trans. 2* **1981**, 77, 1695. (b) Harriman, A.; Hosie, H. J. *J. Photochem.* **1981**, 15, 163.

7. (a) Collman, J. P.; Gagne, R. R.; Reed, C. A.; Halbert, T. R.; Lang, G.; Robinson, W. T. *J. Am. Chem. Soc.* **1975**, 97, 1427. (b) Milgrom, L. R. *J. Chem. Soc., Perkin Trans. 1* **1984**, 1483.

8. (a) Gong, L. C.; Dolphin, D. *Can. J. Chem.* **1985**, 63, 401. (b) Gong, L.C.; Dolphin, D. *Can. J. Chem.* **1985**, 63, 406. (c) Wijesekera, T. Matsumoto, A.; Dolphin, D.; Lexa, D. *Angew. Chem., Int. Ed. Engl.* **1990**, 29, 1028.

9. Binstead, R. A.; Crossley, M. J.; Hush, N. S. *Inorg. Chem.* **1991**, 30, 1259.

10. Evans, B.; Smith, K. M.; Cavaleiro, J. A. S. *J. Chem. Soc., Perkin Trans. 1* **1978**, 768.

11. Baldwin, J. E.; Crossley, M. J.; DeBernardis, J. *Tetrahedron* **1982**, 38, 685.

12. Shine, H. J.; Padilla, A. G.; Wu, S. -M. *J. Org. Chem.* **1979**, 44, 4069.

13. (a) Catalano, M. M.; Crossley, M. J.; Harding,

1537. (c) Crossley, M J.; King, L. G. *J. Chem. Soc., Chem. Commun.* **1984**, 920.

14. (a) Maiya, B. G.; Krishnan,V. *J. Phys. Chem.* **1985**, 89, 5225. (b) Maiya, B. G.; Krishnan, V. *Chemistry and Industry*; Festschrfit volume in honour of Prof. K. K. G. Menon, Oxford & IBH: Bombay, 1987; p303.
15. (a) Maiya, B. G. In *Solvation Dynamics and Charge Transfer*; Bagchi, B.; Krishnan,V., Eds.; World Scientific: Singapore, 1991; p 123. (b) Sirish, M.; Maiya, B. G.; *J. Photochem. Photobiol. A: Chemistry*, **1994**, 77, 189.
16. Lindsey, J. S.; Schreiman, I. C.; Hsu, H. C.; Kearney, P. C.; Marguerettaz, A. M. *J. Org. Chem.* **1987**, 52, 827.
17. Abraham, R. J.; Hawkes, G. E.; Hudson, M. F.; Smith, K. M. *J. Chem. Soc., Perkin Trans. 2* **1975**, 204.
18. Suriyanarayanan, P.; Krishnan, V. *Photochem. Photobiol.* **1983**, 38, 533.
19. Rothemund, P.; Menotti, A. R. *J. Am. Chem. Soc.* **1941**, 63, 267.
20. (a) Subramanian, J., In *Porphyrins and Metalloporphyrins*; Smith, K. M. Ed. Elsevier: Amsterdam, 1975 Chapter 13. (b) Lin, W. C., In *The Porphyrins;* Dolphin, D., Ed.; Academic: New York, 1978; Vol. 4, Chapter 7.
21. (a) Kivelson, D.; Lee, S. -K. *J. Chem. Phys.* **1964**, 41, 1896. (b)Assour, J. M. *J. Chem. Phys.* **1965**, 43, 2477.

22. (a) Nicholson, R. S.; Shain, I. *Analyt. Chem.* **1964**, 36, 706. (b) Kadish, K. M.; Cornillon, J. L.; Yao, C. L.; Malinski, G. *J. Electroanal. Chem. Interface Electrochem.* **1987**, 235, 189.

23. Gouterman, M., In *The Porphyrins*; Dolphin, D. Ed., Academic: New York, 1978; Vol. 5, Chapter 1.

24. Kadish, K. M. *Prog. Inorg. Chem.* **1986**, 34, 435.

25. Fuhrhop, J. -H.; Kadish, K. M.; Davis, D. G. *J. Am. Chem. Soc.* **1973**, 95, 5140.

26. Maiya, B. G.; Mallouk, T. E.; Hemmi, G.; Sessler, J. L. *Inorg. Chem.* **1990**, 29, 3738.

CHAPTER 4

Synthesis, Spectroscopy, Electrochemistry and Singlet State Properties of Aryloxo Derivatives of Phosphorus(V) Porphyrins

4.1 Introduction

In the preceeding chapter, studies on donor-acceptor (D-A) systems in which the porphyrin peripheral (*meso*- and β-pyrrole) positions are utilized for linking the donor/acceptor groups have been described. The present- and also the subsequent chapters of this thesis deal with the synthesis and spectral, redox and photophysical properties of axially substituted porphyrins. Phosphorus(V) (P(V)) porphyrins have been utilized for effecting the 'axial-bonding' between the donor and the acceptor subunits.

The unique structural, spectroscopic and redox properties of phosphorus(V) porphyrins (P(V) porphyrins) have attracted considerable attention over the past two decades.[1-21] While a majority of the early studies[1-10] on these bis axially ligated metalloid porphyrins have focussed on their halide and hydroxide derivatives, recent studies[11-21] have however elaborated on the range of axial ligands coordinated at the phosphorus atom. Specifically, preparation and spectral characterization of complexes of the type $[(por)P(L)_2]^+$, where por is the dianion of a meso-tetraaryl porphyrin and L is an axially bound alkoxo, aryloxo, or arylamido ligand,

have been recently reported by Brothers and co-workers[11] and also by Shimidzu and co-workers.[12-14,18,19]. More recently, Susumu *et al.* have designed and synthesized various "axial-bonding" type hybrid porphyrin trimers.[21] Thus, more than a dozen P(V) porphyrins having organic axial ligands are currently available for study, but the spectral and redox properties of these systems have been rarely investigated in detail.[11,17,19] This chapter deals with the spectral (FAB-mass, UV-vis, IR and ^{1}H and ^{31}P NMR), electrochemical and photochemical properties of a series of newly synthesized P(V) porphyrins having various aryloxo ligands coordinated to the central phosphorus ion. These complexes exist in ionic forms in solution and are represented as $[(TpTP)P(OR)_2]^+$ where OR is a 2,4-dimethylphenoxy (**4a**), 4-methylphenoxy (**4b**), phenoxy (**4c**), 4-(4-nitrophenoxy)phenoxy (**4d**), 4-(2,4-dinitrophenoxy)phenoxy (**4e**), or 4-nitrophenoxy (**4f**) group.

4.2.Experimental details

2,4-dimethylphenol, **3a**, 4-methylphenol, **3b**, phenol, **3c**, and 4-nitrophenol, **3f**, were procured commercially and used after recrystallization from ethanol.

4.2.1 Synthesis of *meso*- 5,10,15,20- tetratolylporphyrin (1)

Compound **1** was synthesized according to the reported procedure[22] (see Scheme 4.1). Pyrrole (4.83 g, 0.07 M) was added to propanoic acid (300 ml) at 120 °C, containing tolualdehyde (8.40 g, 0.07

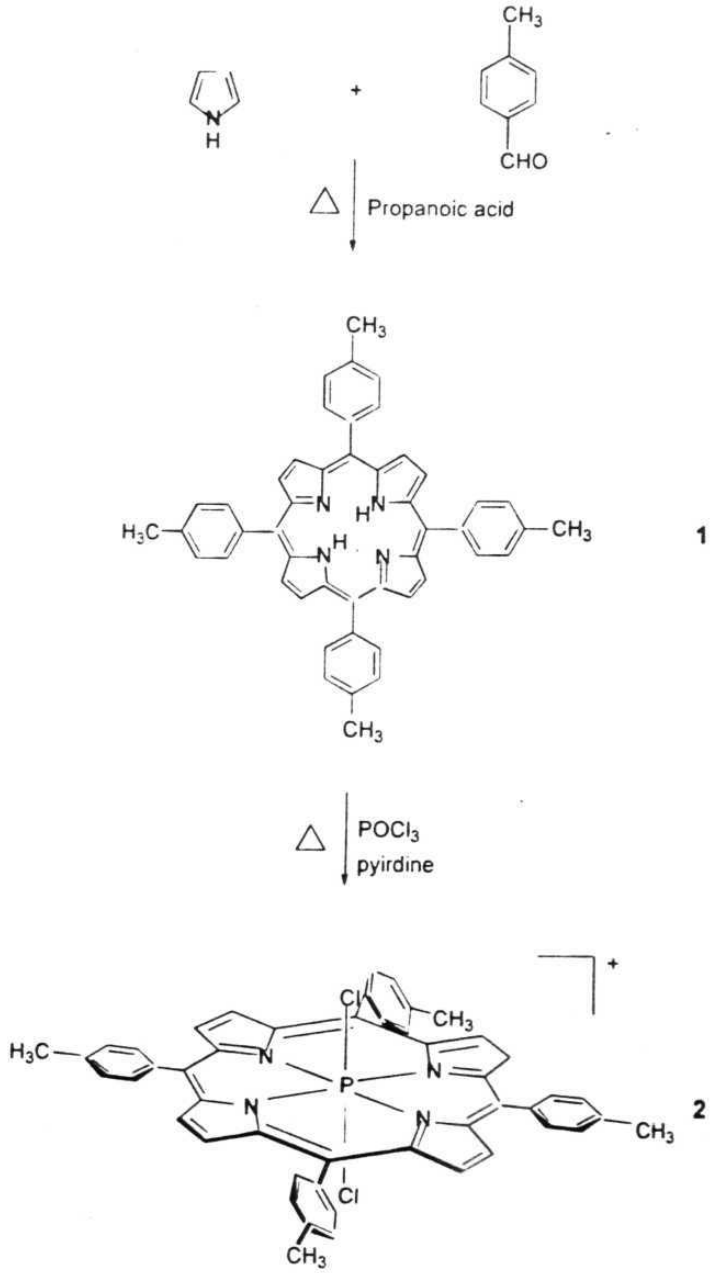
CH3
N
H
+
CHO
Propanoic acid
CH3
H3C
CH3
1
CH3
POCl3
pyirdine
+
Cl
CH3
H3C
N
P
N
N
N
CH3
2
Cl
CH3

Scheme 4.1

M). The mixture was refluxed for 40 minutes and left overnight at 0 °C. The product was filtered and the residue washed with hot water and methanol. The resulting purple residue was chromatographed on a basic alumina column. Elution with chloroform gave the desired product. Yield ≅35%.

4.2.2 Synthesis of 5,10,15,20-tetratolylporphyrinato dichlorophosphorus hydroxide (2)

This compound was synthesized as illustrated in Scheme 4.1 by the method used by Barbour *et al.*[11] Phosphorus oxychloride ($POCl_3$) (8.77 g, 0.057 M) was added to **1** (2.00 g, 0.003 M) in dry pyridine (30 ml) in an atmosphere of nitrogen. The mixture was refluxed for 24 h. under nitrogen. The solvent pyridine and excess $POCl_3$ were removed under reduced pressure. The solid obtained was chromatographed on a silica gel column. Elution with $CHCl_3$ - CH_3OH (90:10, V/V) gave the desired product. The compound was further purified by recrystallization from benzene - octane. Yield ≅70%.

4.2.3 Synthesis of 4-(4- nitrophenoxy)phenol (3d)

Hydroquinone (1.10g, 0.01. M) and K_2CO_3 (1 g) were stirred together in dry DMF (20 ml) for 45 minutes. 4 chloronitrobenzene (1.57g, 0.01 M) dissolved in dry DMF (20 ml) was slowly added to this mixture through a dropping funnel over a period of 1 h. The reaction mixture was stirred overnight at room temperature. The DMF was removed under

reduced pressure and the residue was applied onto a silica gel column. The desired product was obtained using $CHCl_3$ as the eluent. The product was recrystallised twice from ethanol before use. Yield ≅ 60%. M.P. = 169±2 °C.

Analytical data

Found : C,62.24; H,3.94; N,6.58. Calc. for $C_{12}H_9O_4N$: C,62.34; H,3.90; N,6.06.

4.2.4 Synthesis of 4-(2,4-dinitrophenoxy)phenol (3e)

This compound was synthesized in a manner analogous to that described above for compound **3d** by the condensation of hydroquinone with chloro 2,4-dinitrobenzene. Yield ≅ 55%. M.P. = 132±2 °C.

Analytical data

Found : C,51.66; H,2.75; N,10.33. Calc. for $C_{12}H_8O_6N_2$: C,52.17; H,2.90; N,10.14.

4.2.5 Synthesis of aryloxophosphorus porphyrins 4a-f

The method reported by Barbour *et al.* was adopted for the preparation of these compounds (see Scheme 4.2).[11] Compound **2** (0.10 g) was taken in dry pyridine (20 ml). An excess of the corresponding phenol (**3a-f**) (1 g) was added and the mixture was refluxed under nitrogen for 45 minutes. Pyridine was removed under reduced pressure. The solid was

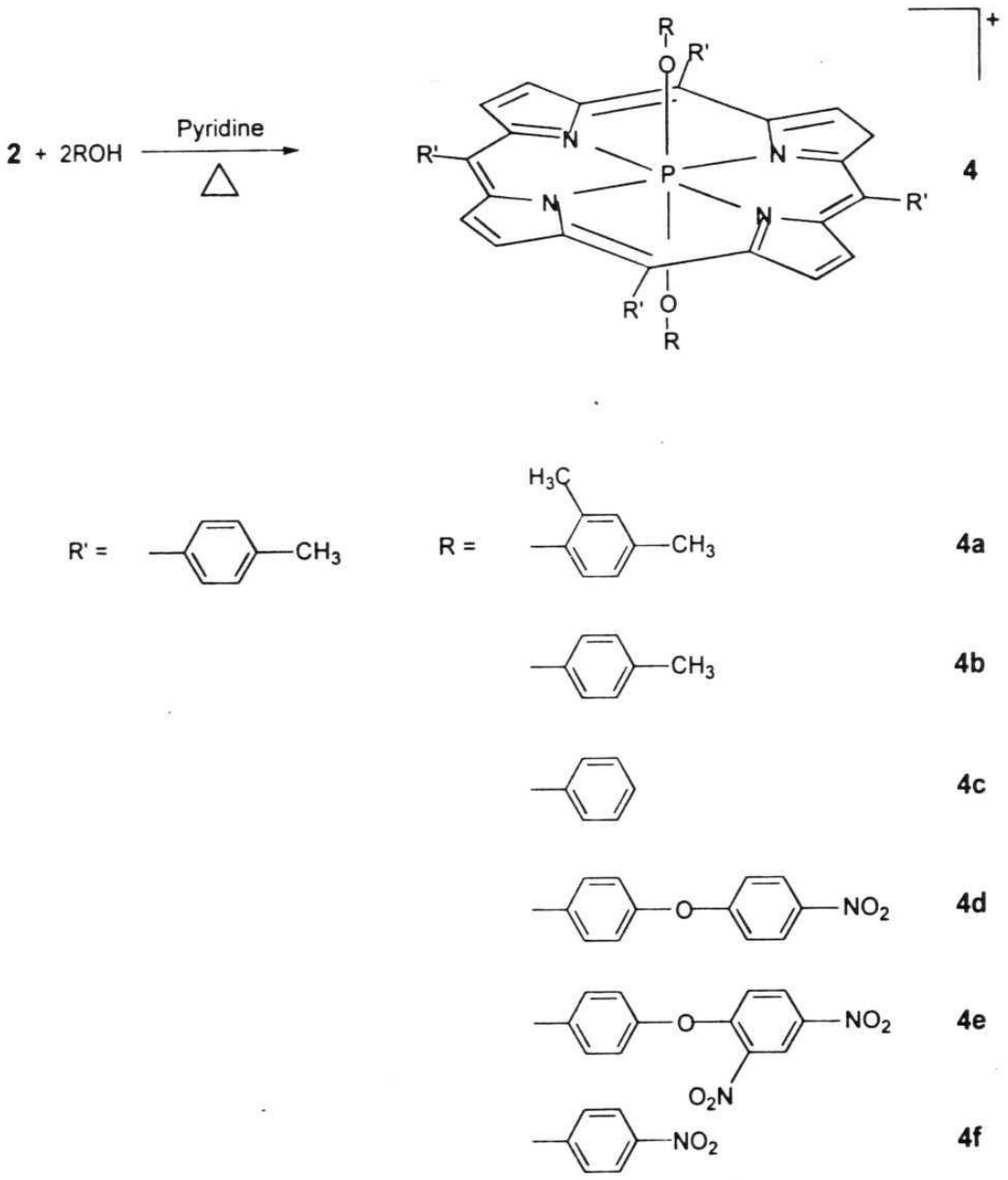

Scheme 4.2

chromatographed on a silica gel column. The desired product was obtained on elution with $CHCl_3$ - CH_3OH (90:10, V/V). The product was recrystallized from benzene-octane. Yield in each case ≈ 60%.

4.2.6 Mass spectral data

(m/z): **4a**: $[M+H]^+$ 942; $[M-C_8H_9O]^+$ 820; $[M-2(C_8H_9O)]^+$ 699 (base peak); **4b**: $[M]^+$, 913; $[M-C_7H_7O]^+$, 806; $[M-2(C_7H_7O)]^+$, 699 (base peak); **4c**: $[M+H]^+$, 885; $[M-C_6H_5O]^+$, 792; $[M-2(C_6H_5O)]^+$, 699 (base peak); **4d**: $[M]^+$, 1159; $[M-C_{12}H_8NO_4]^+$, 929; $[M-2(C_{12}H_8NO_4)]^+$, 699 (base peak); **4e**: $[M]^+$, 1249; $[M-C_{12}H_7N_2O_6]^+$, 974; $[M - 2(C_{12}H_7N_2O_6)]^+$, 699 (base peak) and **4f** : $[M]^+$, 975; $[M-C_6H_4NO_3]^+$, 837; $[M-2(C_6H_4NO_3)]^+$, 699 (base peak);

In each case, a less intense peak at m/z = $[M+OH]^+$ was observed confirming the presence of the hydroxyl counter anion in these systems.

4.3 Results and discussion

4.3.1 Ground state properties

The wavelengths of maximum absorption (λ_{max}) and molar extinction coefficient (log ε) values of all the aryloxo porphyrins are summarized in Table 4.1. Representative UV-vis spectra of **4b** and **4e** are given in Fig. 4.1. Both porphyrins show an intense Soret band and two less intense *Q*-bands between 350 and 650 nm and, log ε values at the absorption maxima of these bands are found to be in a similar range.

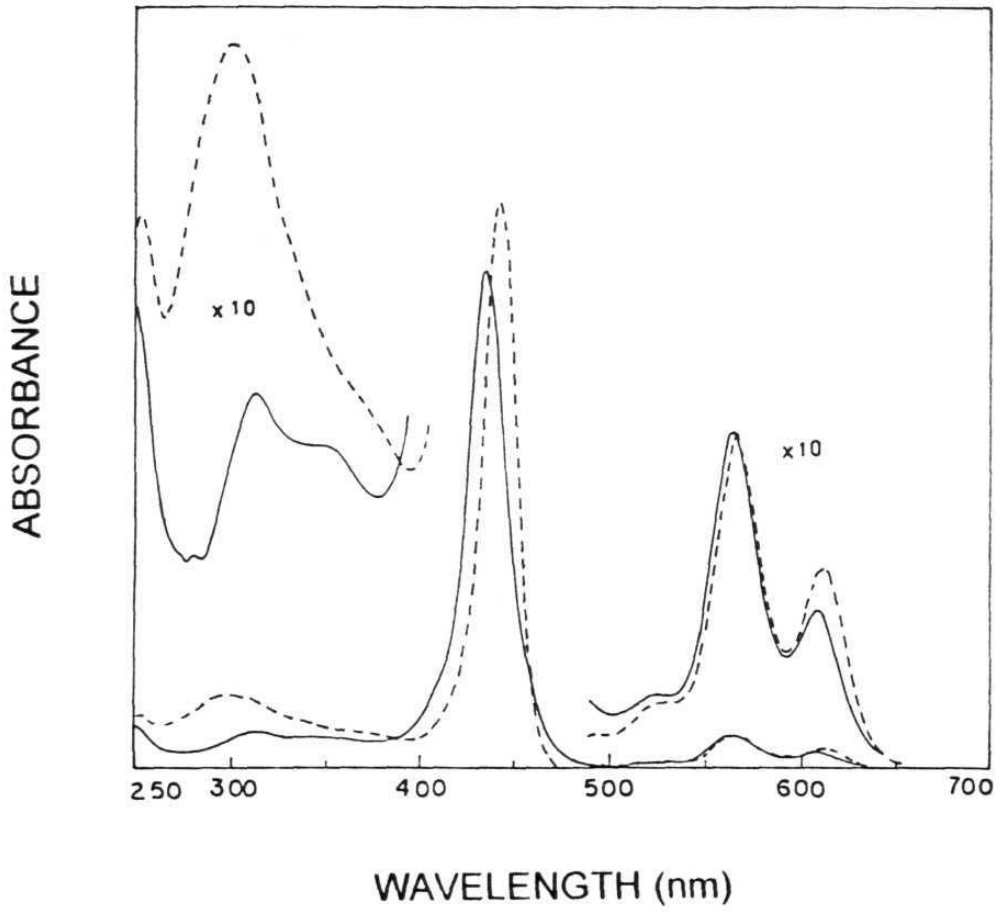

Fig.4.1. UV-visible spectra of **4b** (——) and **4e** (----) in CH_2Cl_2.

Table 4.1 UV-vis (CH_2Cl_2) and IR data

Compound	λ_{max}, nm (log ε)				
	Q-bands		*B*-band	UV	ν_{P-O} cm^{-1}
4a	613 (3.81)	570 (4.11)	436 (5.01)	312 (4.16)	868
4b	610 (3.74)	566 (4.03)	439 (5.23)	311 (4.11)	889
4c	609 (3.97)	565 (4.25)	440 (5.32)	312 (4.34)	885
4d	611 (3.90)	566 (4.13)	440 (4.99)	309 (4.59)	870
4e	616 (4.01)	570 (4.18)	444 (5.41)	314 (4.48)	870
4f	611 (3.94)	566 (4.16)	443 (5.39)	300 (4.52)	885

However, the log ε value of the peak at 314 nm of **4e** is found to be higher than that of the corresponding peak (311 nm) of **4b**. This is due to an additional absorption by the dinitro aromatic chromophore present on the former complex. The data on λ_{max} and log ε values given in Table 4.1 clearly suggest that the spectrum of each aryloxo derivative synthesized in this study also shows an intense Soret band and two less -intense *Q*-bands.

Thus, each of the compounds **4a-f** show what is called a "normal UV-vis absorption spectrum" with one intense Soret band and two less-intense *Q*- bands. This fact indicates the presence of a P(V) species (and not a P(III) species, which shows a "hyper" spectrum[4]) in the porphyrin core for all of them. A closer inspection of these data suggests that these values are not very sensitive to nature of the aryloxo ligands. Nevertheless, as was the case with various metallo- or metalloid-porphyrins containing organic axial ligands,[4,11,26] the Soret bands of the aryloxo phosphorus(V) porphyrins synthesized in this study were also found to be less broad and less intense in comparison with those of **2** or its dihydroxo analogue.

The band due to P-Cl stretching frequency ($\nu_{P\text{-}Cl}$) observed at 425 cm^{-1} in the IR spectrum of **2** was absent in the spectra of the aryloxo derivatives. The IR band due to $\nu_{P\text{-}O}$ for **4b** has been reported[11] to occur at 885 cm^{-1} and based on this fact, the bands observed in the region of 868-889 cm^{-1} can be assigned to the $\nu_{P\text{-}O}$ for various aryloxo porphyrins investigated in this study (see Table 4.1). The absence of the band due to

the P-Cl stretching and the appearance of a new band that is ascribable to the P-O stretching in the IR spectra of these complexes suggest that two axial ligands are attached to the central P(V) atom.

Each new P(V) porphyrin has also been investigated by the ^{31}P NMR spectroscopic method, and the chemical shift data are summarized in Table 4.2. The proton-decoupled ^{31}P NMR signal observed for each compound is between -194 and -200 ppm, and this range is typical of that expected for octahedral six-coordinate phosphorus compounds.[27]

The ^{1}H NMR spectra of **4b** and **4f** are compared in Fig. 4.2. The spectrum of the chloride salt of **4b** has been reported earlier,[11] and the spectrum obtained in this study for the hydroxo salt of the same species is consistent with the reported spectrum. Therefore, proton assignments for the rest of the compounds, **4a** and **4c-f**, can be made on the basis of the known data of **4b**. For example, the peaks due to **4f** as shown in Fig 4.2 can be assigned as follows. The doublet appearing at 9.09 ppm is due to the pyrrole-β protons. These protons show a four-bond coupling with the central P(V) atom ($^{4}J_{PH}$ = 3.8 Hz). The two closely spaced doublets at 7.60 ppm and 7.51 ppm can be assigned to the *o*- and *m*-tolyl (peripheral) protons of the compound, respectively ($^{3}J_{HH}$ = 8.1 Hz). The resonances ascribable to the axial ligand protons of **4f** show expected integrated intensities for eight protons and, moreover, are found to be typically shifted upfield of their normal ranges due to the porphyrin diamagnetic ring-current effect.[28] The *ortho* and *meta* (with respect to the hydroxy substituent) proton resonances of the free ligand **3f**, which were occuring

Table 4.2 ^{1}H NMR and ^{31}P NMR data in $CDCl_3$[a]

Compound	(δ, ppm)								
	Peripheral protons			Axial ligand protons					^{31}P NMR
	H_β ($^4J_{PH}$)	H_o, H_m ($^3J_{HH}$)	CH_3	H_o/CH_3 ($^3J_{HH}$, $^4J_{PH}$) [Δδ]	H_m ($^3J_{HH}$, $^5J_{HH}$) [Δδ]	H_p/CH_3 ($^3J_{HH}$/ $^7J_{PH}$) [Δδ]	H_o ($^3J_{HH}$) [Δδ]	$H_{m'}$ ($^3J_{HH}$, $^4J_{HH}$) [Δδ]	
4a	9.02 (d) (3.5)	7.49 (s) (7.5)	2.60 (s)	0.75 (d),-0.86 (s) (8.3) [3.21]	5.46 (d), 5.73 (s) (8.3) [1.06]	1.64 [0.71]			-197
4b	9.01 (d) (3.1)	7.66 (d), 7.52 (d) (7.9) (7.9)	2.61 (s)	2.08 (dd) (7.8, 2.9) [4.99]	5.69 (d) (7.8) [1.08]	1.64 (2.9) [0.67]			-194
4c	9.02 (d) (3.6)	7.66 (d), 7.52 (d) (8.0) (8.0)	2.61 (s)	2.20 (dd) (7.7, 1.7) [5.06]	5.92 (m) (7.7) [0.98]	6.11 (m) (7.2, 1.7) [0.79]			-195

4d	9.10 (d) (3.1)	7.76 (d), 7.55 (d) (8.0) (8.0)	2.63 (s)	2.32 (dd) (8.1, 2.0) [4.61]	5.68 (dd) (8.1, 1.8) [1.25]	6.31 (d) (8.9) [0.62]	7.91 (d) (8.9) [0.27]	-195
4e	9.10 (d) (3.8)	7.74 (d), 7.55 (d) (7.9) (7.9)	2.62 (s)	2.35 (dd) (9.2, 2.3) [4.62]	5.74 (dd) (9.2, 1.5) [1.23]	6.17 (d) (9.3) [0.80]	8.00 (dd), 8.61 (d) (9.3, 2.4), (2.4) [0.29] [0.22]	-195
4f	9.09 (d) (3.8)	7.60 (d), 7.51 (d) (8.81) (8.81)	2.59 (s)	2.41 (dd) (8.8, 1.7) [4.51]	6.87 (d) (8.8) [1.31]			-199

a Internal standards ^{1}H NMR: TMS, ^{31}P NMR: 80% aqueous H_3PO_4.

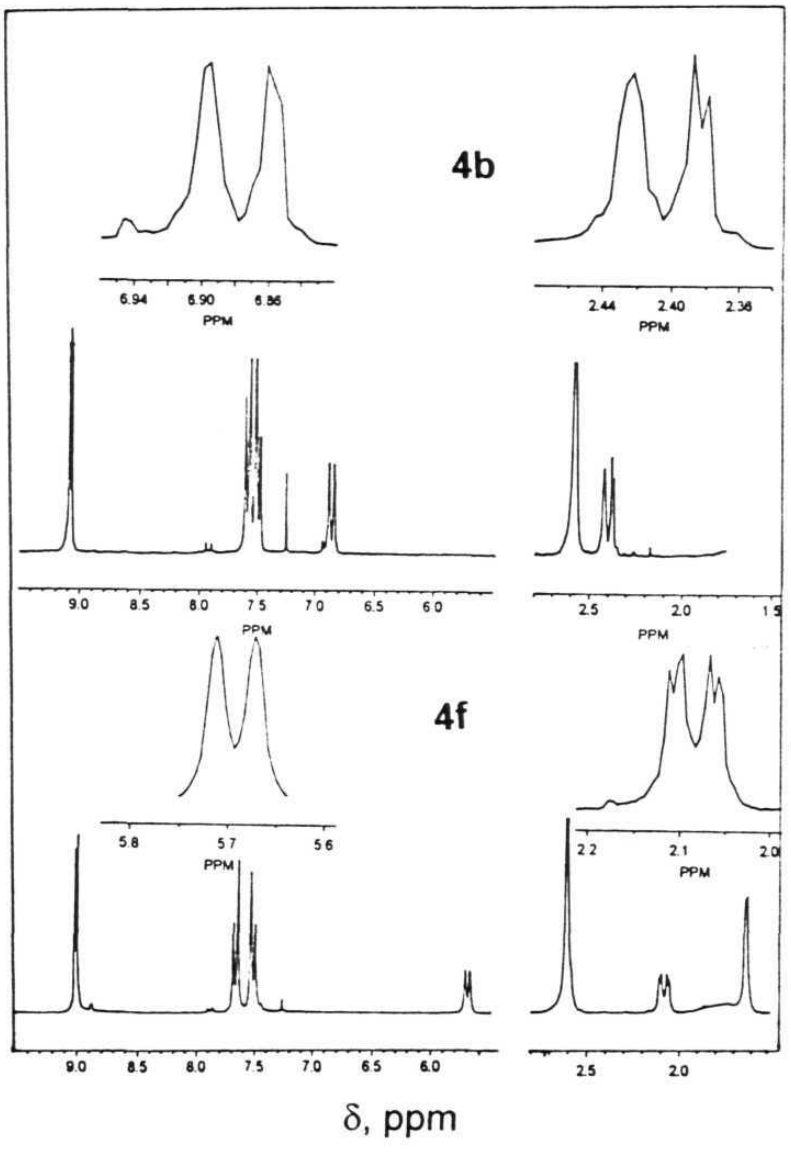

Fig. 4.2. ^{1}H NMR spectra of **4b** and **4f** in $CDCl_3$.

at 6.92 ppm and 8.18 ppm as two doublets, now appear at 2.41 ppm as a doublet of a doublet and at 6.87 ppm as a doublet respectively, when this ligand is bound to **4f**. The change in the chemical shifts ($\Delta\delta$) observed for the *ortho* protons ($\Delta\delta$ = 6.92 - 2.41 = 4.51 ppm) is more than that for the *meta* protons ($\Delta\delta$ = 8.18 - 6.87 = 1.31 ppm). Furthermore, *ortho* protons of the axial ligands resonate as a doublet of a doublet in **4f** due to a three-bond coupling with the adjacent *meta* protons ($^3J_{HH}$ = 8.8 Hz) and a four-bond coupling with the central phosphorus atom ($^4J_{PH}$ = 1.7 Hz).

The data given in Table 4.2 suggests that the remaining aryloxo P(V) porphyrins follow a similar trend in that they all show a doublet β-pyrrolic proton resonance, a pair of doublet resonances due to peripheral *p*-tolyl substituents, and upfield-shifted resonances due to the coordinated axial aryloxo substituents. In each case, resonances due to the peripheral β -pyrrolic protons and ortho protons of the axial ligand both show a four bond coupling with the central phosphorus atom. In a few cases $^5J_{PH}$ and $^7J_{PH}$ coupling constants were also noticed and these values are listed in Table 4.2. Finally, the $\Delta\delta$ values given in Table 4.2 follow a trend that is consistent with the porphyrin ring-current model.[28]

Fig. 4.3 gives the cyclic voltammetric traces obtained for each aryloxo P(V) porphyrin investigated in this study in CH_3CN, 0.1 M TBAP at 293 ± 3 K and Table 4.3 summarizes the redox potential data obtained at both 293±3 and 273±3 K. Except for compounds **4d** and **4e**, which show three reduction peaks, each complex undergoes two stepwise reactions. Wave analysis suggested that most of these electrode proceeses

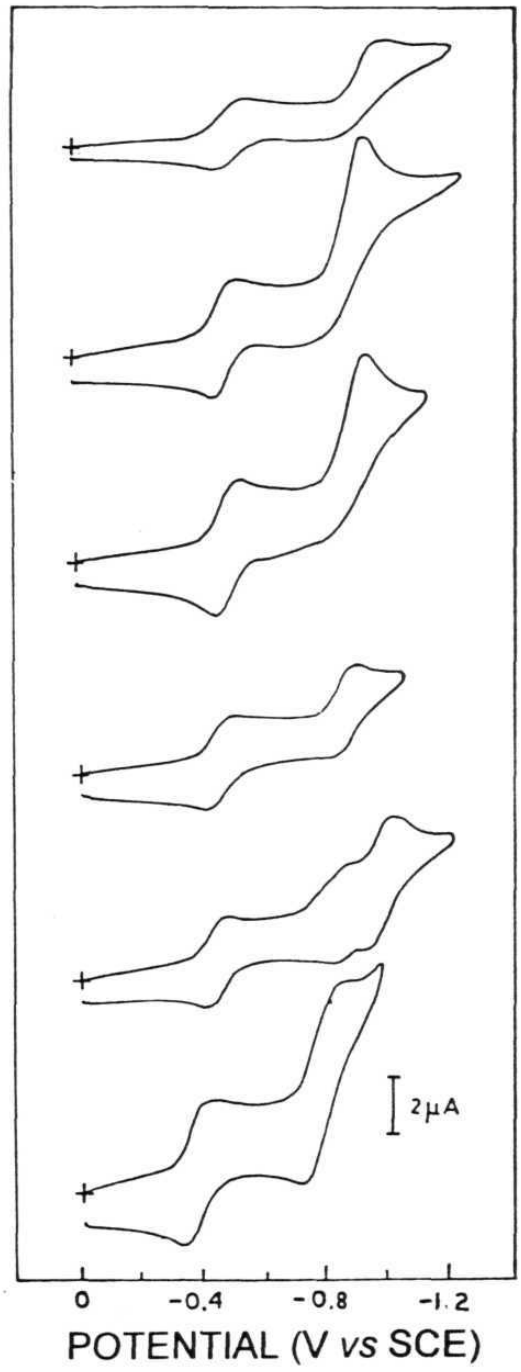

Fig. 4.3. Cyclic voltammograms of (top to bottom) **4a**, **4b**, **4c**, **4d**, **4e** and **4f** in CH_3CN, 0.1M TBAP at 293±3 K (scan rate, 100 mV s^{-1})

Table 4.3 Redox potential data in CH_3CN, 0.1 M TBAP (V *vs* SCE)

Compound	Porphyrin ring					Axial ligand[c]		$E_{CT}(1)$ (eV)	$E_{CT}(2)$ (eV)
	293 K			273 K					
	$-E_{1/2}$ (I)	$-E_{1/2}$ (II)	$\Delta E_{1/2}$	$-E_{1/2}$ (I)	$-E_{1/2}$ (II)	$-E_{1/2}$	$E_{1/2}$[d]		
4a	0.51	1.00[a]	0.49	0.51	0.98[a]		0.92	> 3.1	1.43
4b	0.49	0.94[a]	0.45	0.50	0.95[a]		0.92	> 3.1	1.41
4c	0.48	1.00[a]	0.52	0.49	0.95[a]		1.12	> 3.1	1.60
4d	0.45	0.87	0.42	0.45	0.87	1.28 (1.22) *b*	1.21	> 3.1	1.66
4e	0.44	0.85	0.41	0.43	0.86	0.90 (0.98) *b*	1.35	> 2.7	1.79
4f	0.36	0.77	0.41	0.37	0.77	1.02	1.33	> 2.8	1.69

[a] Irreversible/quasireversible. [b] These values are for the bound aryloxy ligands. [c] Redox potentials are for free phenols. [d] Peak potentials obtained from differential pulse voltammetry.

represent reversible (i_{pc}/i_{pa} = 0.9 - 1.0), diffusion controlled ($i_{pc}/\nu^{1/2}$ = constant in the scan rate (ν) range 50 - 500 mV/s), one-electron transfer (Δ Ep = 60 - 70 mV; ΔEp = 65 ± 3 mV for ferrocene^{+}/ferrocene couple) reactions[29]. On the other hand, the second reduction steps of **4a**, **4b** and **4c** and also the third reduction steps of **4d** and **4e** are found to be either quasi-reversible (E_{pa} - E_{pc} = 90-200 mV and i_{pc}/i_{pc} = 0.2-0.7 in the scan rate (ν) over the range of 100-500 mVs^{-1}) or totally irreversible. On the basis of the redox potential data reported earlier for various P(V) porphyrins of the type $[(por)P(X)_2]^{+}$ (where por = either a meso-tetraaryl porphyrin or the octaethyl porphyrin and X = Cl, OH, $O(Si(CH_3)_3)$ or OCH_3) [5,8,9,17] and also on the basis of the diagnostic criteria developed by Fuhrhop, Kadish and Davis[30] for porphyrin ring reduction ($\Delta E_{1/2}$ (i.e. the difference in potential between the first one-electron and second one-electron addition) = 0.42 ± 0.05 V; where $\Delta E_{1/2}$ = 0.49 - 0.41 V as seen in Table 4.3), the first two reduction waves observed for the hydroxide salts of the aryloxo P(V) porphyrins investigated here can be assigned to two successive, one-electron additions to the porphyrin ring. The third reduction peaks observed for **4d** and **4e** can be assigned to the electron additions to the bound nitroaromatic axial ligands in each case. Interestingly, these observed potentials are found to be close to those of the corresponding free phenolic precursors as shown in Table 4.3.

Scanning the potential in the positive range (0 -1.8 V) for solutions containing these porphyrins gave ill-defined voltammograms with a large background current. However, all of the phenols (Ph-OH)

employed here for the synthesis of **4a-f** could be irreversibly oxidized (E(Ph-OH^{+}/Ph-OH) in CH_3CN, 0.1 M TBAP. These data are summarized in Table 4.3.

A comparison of the electrochemical properties of the aryloxo P(V) porphyrins reported in this study with those of the previously studied P(V) porphyrins is interesting. Whereas compound **2** has been reported to undergo a series of chemical reactions following electron transfer in CH_2Cl_2, 0.1M TBAP at 295 K, the methoxo analogue has been shown to be relatively stable with respect to electroreduction under similar experimental conditions.[17] By comparison, except for the second one-electron reduction peaks of the three complexes mentioned above, electrochemical reduction steps of the aryloxo P(V) complexes reported here are reversible within the voltammetric time-scale in CH_3CN, 0.1 M TBAP at 293 ± 3 K. Low temperature (273 ± 3 K) voltammetric behaviour of these investigated compounds was found be essentially similar to that obtained at the room temperature as can be seen in Table 4.3. Interestingly, as was the case with the previously studied P(V) porphyrins having 'oxo' type ligands (dihydroxo- and dimethoxo phosphorus(V) 5,10,15,20-tetratolyl porphyrins), all of the aryloxo P(V) porphyrins reported here are more difficult ($E_{1/2}$(I) = - 0.36 to - 0.51 V) to reduce than the dichloro complex ($E_{1/2}$(**2**) = - 0.33 V) under the same experimental conditions.[8,9,17] In addition, the reduction potentials of these porphyrins seem to follow a trend that is consistent with the electron donating ability of the axial ligands.[19]

It has been well established that for many different metalloporphyrins $E_{1/2}$(ox) - $E_{1/2}$(red) (i. e. the potential difference between the first ring oxidation and first ring reduction) is in the range of 2.1 - 2.2 V.[31] Aryloxo P(V) porphyrins are also expected to confine to such a rule and, in such a case, the first one-electron oxidation peaks for these porphyrins can occur at potentials more positive than ca. 1.8 V. Similarly, the fact that all of the phenols utilized here for the synthesis of **4a-f** could be oxidized between 0.92 and 1.35 V (see Table 4.3) suggests that peaks due to oxidation of the bound aryloxo ligands can be expected during the positive potential scan for solutions containing these porphyrins. However, as mentioned above, neither the porphyrin ring-oxidation potentials nor the oxidation potentials of the bound aryloxo ligands could be measured under these experimental coditions. Nonetheless, the low ring-reduction potentials and the high ring-oxidation potentials of these aryloxo P(V) porphyrins suggest that it is easier to add an electron to their excited states than to abstract one from them. This is indeed the case as will be shown in the next Section.

4.3.2 Excited state properties:

Each aryloxo P(V) porphyrin investigated in this study shows a two-banded fluorescence spectrum in CH_2Cl_2 (see Fig. 4.4) that is typical of a metallo-porphyrin. The fluorescence quantum yields (ϕ) were estimated using *meso*-5,10,15,20-tetraphenylporphyrinatozinc(II) as the standard.[23] Refractive index corrections have been incorporated while

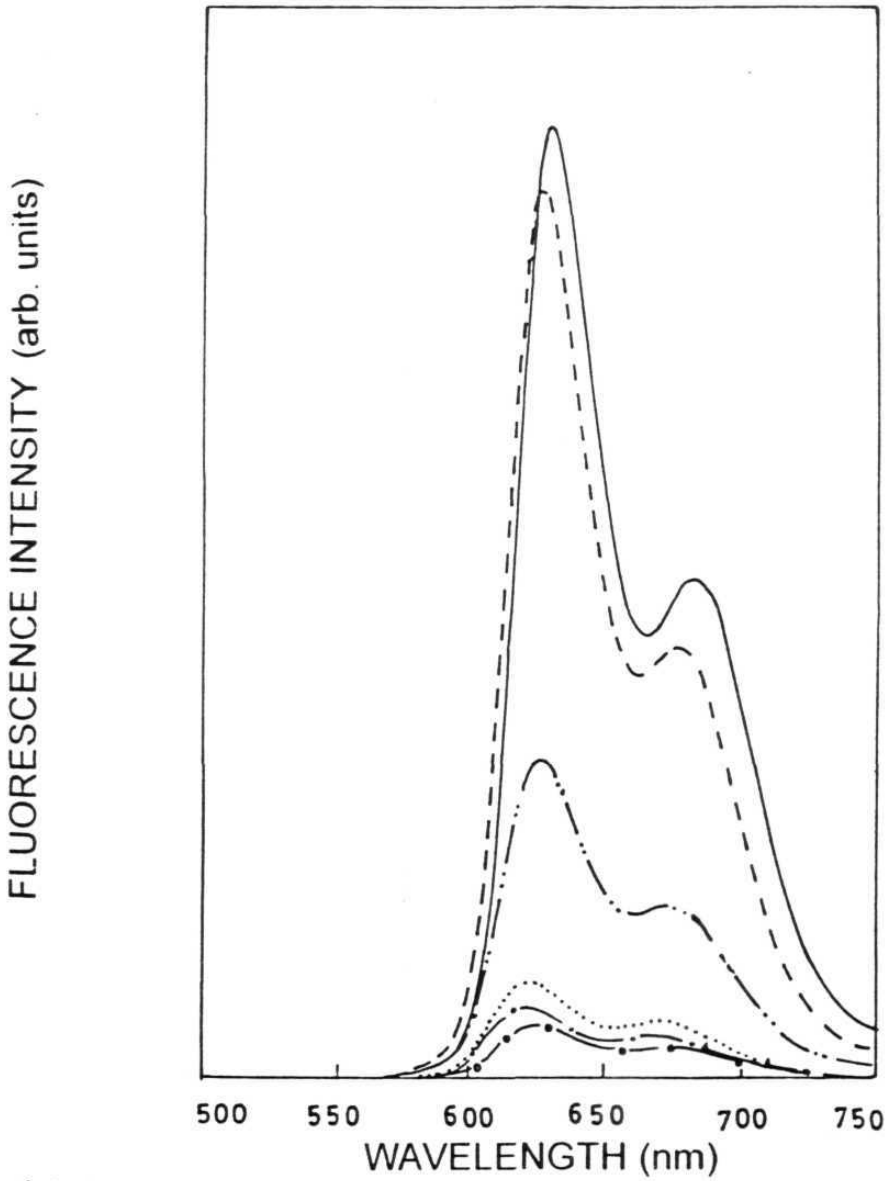

Fig. 4.4. Steady state fluorescence spectra of (bottom to top) **4a** (—•—•—), **4d** (—·—·—), **4b**, (.....), **4e** (—··—··—), **4c** (-----) and **4f**(——) in CH_2Cl_2.

reporting the fluorescence data in various solvents.[23-25] The energies of the singlet states (E^S) and the Stoke's shifts ($\Delta\upsilon$) of these porphyrins (see Table 4.4) are in the same range as the corresponding parameters of **2** (E^S = 2.00 eV, $\Delta\upsilon$ = 0.035 eV). However, the ϕ values of most of these aryloxo derivatives are found to be quite low compared to that of **2** ($\phi \cong$ 0.035). As seen from the data given in Table 4.4, the ϕ values follow a trend with respect to the nature of the axial ligand, as follows: **4f** > **3c** > **4e** > **4b** ≥ **4d** ≈ **4a**. In addition, the solvent polarity also seems to have an influence on the fluorescence properties of these porphyrins, and in general, except for **4f**, the quantum yields follow the order toluene > CH_2Cl_2 > CH_3CN > DMF.

A variety of excited state processes including enhanced internal conversion and intersystem crossing, ion-association, excitation energy transfer (EET), photoinduced electron transfer (PET) etc. can be thought of to be operative in the quenching of fluorescence observed for the aryloxo P(V) porphyrins in various solvents. Obviously, it is not going to be easy to estimate the contribution from each of these excited state processes based only on the steady state fluorescence data. However, an intramolecular EET from the singlet P(V) porphyrin to the appended aryloxo ligand is less likely to occur and hence, the contribution of this process to the overall decrease in the ϕ values is considered to be the minimum for these complexes. Similarly, as shown in Table 4.4, the observed general dependence of ϕ values on the electron donating/withdrawing ability of the axial ligand and also on the solvent

Table 4.4 Fluorescence data in various solvents.

Compound	λ_{max}, (nm) ϕ				Stokes shift	
	toluene	CH_2Cl_2	CH_3CN	DMSO	$\Delta\upsilon$ (eV)	E^S (eV)
4a	618, 667	619, 669	618, 667	620, 668	0.052	2.016
	0.004	0.002	0.003	0.001		
4b	618, 668	623, 669	619, 669	620, 670	0.052	2.016
	0.010	0.004	0.005	0.003		
4c	627, 670	627, 667	626, 674	631, 678	0.058	2.008
	0.027	0.037	0.025	0.021		
4d	622, 667	626, 672	623, 669	628, 670	0.049	2.005
	0.003	0.003	0.002	0.001		
4e	619, 670	624, 672	621, 670	623, 670	0.050	2.000
	0.025	0.013	0.012	0.006		
4f	633, 683	630, 682	630, 680	634, 684	0.058	1.999
	0.033	0.040	0.030	0.028		

polarity indicate that it is difficult to rationalize these trends solely on the basis of differences in the rates of internal conversion and intersystem crossing reactions of the aryloxo porphyrins among themselves and also in relation to the dichloro analogue. Ion-association is another phenomenon that is imminent in these charged species and, the extent of this process is expected to be dependent on the solvent properties and also on the structure of the fluorophore. Currently, there exists no direct or indirect evidence/s to show the correspondence between the trends observed for the ϕ values and the extent of ion-association in these complexes. Finally, as far as the PET-based mechanisms are concerned, two types of reactions can be envisaged here (equns 1 and 2).

$$P(V)^{*} -- OR \text{ ------> } P(V)^{+} -- OR^{-} \quad ..(4.1)$$

$$P(V)^{*} -- OR \text{ ------> } P(V)^{-} -- (OR)^{+} \quad ..(4.2)$$

In the above equations, P(V)* - OR represents singlet excited state of the aryloxo P(V) porphyrins, $P(V)^{+}$ - OR^{-} and $P(V)^{-}$ - OR^{+}, the charge separated species where, P(V)* - OR represents the singlet state of the aryloxo P(V) porphyrins and, $P(V)^{+}$ - OR^{-} and $P(V)^{-}$ - OR^{+} represent the charge separated species. Note that the positive charge present on the P(V) porphyrin has been omitted for clarity in the presentation of these equations. Thus, $P(V)^{+}$-$(OR)^{-}$ represent a porphyrin "dication radical" and an anion radical of the aryloxo ligand. Similarly, $P(V)^{-}$ - $(OR)^{+}$ represents

a "neutral" porphyrin radical species and a cation radical of the aryloxo ligand.

Calculations based on the available redox potential data of these systems suggest that while, the energies of the charge transfer states corresponding to $P(V)^+ - OR^-$ (i. e. $E_{P(V)^+ - OR^-}$) are all more positive than at least ca. 2.7 eV, those of the $P(V)^- - OR^+$ states (i. e. $E_{P(V)^- - OR^+}$) range between 1.79 and 1.41 eV as shown in Table 4.4. Note here that

$$E_{P(V)^+ - OR^-} = E(P(V)^+/P(V)) - E(Ph\text{-}OH/Ph\text{-}OH^-) \quad (4.3)$$

and

$$E_{P(V)^- - OR^+} = (E(Ph\text{-}OH^+/Ph\text{-}OH)) - E(P(V)/P(V)^-) \quad (4.4)$$

where, $E(P(V)^+/P(V))$ and $E(P(V)/E(P(V)^-)$ are the ring oxidation and ring reduction potentials of the P(V) porphyrin, $E(Ph\text{-}OH^+/Ph\text{-}OH)$ and $E(Ph\text{-}OH/Ph\text{-}OH^-)$ are the oxidation and reduction potentials of the phenolic precursors, respectively. $E(P(V)/P(V)^-)$ and $E(Ph\text{-}OH^+/Ph\text{-}OH)$ for all the porphyrins and $E(Ph\text{-}OH/Ph\text{-}OH^-)$ for **4e** $[(TpTP)P(O\text{-}p\text{-}C_6H_4\text{-}O\text{-}o,p\text{-}C_6H_3(NO_2)_2)_2]^+$, **4d** $[(TpTP)P(O\text{-}p\text{-}C_6H_4\text{-}O\text{-}p\text{-}C_6H_4NO_2)_2]^+$ and **4f** $[(TpTP)P(O\text{-}p\text{-}C_6H_4NO_2)_2]^+$ are taken from Table 4.3. $E(Ph\text{-}OH/Ph\text{-}OH^-)$ values for rest of the porphyrins are expected to be more negative than those observed for these two complexes. As discussed earlier, $E(P(V)^+/P(V))$ values are more positive than at least 1. 8 V. It should be noted here that the energies of the charge transfer states estimated here are

only 'apparent' values. This is because we have employed oxidation potentials of the precursor 'free' phenols and not those of the bound aryloxo ligands in the calculation and, in addition, nor are the oxidation potentials of the P(V) porphyrins known with certainty

Interestingly, as observed in Table 4.4, the $P(V)^{+}$ - OR^{-} state of each complex lies above the E^{S} (=2.008 ± 0.008 eV) of the P(V) porphyrin and thus, an electron transfer from the singlet porphyrin to the axially bound aryloxo subunit is not possible on the thermodynamic grounds for these systems. On the other hand, the $E_{P(V)^{-}}$ - OR^{+} values are all less positive than the E^{S} suggesting that charge transfer from the axial aryloxo subunits to the P(V) porphyrin is thermodynamically favourable in each case. Relaxation of the singlet state to this thermodynamically accessible charge transfer state can, in principle, rationalize the observed fluorescence quenching of the porphyrin chromophore in these compounds. Consistent with this analysis is the fact that the fluorescence due to **4a** and **4b** (which possess electron donating methyl groups) are quenched much more than that due to **4f** and **4e** (which possess electron accepting nitro groups). The observed decrease of ϕ values with increasing polarity of the solvent is also consistent with the participation of a charge transfer state in the excited state deactivation for these compounds.[19,23-25]. In this regard, it can be noted here that recent fluorescence studies which include those on a series of 'wheel-and-axle' type dimeric and oligomeric P(V) porphyrins,[18,19] on bis-axially ligated 'oligothiophenoxy' derivatives of P(V) porphyrins[13] and on P(V)

porphyrin-based, aryloxo-ligand bridged, hybrid porphyrin trimers[20,21] all have indicated that relaxation of the singlet excited states of these complexes involves significant contribution from the charge transfer states. Despite these, we note that it is not generally correct to consider exclusively a PET-based mechanism relying only on the thermodynamic criteria and the solvent dependence of the ϕ values. Thus, it is reasonable to expect that contribution from a PET-based mechanism is the maximum for a compound having a highly electron donating axial ligand and it is the minimum for a compound having a highly electron withdrawing axial ligand in this series of P(V) porphyrins.

4.4 Summary

In summary, six aryloxo derivatives of phosphorus(V) porphyrins of the type $[(TpTP)P(OR)_2]^+$ where TpTP is the dianion of *meso*-5,10,15,20 tetratolylporphyrin and OR is an axial aryloxo (2,4-dimethylphenoxy (**4a**), 4-methylphenoxy (**4b**), phenoxy (**4c**), 4-(4-nitrophenoxy)phenoxy (**4d**), 4-(2,4-dinitrophenoxy)phenoxy (**4e**), or 4-nitrophenoxy (**4f**)) ligand have been synthesized and fully characterized by FAB-mass, UV-vis, fluorescence, infrared, and nuclear magnetic resonance (^1H and ^{31}P) spectroscopies and cyclic voltammetric methods. Each porphyrin shows a typical "normal UV-vis absorption spectrum" indicating the presence of a P(V) ion in the porphyrin cavity. The proton-decoupled ^{31}P NMR signal observed for these compounds, between - 194 and - 200 ppm, suggests that there exists an octahedral coordination

around the phosphorus atom, and this supposition is further substantiated by the porphyrin ring-current-inducedupfield shifts observed for protons on the two axial aryloxo ligands in the ^{1}H NMR spectra. Cyclic voltammetric studied reveal that each porphyrin undergoes two successive one-electron reductions with the site of electron transfer being the porphyrin ring. The fluorescence quantum yield values of these porphyrins are found to be sensitive to the nature of the aryloxo ligand and also to the solvent polarity. The singlet state properties of these systems have been discussed in light of both the fluorescence and the redox potential data. Thermodynamic considerations based on the electrochemical and fluorescence data indicate that a charge transfer state of the type $P(V)^{-}$ - OR^{+} can participate in the excited state deactivation of these compounds.

4.5 References

1. Sayer, P.; Gouterman, M.; Connell, C. R. *J. Am. Chem. Soc.* **1977**, 99, 1082.
2. Carrano, C. J.; Tsutsui, M. *J. Coord. Chem.* **1977**, 7, 79.
3. Gouterman, M.; Sayer, P.; Shankland, E.; Smith, J. P. *Inorg. Chem.* **1981**, 20, 87.
4. Sayer, P.; Gouterman, M.; Connell, C. R. *Acc. Chem. Res.* **1982**, 15, 73.

5. Marrese, C. A.; Carrano, C. J. *J. Chem. Soc. Chem. Commun.* **1982**, 1279.

6. Mangani, S.; Meyer, E. F.; Cullen, D. L.; Tsutsui, M; Carrano, C. J. *Inorg. Chem.* **1983**, 22, 400.

7. Harriman, A. *J. Photochem.* **1983**, 23, 37.

8. Marrese, C. A.; Carrano, C. J. *Inorg. Chem.* **1983**, 22, 1858.

9. Marrese, C. A.; Carrano, C. J. *Inorg. Chem.* **1984**, 23, 3961.

10. Pandian, R. P.; Chandrashekar, T. K.; Chandrasekhar, V. *Ind. J. Chem.* **1991**, 30A, 579.

11. Barbour, T.; Belcher, W. J.; Brothers, P. J.; Rickard, C. E. F.; Ware, D. C. *Inorg. Chem.* **1992**, 31, 746.

12. Segawa, H.; Kazuhiko, K.; Nakamoto, A.; Shimidzu, T. *J. Chem. Soc,. Perkin Trans.* **1992**, 939.

13. Segawa, H.; Nakayama, N.; Shimidzu, T. *J. Chem. Soc,. Chem. Commun.* **1992**, 784.

14. Kunimoto, K.; Segawa, H. Shimidzu, T. *Tetrahedron Lett.* **1992**, 33, 6327.

15. Lin, Y.-H.; Lin, C.-C.; Chen, J.-H.; Zeng, W.-F.; Wang, S.-S. *Polyhedron*, **1994**, 13, 2887.

16. Lin, Y.-H.; Sheu, M.-T.; Lin, C.-C.; Chen, J.-H.; Wang, S.-S. *Polyhedron*, **1994**, 13, 3091.

17. Liu, Y. H.; Benassy, M. -F.; Chojnacki, S.; D'Souza, F.; Barbour, T.; Belcher, J. W.; Brothers, P. J.; Kadish, K. M. *Inorg. Chem.* **1994**, 33, 4480.

18. (a) Segawa, H.; Kunimoto, K.; Susumu, K.; Taniguchi, M.; Shimidzu, T. *J. Am. Chem. Soc.* **1994**, 116, 11193 (b) Susumu, K.; Kunimoto, K.; Segawa, H.; Shimaizu, T. J. *J. Phys. Chem.* **1995**, 99, 29.

19. Susumu, K.; Kunimoto, K.; Segawa, H.; Shimidzu, T. *J. Phys. Chem.* **1995**, 99, 29.

20. Rao, T. A.; Maiya, B. G. *J. Chem. Soc., Chem. Commun.* **1995**, 939.

21. Susumu, K.; Segawa, H.; Shimidzu, T. *Chemistry Lett.* **1995**, 929

22. Fuhrhop, J. H.; Smith, K. M. In *Porphyrins and Metalloporphyrins*; Smith, K. M., Ed.; Elsevier : Amsterdam, 1975; p 769.

23. Sirish, M.; Maiya, B. G. *J. Photochem. Photobiol. (A)* **1994**, 77, 189.

24. Rao, T. A.; Maiya, B. G. *Polyhedron* **1994**, 12, 1863.

25. Sirish, M.; Maiya, B. G. *J. Photochem. Photobiol. (A)* **1995**, 85, 127.

26. Guilard, R.; Lecomte, C.; Kadish, K. M. *Structure and Bonding* **1987**, 64, 205.

27. *Multinuclear NMR*; Mason, J; Ed.; Plenum Press: New York, 1987; p.369.

28. Abraham, R. J.; Bedford, G. R.; McNeillie, D.; Wright, B. *Org. Magn. Reson.* **1980**, 14, 418.

29. Nicholson, R. S.; Shain, I. *Anal. Chem.* **1964**, 36, 706.

30. Fuhrhop, J. H.; Kadish, K. M.; Davis, D. G. *J. Am. Chem. Soc.* **1973**, 95, 5140.

31. Kadish, K. M. Prog. *Inorg. Chem.* **1986**, 435.

CHAPTER 5

Axial-Bonding Type', Vertically-Linked Hybrid Porphyrin Arrays: Design, Synthesis and Modulation of Redox and Photophysical Properties

5.1 Introduction

This chapter deals with the design, synthesis, spectral characterization, electrochemistry and photochemical properties of mainly a series of hybrid-porphyrin trimers in which a phosphorus(V) 'basal' porphyrin has been axially ligated, *via* aryloxy bridges, by free-base-, vanadyl(IV) (VO(IV)), cobalt(II) (Co(II)), nickel(II) (Ni(II)), copper(II) Cu(II)), zinc(II) (Zn(II)) or phosphorus(V) (P(V)) porphyrins. It also deals with similar studies carried out on a homologous hybrid hepatameric array.

Photochemically-active molecular arrays comprising of porphyrin or other structurally related macrocyclic systems are currently being investigated in connection with their ability to transport charge, ion or energy. Specifically, porphyrin oligomers have been employed as components of supramolecular structures in studies related to molecular catalysis, molecular electronics, biomimetic photosynthesis *etc.*[1,2] Although a great variety of homologous porphyrin arrays have been reported so far, relatively less attention seems to have been paid towards

the construction of functionally active, hybrid-type systems. Moreover, majority of the hither-to reported porphyrin arrays (hybrid or otherwise) have been obtained *via* multi-step and often, cumbersome organic reaction sequences carried out at the porphyrin peripheral position/s (i. e. β-pyrrole or *meso*).[1,2] On the other hand, utilization of 'inorganic' reactions, which can be readily conducted either at the porphyrin central cavity (*ca.* metal/non-metal ion insertion) or on the resident metal/metalloid ion therein (*ca.* metal-metal interaction, metal-ligand coordination, covalent bond formation etc.), appears to be an attractive and a viable alternative for the facile construction of hybrid-type multiporphyrin arrays. This is indeed the case as will be shown in this chapter.

During the course of investigations on the donor-acceptor type, hexa-coordinated, bis-(aryloxo)phosphorus(V) (P(V)) porphyrins described in the previous chapter, it was realized that the inherent simplicity and the flexibility of this new, 'axial-bonding' approach can be conveniently employed for the design and synthesis of elaborate, hybrid-type, porphyrin arrays having diverse structures and functions. For example, it should be possible to utilize P(V) porphyrin as the basal scaffolding unit and free-base-, metallo- or metalloid-porphyrins as the axial donor/acceptor subunits for the fabrication of arrays with varying spectral, redox and photophysical properties. It should also be possible to extend this 'building-block' approach and construct higher, branched-chain oligomers. Continued research efforts in these directions showed that the above concepts are readily achievable. The present chapter reports

on the design, synthesis and modulation of the photochemical functions of a series of P(V) porphyrin-based, 'axial-bonding' type hybrid trimers and a 'branched-chain', heptameric array, (Figs.5. 1 and 5. 2).

There have been a few studies carried out earlier on the axially-substituted porphyrin arrays. For example, axial-bonding type, homologous porphyrin oligomers have been known in the literature but, many of them were obtained only as solid-state polymers.[3] Similarly, strategies involving metal-ligand coordination and covalent bond formation reactions at the porphyrin central metal/metalloid ion have been employed to prepare mostly homologous porphyrins arrays.[2,4] In addition, metal-complex-interspersed porphyrin arrays such as, for example, entwined porphyrin conjugates [1b] are well-known in the literature but, these fall outside the theme of the present study. More relevant reports that fit into the theme of the present study are those on novel axial-bonding 'wheel-and-axle' type porphyrin arrays reported by Shimidzu and co-workers but, even these soluble oligomers are composed of only one type of porphyrin in their arrays.[5] Nonetheless, 'axial-bonding' type, hybrid porphyrin oligomers have been synthesized recently and, they are limited to Ru(II)-free-base and P(V)-free-base trimers.[6]

5.2 Experimental details

5,10,15,20-tetratolylporphyrinatodichlorophosphorus(V)hydroxide **(1)** was synthesized as described in Chapter 4, Section 4.2.2.

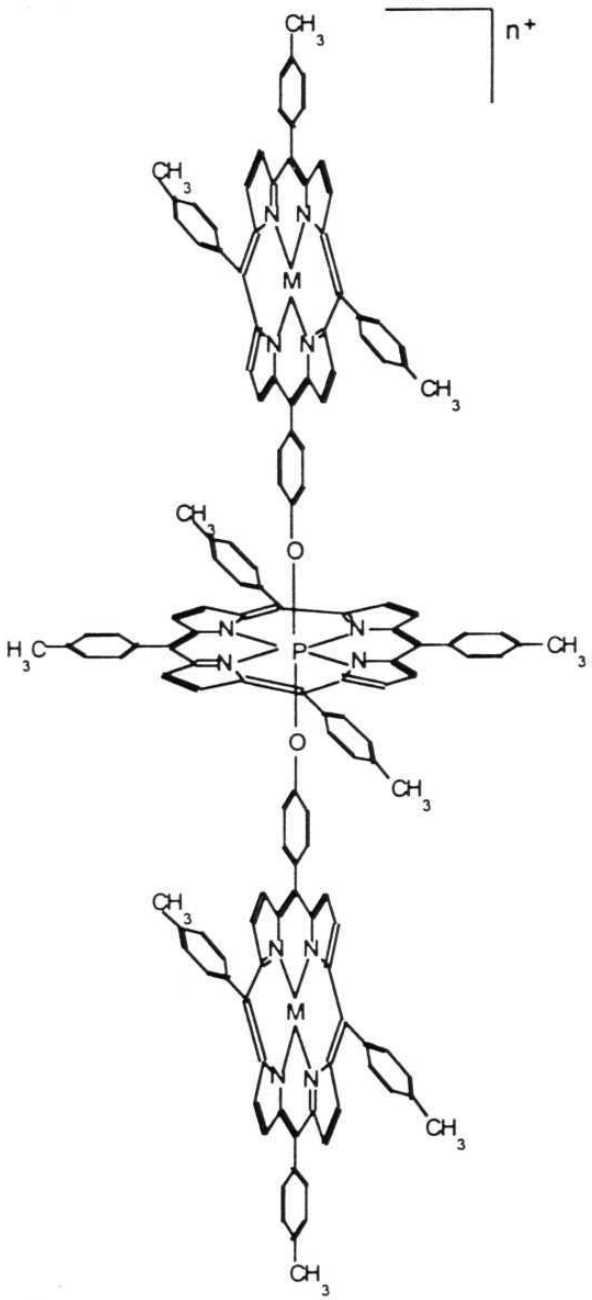

M = 2H (3a), VO(IV) (3b), Co(II) (3c), Ni(II) (3d), Cu(II) (3e), Zn(II) (3f), or P(V)Cl2 (3g)

n = 1 or 3

Fig. 5.1. Structures of trimers **3a-g**.

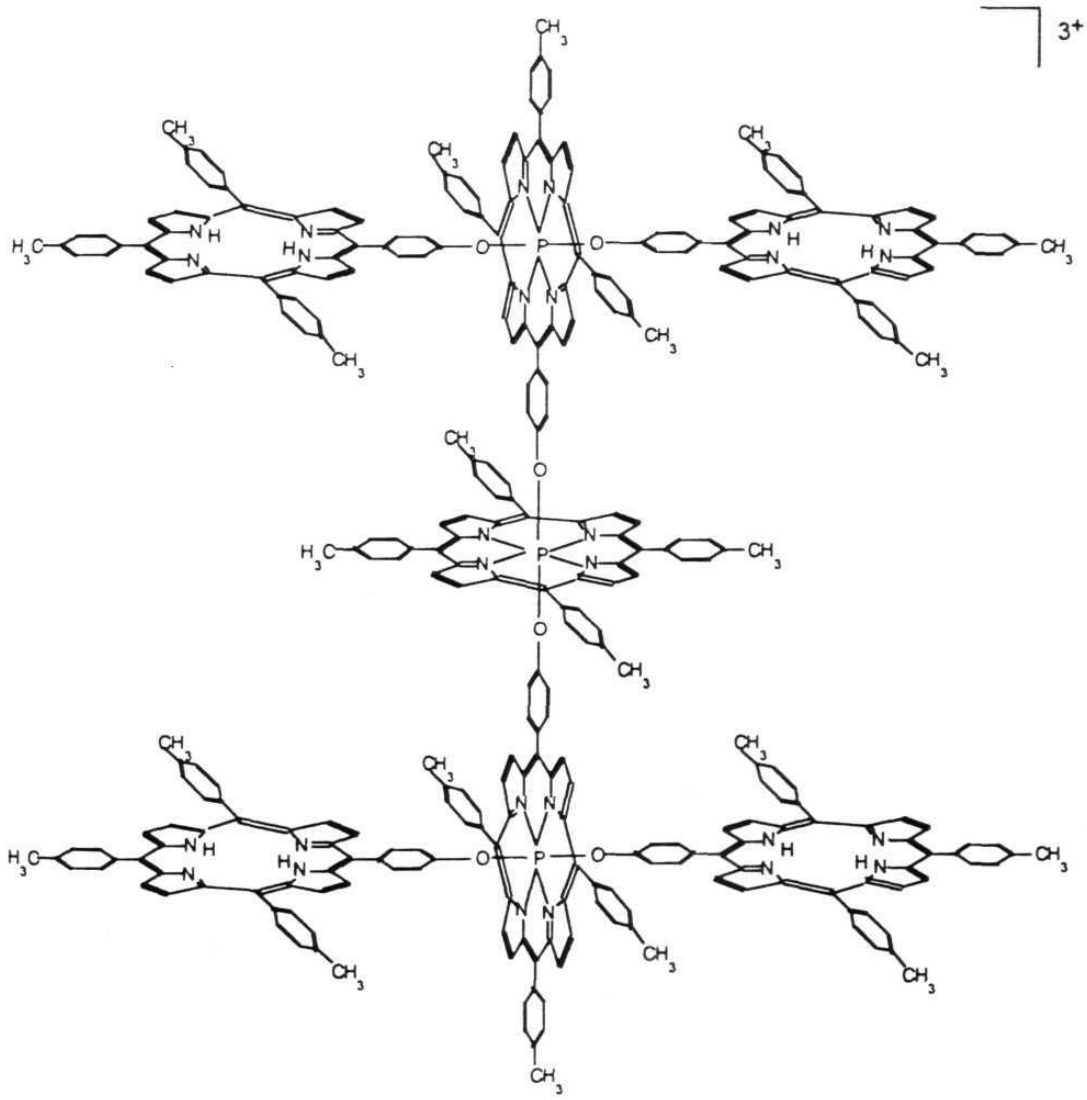

Fig. 5.2. Structure of the heptamer **4**.

5.2.1 Synthesis of 5-(4-hydroxyphenyl),10,15,20-tritolyl porphyrin 2

6.1 g (50 mM) of 4-hydroxybenzaldehyde in 350 ml of propanoic acid was stirred at 120 °C for 30 min.. To the resulting solution, 12 g (100 mM) of *p*-tolualdehyde followed by 10.5 g (157 mM) of pyrrole were added. The mixture was refluxed for 45 minutes, left overnight at 10 °C and then filtered. The black-violet residue was washed several times with hot water, followed by methanol and purified by chromatography on a basic alumina column. Elution with chloroform gave 5,10,15,20-tetratolyl porphyrin. Elution with $CHCl_3$ - CH_3OH (97:3, V/V) gave the desired product **2** in ~ 30% yield.

5.2.2 Synthesis of '(free-base porphyrin)$_2$ - P(V) porphyrin' trimer 3a

This compound was prepared as illustrated in Scheme 5.1. 100 mg (0.13 mM) of 5,10,15,20-tetratolylporphyrinato dichlorophosphorus(V) hydroxide (**1**) was taken in 25 ml of dry pyridine. 400 mg (0.59 mM) of 5-(4-hydroxyphenyl),10,15,20-tritolyl porphyrin **2** was added and the mixture refluxed under nitrogen for 5 h. The solvent was evaporated and the resultant brown residue was loaded onto a silica gel column. The desired product, **3a**, was eluted out with $CHCl_3$-CH_3OH (9:1, V/V) after which it was recrystallized using a mixture of $CHCl_3$ and hexanes. Yield: 50%.

5.2.3 Synthesis of '(metallo/metalloid porphyrin)$_2$ - P(V) porphyrin' trimers 3b-g

Compounds **3b-g** were prepared by insertion of the appropriate metal/metalloid ion into the free-base units of **3a** (Scheme 5.1). Refluxing 10 mg (4.9 x 10^{-3} mM) of **3a** in 20 ml chloroform with 15 mg of the corresponding metal acetate in 5 ml CH_3OH for 30 minutes gave the compounds **3c-f**. A 0.5 ml acetic acid was also added to the reaction mixture in the case of metallation with copper(II). The solvents were evaporated, and purified in the same manner as described above for **3a**. Insertion of VO(IV) into the axial porphyrins was achieved by mixing 15 mg (7.3 x 10^{-3} mM) of **3a** and 15 mg (9 x 10^{-2} mM) of vanadylacetylacetonate in 5 ml of phenol and refluxing for 30 minutes. The phenol was removed under reduced pressure and the crude product **3b** was purified as described above for **3a**. **3g** was obtained by the reaction of **3a** with $POCl_3$ by adopting the same procedure as described for the synthesis of compound **2** in Chapter 4.

While trimers **3a-f** were obtained in almost quantitative yields, the 'all-phosphorus' array **3g** was obtained in 40% yield. Each new trimer was recrystallized using a mixture of $CHCl_3$ and hexanes before use.

5.2.4 Synthesis of the '(free-base porphyrin)$_4$ - (P(V) porphyrin)$_3$' heptamer 4

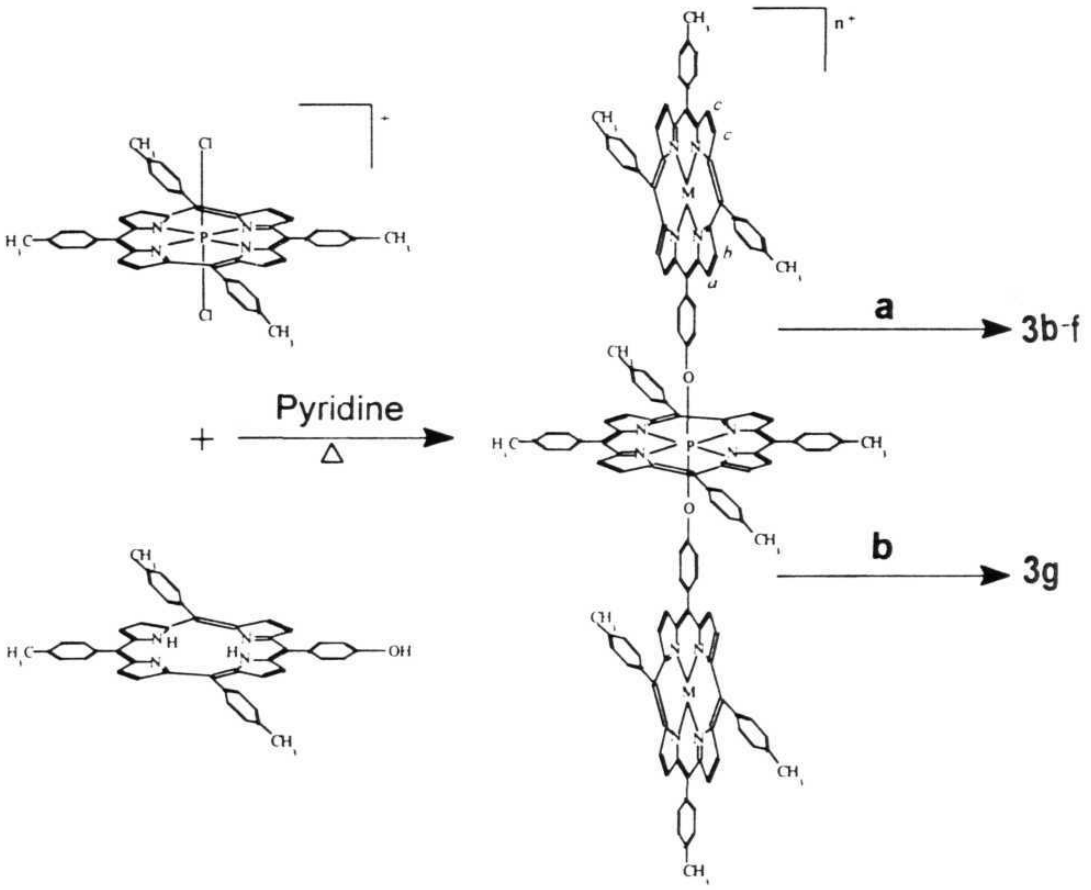

M = 2H (**3a**), VO(IV) (**3b**), Co(II) (**3c**), Ni(II) (**3d**), Cu(II) (**3e**) Zn(II) (**3f**) or P(V)Cl2 (**3g**), n = 1 or 3

a M-acetate/ VO(acac) $CHCl_3/CH_3OH$

b $POCl_3$ Pyridine Δ

Scheme 5.1

Synthesis of this heptamer was achieved by following a method similar to that adopted for the synthesis of **3a** (Scheme 5.2). To a solution of 25 mg (1.1 x 10^{-2} mM) of **3g** in 10 ml of dry pyridine, 150 mg (0.3 mM) of **2** was added and the mixture was refluxed under nitrogen for 5h. The solvent was evaporated and the residue loaded onto a silica gel column. Elution with $CHCl_3$ - CH_3OH (9:1, V/V) gave **4**. The compound was recrystallized using a mixture of $CHCl_3$ and hexanes. Yield: 30%.

5.3 Results and discussion

The new 'axial-bonding' type hybrid porphyrin arrays could be easily prepared in good-to-moderate yields by utilizing the axial bonding capability of the P(V) porphyrin. As seen in the previous chapter and also by the work of Brothers and co-workers[7], the axial halide ligands on the P(V) porphyrin can be easily replaced by the aryloxide species.

5.3.1 Ground state properties

The FAB- mass spectrum of **3a** (Fig. 5.3) shows a minor peak at *m/z* 2058 ascribable to $[M + OH]^+$ ($M = C_{142}H_{106}N_{12}O_2P$) thus confirming the presence of OH^- as the counter anion. The major molecular ion peak for this trimer appears at *m/z* = 2042. The major peak at 2045 (M + 3H) observed in the FAB - mass spectrum of **4** is ascribable to the trimer fragments ((free-base porphyrin)$_2$- P(V) porphyrin type) derived from symmetric bond scissions at the P-O linkages of the central porphyrin. Another peak seen for this compound at *m/z* = 2108 might be taken as an

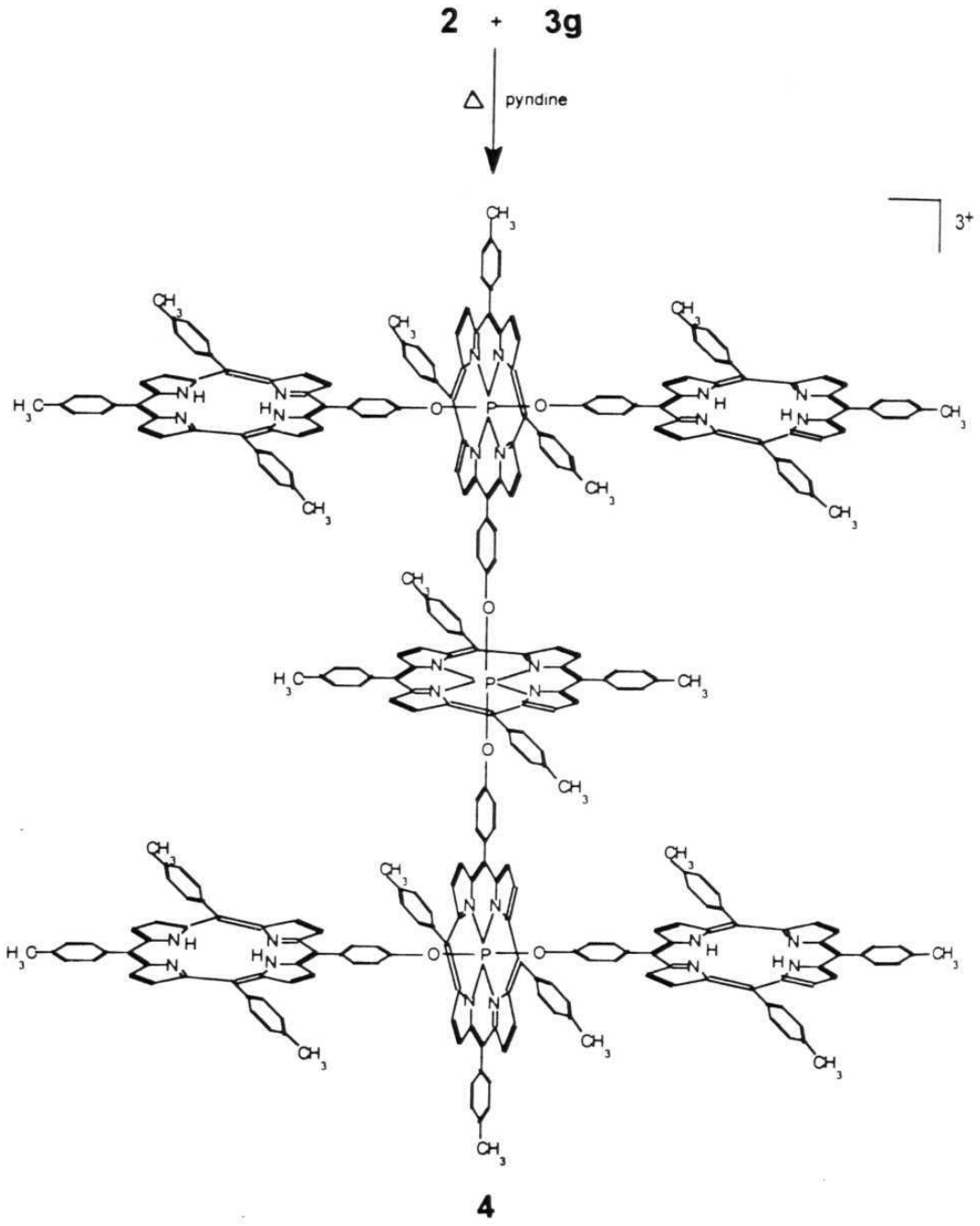

Scheme 5.2

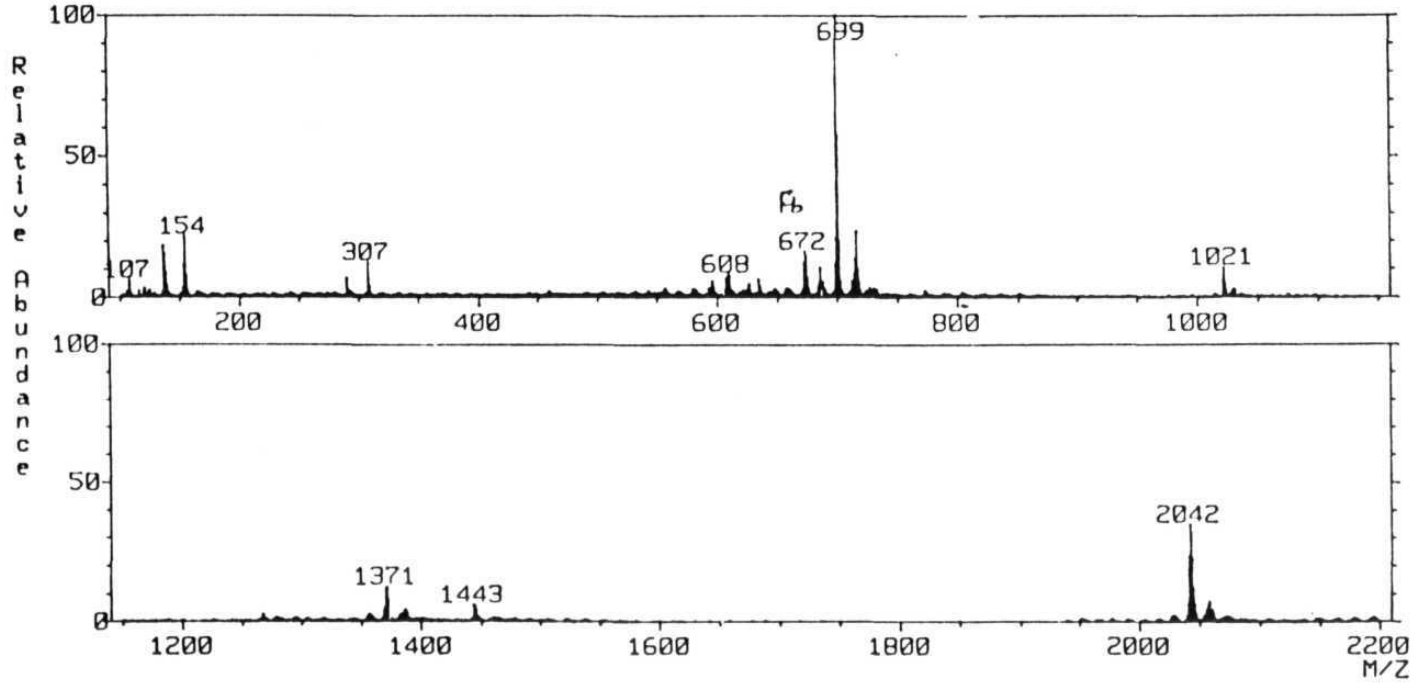

Fig. 5.3. FAB Mass spectrum of **3a**.

evidence for the presence of the "all-phosphorus" trimer fragment. A major fragment appearing at *m/z*= 1371 matches the P(V) porphyrin-free-base porphyrin dimeric unit (M + H). The base peak appears at *m/z* = 701 in each array and corresponds to the P(V) porphyrin monomeric unit.[7]

The wavelengths of maximum absorbance (λ_{max}) and molar extinction coefficient (ε) values of the trimers and the heptamer synthesized in this study are presented in Table 5.1. Fig. 5.4 shows the UV-vis spectra of **3a** and **3d**. These data reveal that the spectrum of each trimer is more or less similar to the spectrum resulting from a combination (1:2 mole/mole ratio of P(V) porphyrin and free-base/metalloporphyrin) of the corresponding individual precursors. The spectra of compounds **3a-f** and **4** exhibit two partially overlapping Soret bands; the more intense band (414-426 nm) corresponds to the axial porphyrin units and the less intense one (436-445 nm) to the central P(V) porphyrin. The *Q*- band region of the spectrum of each trimer also shows features similar to those of the precursors. For example, the spectral features of trimer **3g**, in which all the three units are phosphorus porphyrins, seem to be more or less identical to those of the spectrum of **1**. This spectrum consists of a single Soret band at 444 nm and two *Q*-bands at 571- and 617 nm. The ε values of the bands due to each trimer are also close to a simple addition of the ε values of the respective bands due to precursor porphyrins.

While the λ_{max} values of the heptamer **4** were found to be in the same range as those due to the trimer **3a**, the corresponding ε values were

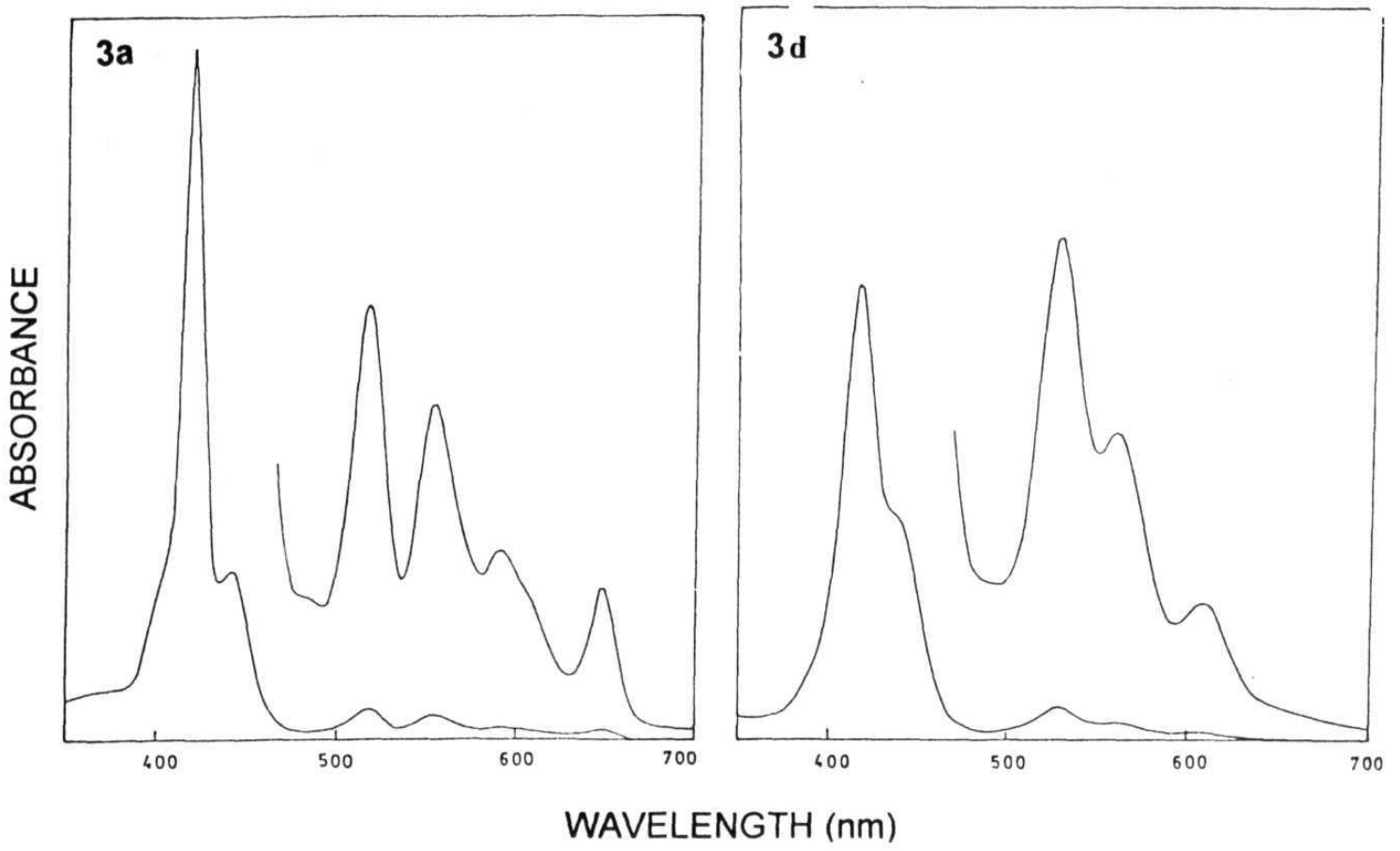

Fig. 5.4 UV-vis. spectra of **3a** and **3d** in CH_2Cl_2.

Table 5.1 UV-vis data in CH_2Cl_2

Compound	λ_{max}, nm (log ε)					
	Q-bands				*B*-band(s)	
1	617		571		443	
	(4.01)		(4.14)		(5.46)	
2	650	592	551	516		418
	(3.76)	(3.64)	(3.90)	(4.17)		(5.30)
3a	648	592	555	517	441	420
	(4.00)	(4.16)	(4.40)	(4.49)	(5.40)	(6.02)
3b		609	552		443	426
		(4.06)	(4.54)		(5.47)	(5.75)
3c		607	562	529	436	414
		(4.05)	(4.40)	(4.37)	(5.52)	(5.34)
3d		609	561	528	438	416
		(3.94)	(4.29)	(4.50)	(5.32)	(5.63)
3e		608	567	540	440	416
		(3.92)	(4.27)	(4.58)	(5.28)	(5.84)
3f	611	587	551		445	421
	(3.99)	(4.20)	(4.62)		(5.13)	(5.76)
3g	618		571		445	
	(4.42)		(4.56)		(5.85)	
4	648	591	555	517	440	420
	(4.46)	(4.59)	(4.81)	(4.91)	(5.79)	(6.26)

different as expected. For example, the ratio (ε_{420} /ε_{440}) **4**/(ε_{420} /ε_{440}) **3a** = 0.70 as estimated from the UV-vis spectra (see Fig. 5.5) and, this value is close to that expected (i.e. 4/3/2/1= 0.67) for these arrays in the absence of any inter-chromophoric interaction.

All of the above features seen in the UV-vis spectra of these hybrid arrays, while establishing, to a certain extent, their structural integrities, reflect a lack of any exciton coupling interactions between the individual porphyrin units.[8] In molecular arrays of the type investigated here, exciton coupling is known to occur when there is complete delocalization of excitation over the entire super-molecule and excitation of any particular component of the molecule is not possible. For example, in the case of a homo-dimer, the excitation is distributed over both the molecules. and the resulting exciton splitting is manifested in a much narrower spectrum compared to that of the monomer. An illustration refers to exciton coupling studies on porphyrin dimer and trimer by Tran-Thi *et al.*[9a] They have observed blue shifted Soret bands and red-shifted Q-bands of the porphyrin arrays with respect to the corresponding monomer. This behaviour has been found to be typical of "face-to-face" compounds as predicted by the molecular exciton theory and has been applied to a number of porphyrin systems including the 'wheel-and-axle' porphyrins mentioned above.[5, 9] Such a behaviour is obviously absent in the trimers and the heptamer investigated in this study indicating the absence of any exciton coupling.

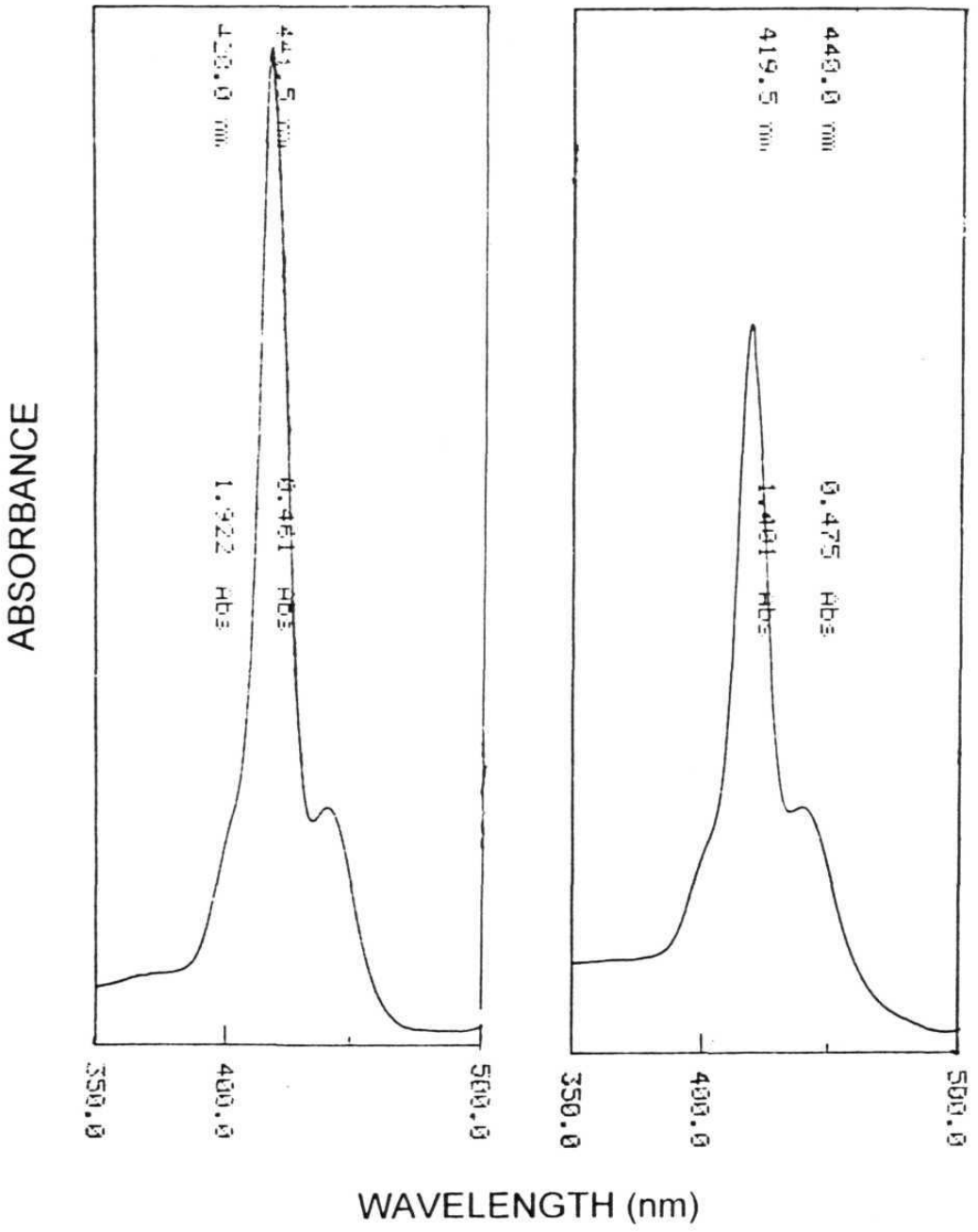

Fig. 5.5. UV-visible spectra of **3a** and **4** in the Soret band region.

^{1}H NMR data of the diamagnetic arrays **3a**, **3d**, **3f**, **3g** and **4** are summarized in Table 5.2. Representative spectra of **3a** and **3g** are shown in Fig. 5.6.

In each trimer, the pyrrole-β protons of the central phosphorus porphyrin unit are seen to resonate (9.18-9.34 ppm) as a doublet due to a four-bond coupling with the phosphorus atom. This observation is consistent with that reported earlier for various alkoxo and aryloxo derivatives of P(V) porphyrins.[7] The resonances due to the pyrrole-β protons on the axial porphyrins in the trimers are shifted upfield relative to their position in the 'free' (unlinked) precursor porphyrins (**2** or its metal(II) derivatives) and are also split into a singlet (*c*) and a pair of doublets (*a*, *b*) in the case of **3a**, **3d**, and **3f**. In the case of **3g**, these same protons are similarly shifted upfield but, are split into three pairs of doublets (*a*, *b* and *c*). The three types of axial pyrrole-β protons *a*, *b* and *c* are indicated in Fig. 5.7. The four 'type *a*' protons resonate in the region of 7.85-8.22 ppm; these protons experience the maximum shielding effect due to ring-current effect of the central P(V) porphyrin.[10] The four 'type *b*' protons, resonating in the region of 8.49-8.85 ppm, reflect a diminished shielding effect compared to 'type *a*' protons as they are situated 'far off' from the central P(V) porphyrin. The eight 'type *c*' protons, facing away from the central porphyrin, are least affected by the shielding ring-current and resonate in a more downfield shifted region (8.71-8.90 ppm) compared to the 'type *a*- and *b*' protons. A similar ring-current induced shielding effect is also seen for the 'bridging' meso-aryl

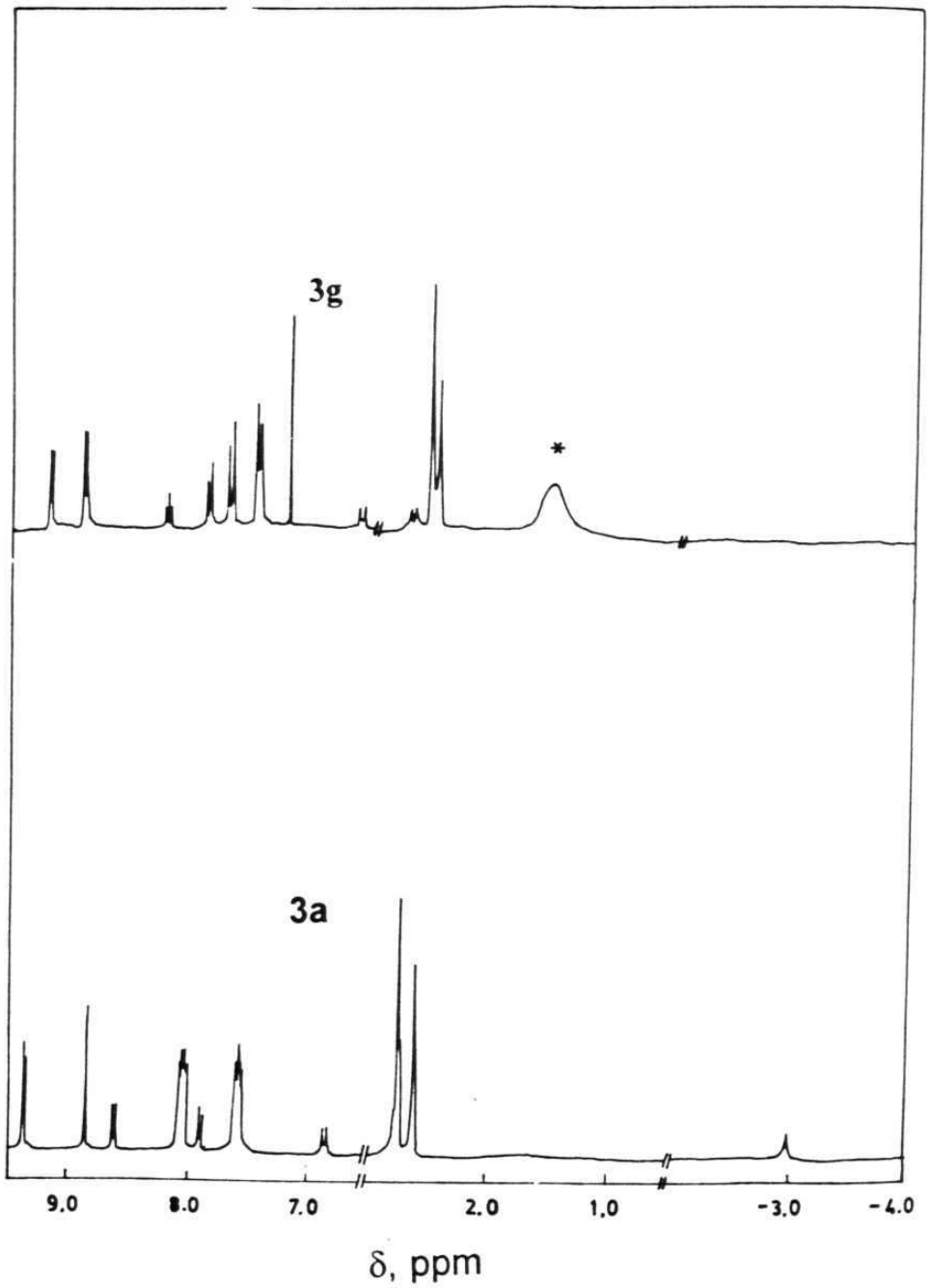

Fig. 5.6. ^{1}H NMR spectra of **3a** and **3g** in $CDCl_3$. Peaks marked * are due to solvent or impurities.

Table 5.2 ^{1}H NMR data in $CDCl_3$

Compound	δH, ppm					
	β (central)	β (axial)	*meso*-phenyl	*meso*- bridging phenyl	*meso*- CH_3	-NH
3a	9.34 (d) 8H	8.83 (s) 8H	*o*- 8.04 (m) 20H	*o*-6.86 (d) 4H	2.74 (s) 18H	-2.99 (s) 4H
		8.60 (d) 4H	*m*- 7.56 (m) 20H		2.59 (s) 12H	
		7.89 (d) 4H				
3d	9.28 (d) 8H	8.87 (s) 8H	*o*- 7.96 (d) 8H	*o*- 6.60 (d) 4H	2.65 (s) 18H	
		8.49 (d) 4H	7.81 (m) 12H		2.64 (s) 12H	
		7.81 (m) 4H	*m*- 7.49 (m) 20H			
3f	9.32 (d) 8H	8.87 (s) 8H	*o*- 8.03 (m) 20H	*o*- 6.83 (d) 4H	2.70 (s) 18H	
		8.63 (d) 4H	*m*- 7.55 (m) 20H		2.59 (s) 12H	
		7.93 (d) 4H				

.....

3g	9.18 (d) 8H	8.89 (m) 12H 8.22(m) 4H	*o*- 7.89 (d) 8H, 7.70 (d) 12H *m*- 7.47 (m)	*o*- 6.60 (d) 4H *m*- 2,69 (d) 4H	2.54 (s) 18H 2.47 (s) 12H	
4	9.33 (d) 16H	8.82 (s) 16H 8.58 (d)12H 7.87 (d) 12H	*o*- 8.04 (m) *m*- 7.57 m	*o*- 6.85 (d) 12H	2.71 (s) 48H 2.58 (s) 40H	-3.01 (s) 12H

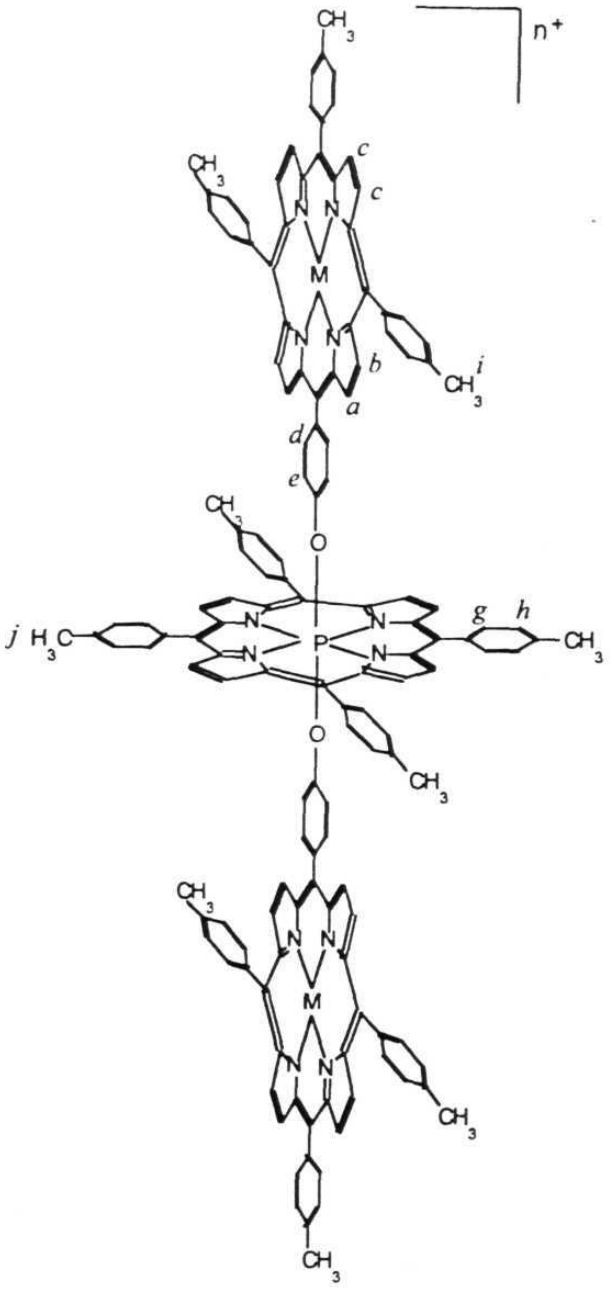

Fig. 5.7. Structure of **3a** illustrating the various types of protons.

protons (*d* and *e*) and the central imino protons (-NH, *f*) (see Fig. 5.7). The 'bridging' meso-aryl protons resonate as two pairs of doublets at 6.59-6.86 ppm (meta to the central porphyrin, *d*) and 2.64-2.75 ppm (ortho to the central porphyrin, *e*), respectively. The latter protons are 'enveloped' by the intense signal due to the methyl protons of the *meso*-tolyl groups and could only be recognized by 2D-COSY ^{1}H NMR spectrum as illustrated in Fig. 5.8 for trimer **3a**. The imino protons of **3a** resonate at -2.99 ppm and this can be compared with the resonance due to the same protons appearing at -2.73 ppm in the unlinked porphyrin **2**. Thus, in all, it can be visualized that the pyrrole-β,'bridging' phenyl and the central imino protons of the two axial porphyrins in these trimers simultaneously experience the shielding effect due to the central porphyrin and deshielding effect due to the axial porphyrins. This is not the case for the protons on the peripheral meso-tolyl groups of each porphyrin.

The phenyl protons of the *meso*-tolyl groups (*g* and *h*, see Fig. 5.7) on each porphyrin in compounds **3a**, **3d**, **3f** and **3g**, being located in a deshielding zone of the respective porphyrin ring current, resonate at 7.88-8.04 ppm (protons *ortho* to the porphyrin ring, *g*) and at 7.47-7.84 ppm (protons *meta* to the porphyrin ring, *h*). The *ortho*-phenyl protons of the *meso*-tolyl groups of **3g** are further split into two pairs of doublets, with one of them representing eight protons of the central phosphorus porphyrin (7.89 ppm) and the other representing twelve protons of the axial P(V) porphyrins (7.70 ppm). Finally, singlet resonances appearing at

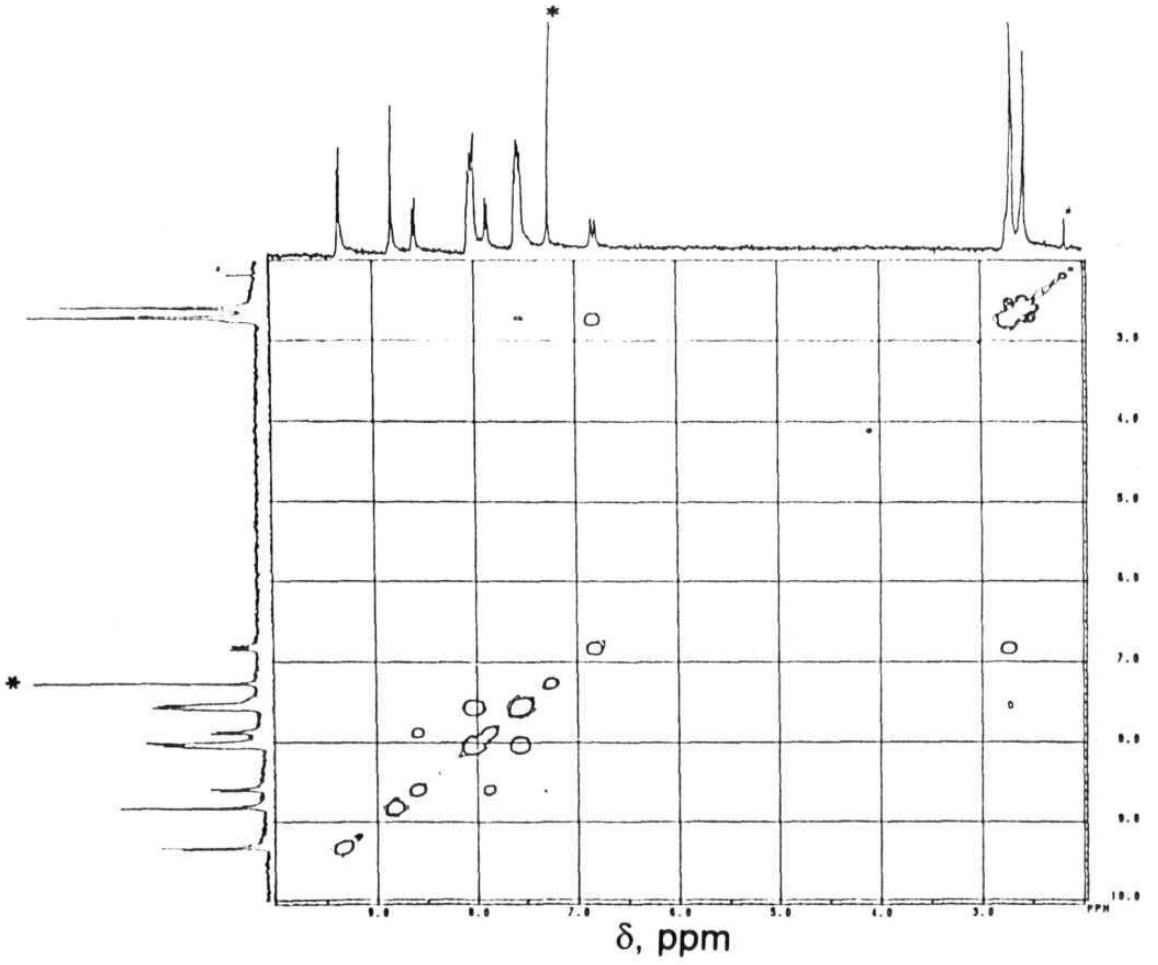

Fig. 5.8. 2D COSY ^{1}H NMR spectrum of **3a** in $CDCl_3$.

2.54-2.73 ppm and 2.47-2.64 ppm in these trimers are ascribable to the methyl protons (*i and j*, see Fig. 5.7) of the *meso*-tolyl groups of the axial- and central porphyrins, respectively.

The ^{1}H NMR spectrum of the heptamer **4** (Fig. 5.9) is nearly identical to that of its lower homologue - trimer **3a**. Similar splitting patterns and shielding effects are observed for the protons on all of the four free-base axial porphyrin subunits due to the ring-current effects of the three central P(V) porphyrin units for this array.

A comparison of the ^{1}H NMR data of our arrays with those of 'wheel-and-axle' type phosphorus porhyrins reported by Shimidzu and co-workers is interesting.[5] The individual porphyrins in the 'wheel-and-axle' type arrays are arranged face-to-face along a central axis composed of methylinic spacers. It has been observed that the bridging methylinic protons are shifted upfield due to the *additive* ring currents of the porphyrins. In addition, the pyrrole-β protons of the oligomers have been reported to show large upfield shifts depending on the number of porphyrins in the system, as compared to the corresponding monomer. In our study, while upfield shifts are observed in the case of trimers **3a**, **3d**, **3h**, and **3g**, as compared to their corresponding precursors, it should be noted that such shifts are only the resultant of opposing shielding and deshielding ring-current effects due to the 'basal' and axial porphyrinunits. In addition, as discussed above ^{1}H NMR data of the heptamer **4** is similar to that of trimer **3a**. This fact indicates that there is no dependence of the chemical shifts on the number of porphyrins in our

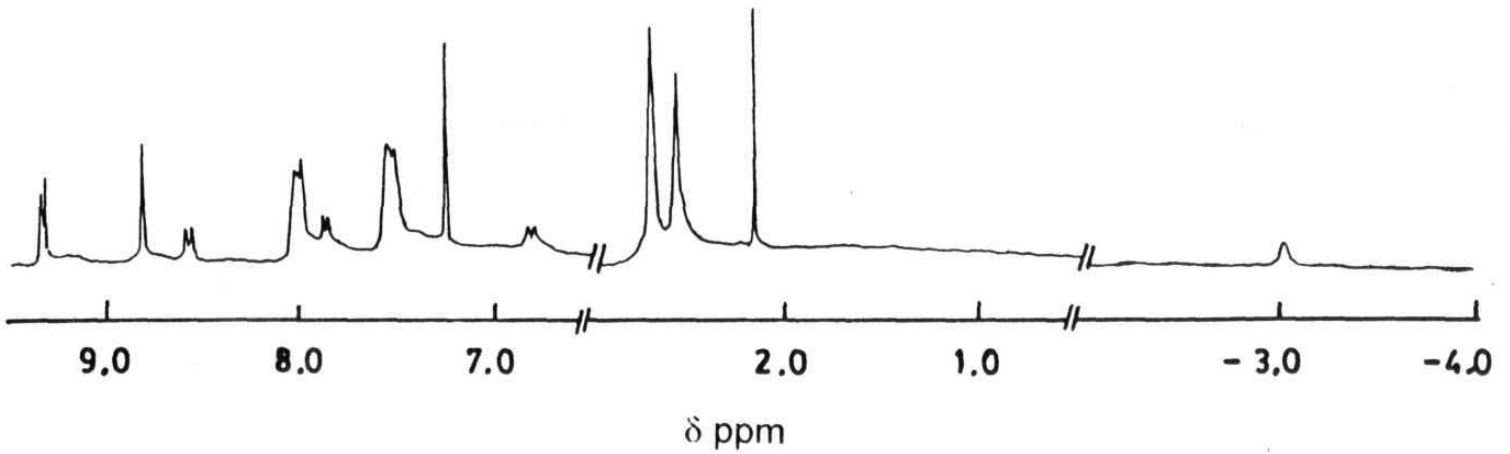

Fig. 5.9. ^{1}H NMR spectrum of the heptamer **4** in $CDCl_3$.

arrays unlike the case with the 'wheel-and-axle' type systems. On the other hand, the key features of the ^{1}H NMR spectral data of our arrays are analogous to those recently reported for the 'vertically' linked porphyrin arrays of Imamura and co-workers.[6]

^{31}P NMR spectra were recorded for **1**, **3g**, **3a** and **4** and they showed signals in the region typical for aryloxo substituted P(V) porphyrins (Fig. 5.10).[11] While the precursor **3g** showed two characteristic resonances, one at -196 ppm (central porphyrin) and the other at -229 ppm (axial porphyrins), the heptamer **4** showed only one peak at -194 ppm as is the case with its lower homologur **3a** or precursor **1**.

The ESR spectral features and the derived spin-hamiltonian parameters of the paramagnetic arrays (**M** = VO(IV) **3b**, and Cu(II) **3e**) were indistinguishable from those of the corresponding paramagnetic monomers (see Table 5. 3 and Figs. 5.11a and 5.11b).

All of the above observations indicate that there exists a symmetric but, a non-parallel disposition of the two axial porphyrins with respect to plane of the central porphyrin thus conferring a unique architectural identity for these arrays.

The reduction and oxidation potentials of compounds **3a-g** along with those of the individual precursors **1**, **2** and metalloderivatives of **2**, (M(**2**), where M = VO(IV), Co(II), Ni(II), Cu(II) or Zn(II)) as determined by the cyclic voltammetric experiments in CH_2Cl_2, 0.1 M TBAP, are given in Table 5.4. Representative voltammograms of reductions of **3a**

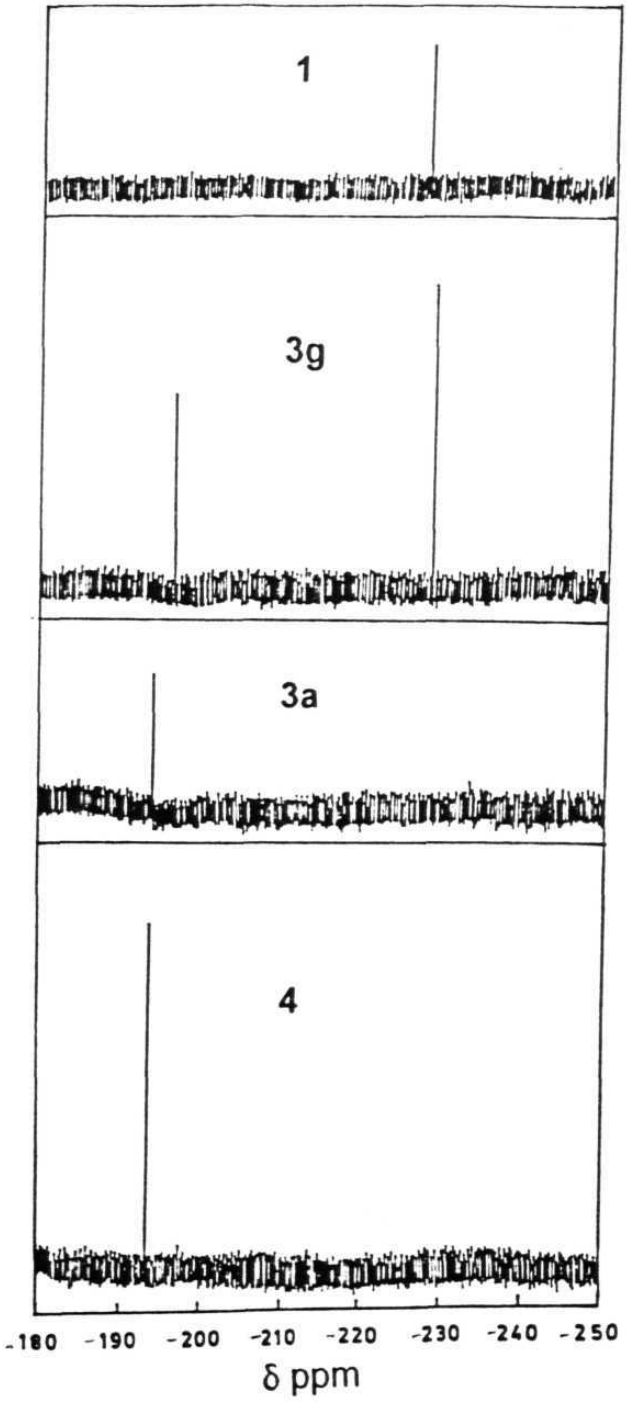

Fig. 5.10. ^{31}P NMR spectra of **1**, **3g**, **3a** and **4** in $CDCl_3$.

Table 5.3. ESR spectral data of **3b** and **3e** along with the respective precursors Cu(II)(**2**) and VO(IV)(**2**) in toluene at 100±3K

Compound	$g_{//}$	$g_{\perp}$	$A_{//}$	$A_{\perp}$	$A_{//}^{N}$	$A_{\perp}^{N}$
			($\times 10^{4}$ cm^{-1})			
VO(IV)(**2**)	1.961	1.986	160	57.0	—	—
3b	1.965	1.990	165	60.0	—	—
Cu(II)(**2**)	2.187	2.045	202	33.0	15.4	14.5
3e	2.180	2.040	200	30.0	15.3	14.0

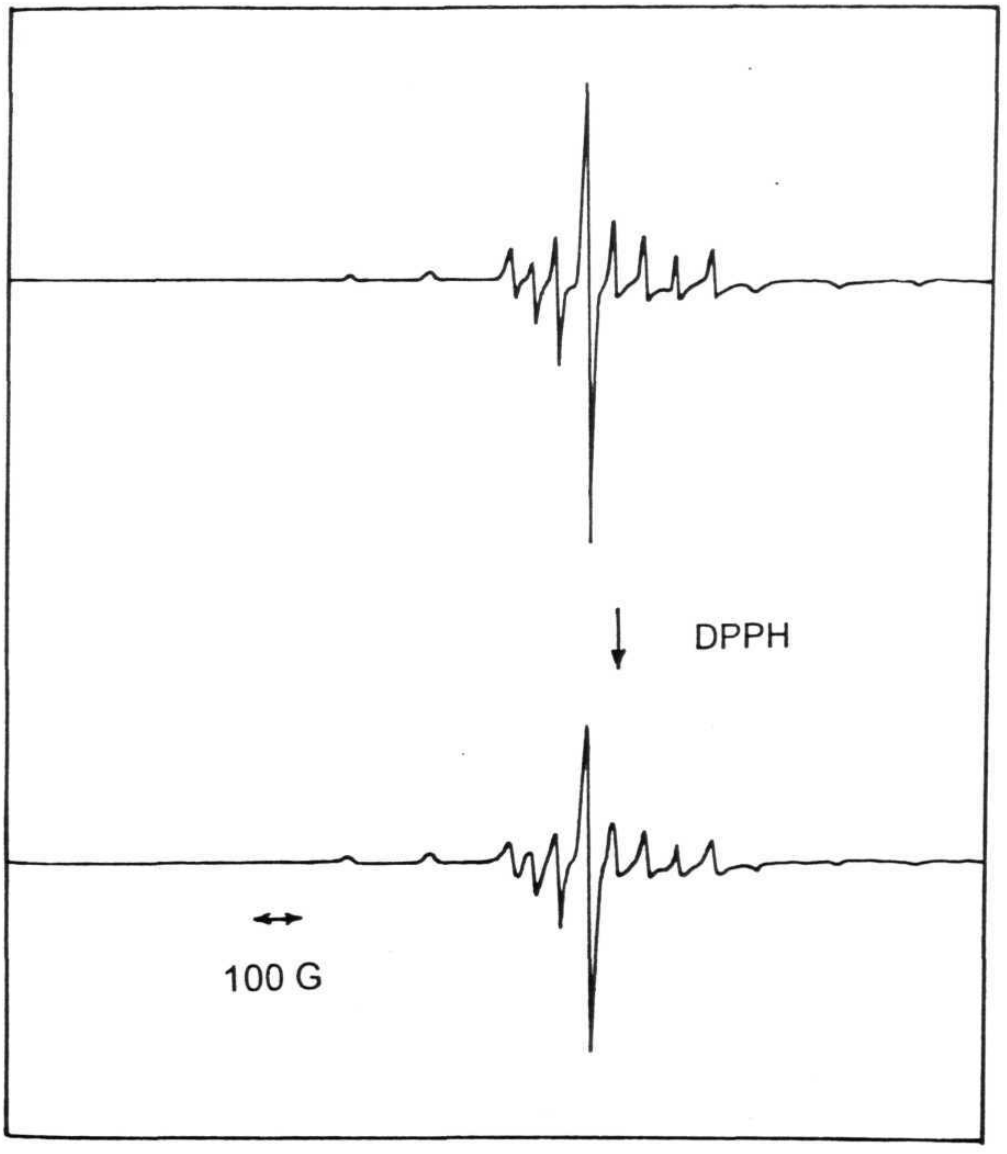

Fig. 5.11a. EPR spectra of VO(**2**) and **3b** in toluene (100 ± 3K).

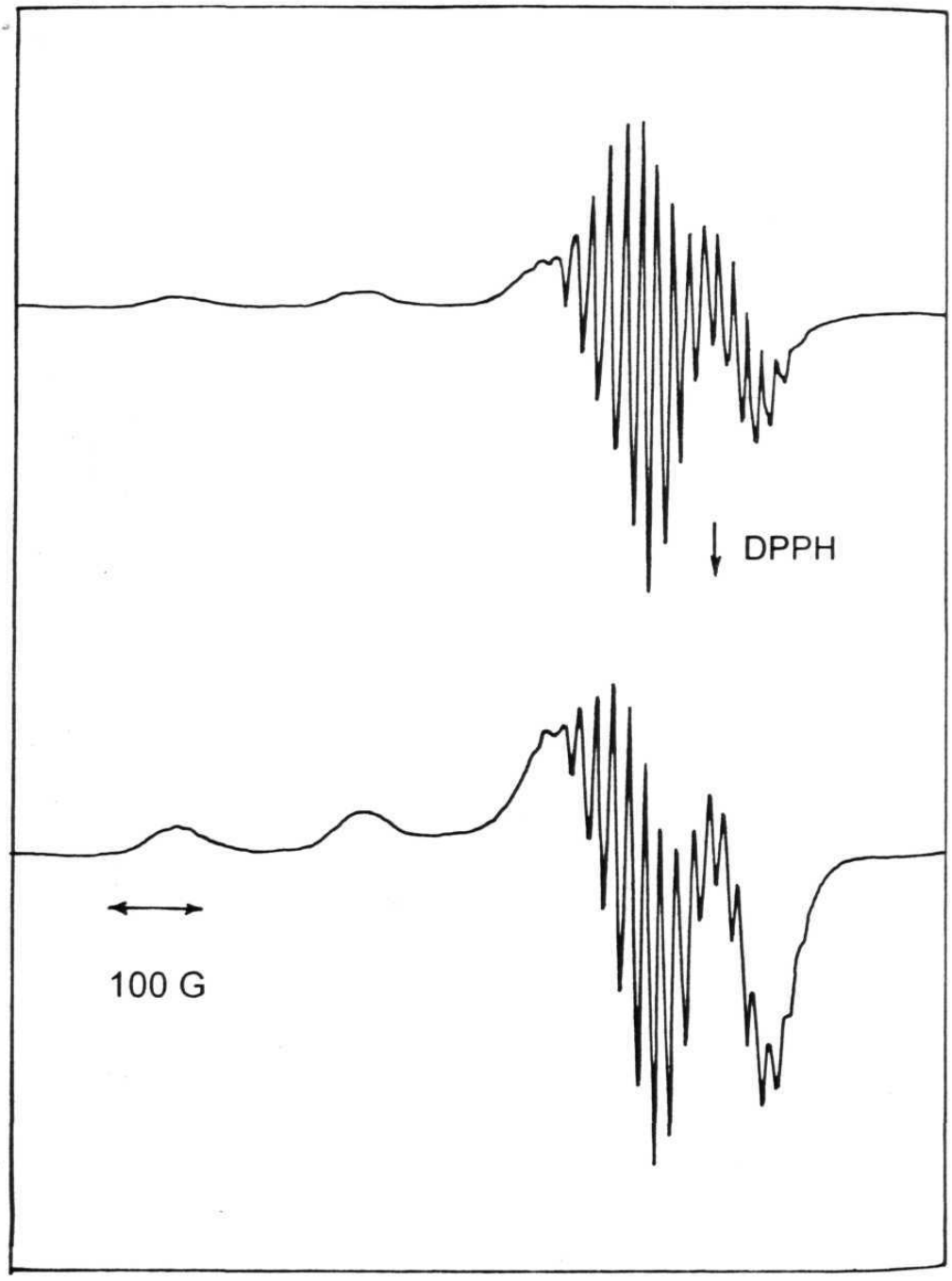

Fig. 5.11b. EPR spectra of Cu(**2**) and **3e** in toluene (100 ± 3K).

and **3b** are are shown in Fig.5.12. Wave analysis suggested that most of these electrode proceeses represent reversible (i_{pc}/i_{pa} = 0.9 - 1.0), diffusion controlled ($i_{pc}/\nu^{1/2}$ = constant in the scan rate (ν) range 50 - 500 mV/s), one-electron transfer (ΔE_p = 60 - 70 mV; ΔE_p = 65 ± 3 mV for ferrocene$^+$/ferrocene couple) reactions.[12]

A comparison of the cyclic voltammograms of the trimers with those of the corresponding individual constituent monomeric porphyrins suggests that the current-voltage responses seen for the trimers in the range of -0.44 to -0.53 V and -0.97 to -1.12 V correspond, respectively, to the first- and second one-electron reduction potentials of the central P(V) porphyrin.[13] The third current-voltage response seen during the cathodic scan for each trimer corresponds to an electron addition to the axial porphyrin units. In a few cases, peaks corresponding to the second one-electron addition to the axial porphyrins were also noticed and these data are given in Table 5.4. Trimers **3a-f** also exhibited two oxidation waves during the anodic scan. These are due to two successive one-electron abstractions from the axial porphyrins and not due to the central P(V) porphyrin as the precursor **1** does not show any oxidation under the present experimental conditions.[13] Compound **3g** could be reduced at -0.24 V and, as expected, this 'all phosphorus' trimer did not show any oxidative response. Finally, the heptamer **4** showed four successive one-electron reduction peaks (see Fig. 5.13) and two successive one-electron oxidation peaks as is the case with trimer **3a**.

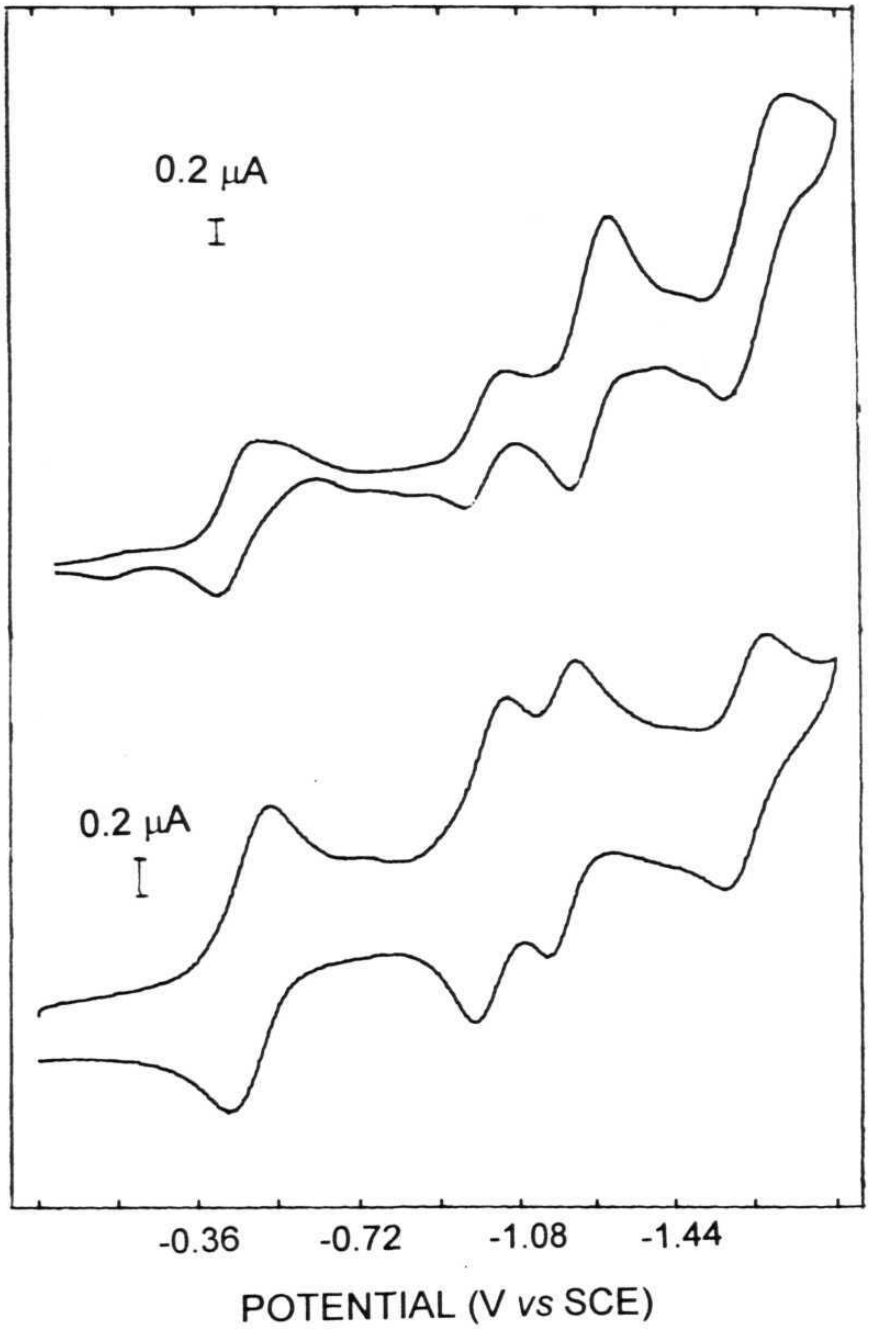

Fig. 5.12. Cyclic voltammograms of **3a** and **3b** in CH_2Cl_2, 0.1M TB (scan rate, 100 mV s^{-1}).

Table 5.4 Redox data in CH_2Cl_2, 0.1M TBAP

Compound	(V *vs* SCE)					
	$E^{1/2}_{red}$				$E^{1/2}_{ox}$	
	(I)	(II)	(III)	(IV)	(I)	(II)
1	-0.33	-0.72				
2	-1.26	-1.64			0.86	1.30
(VO)(**2**)	-1.24	-1.55			1.06	1.22
Co(**2**)	-0.92	-1.40			0.66	0.92
Ni(**2**)	-1.37	-1.82			0.99	1.45
Cu(**2**)	-1.40	-1.75			0.88	1.14
Zn(**2**)	-1.40	-1.80			0.72	1.00
3a	-0.43	-0.97	-1.22	-1.60	0.99	1.37
3b	-0.44	-0.97	-1.16	-1.55	1.09	1.28
3c	-0.45	-0.85	-0.99	-1.39	0.82	1.18
3d	-0.53	-1.12	-1.48		1.06	
3e	-0.52	-1.08	-1.45		0.99	1.24
3f	-0.48	-1.05	-1.44		0.72	1.01
3g	-0.24					
4	-0.42	-0.97	-1.22	-1.60	1.00	1.33

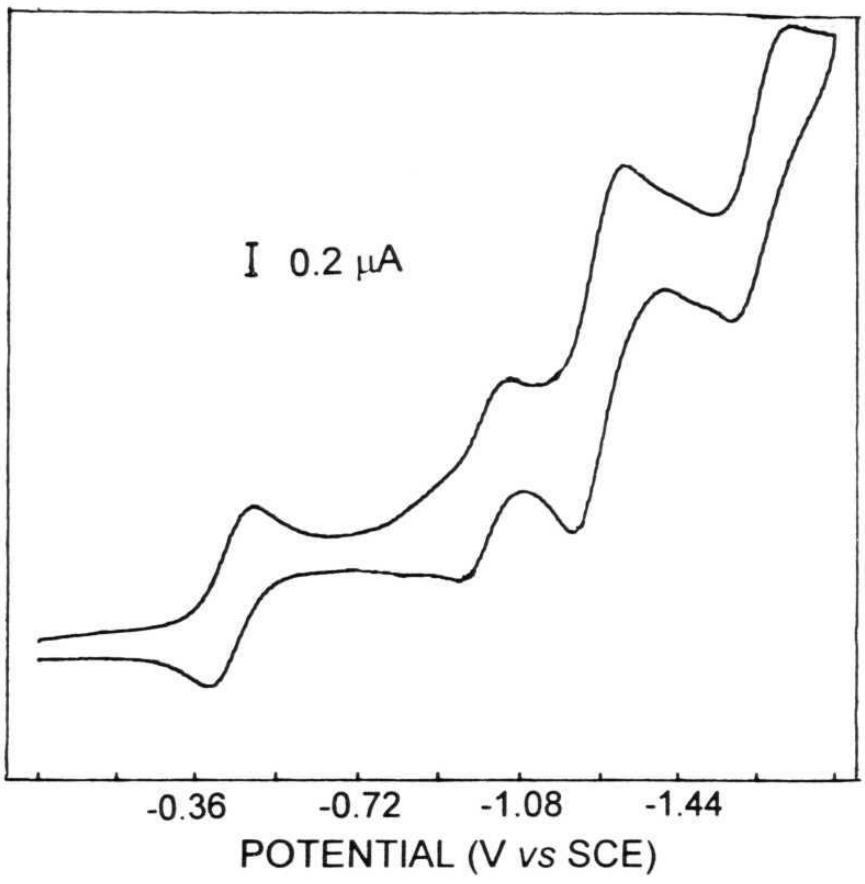

Fig. 5.13. Cyclic voltammogram of the heptamer **4** in CH_2Cl_2, 0.1M TBAP (scan rate, 100mV s^{-1}).

It is interesting to note that the oxidation and reduction potentials of these arrays are dependent on the metal/metalloid ion present (or the absence of it) in the cavities of the constituent monomers thus enabling a facile modulation of the ground state redox properties. As will be shown in the next Section, the excited state redox properties of these arrays are also dependent on the type and electropoisitivity of the metal/metalloid ion present in the porphyrin cavities.

5.3.2 Excited state properties

Fig. 5.14 illustrates the fluorescence spectra of trimer **3a** and heptamer **4** along with those of their precursor compounds **1** (dihydroxo analogue) and **2**. For the arrays, excitation at 405 nm corresponds to a predominant axial free-base porphyrin absorption while that at 445 nm to a predominant central P(V) porphyrin absorption. Thus, as seen in this Fig., shape of the spectra and λ_{max} values obtained upon exciting trimer **3a** at 405 and 445 nm correspond to those of free-base porphyrin and P(V) porphyrin, respectively. In addition, the singlet state energies ($E_{0\text{-}0}$) of the P(V) (2.006 eV) and free-base (1.89 eV) components of this trimer are also close to those of **1** and **2**, respectively.[14] On the other hand, the fluorescence quantum yields (ϕ) of **3a** are quite low compared to the ϕ values of **1** and **2**. Similar observations were also made for the trimer **3f** and the heptamer **4** (see Fig. 5.14). The λ_{max} and ϕ values of these arrays along with those of their respective constituent monomeric components measured in three different solvents are summarized in Table 5.5. An

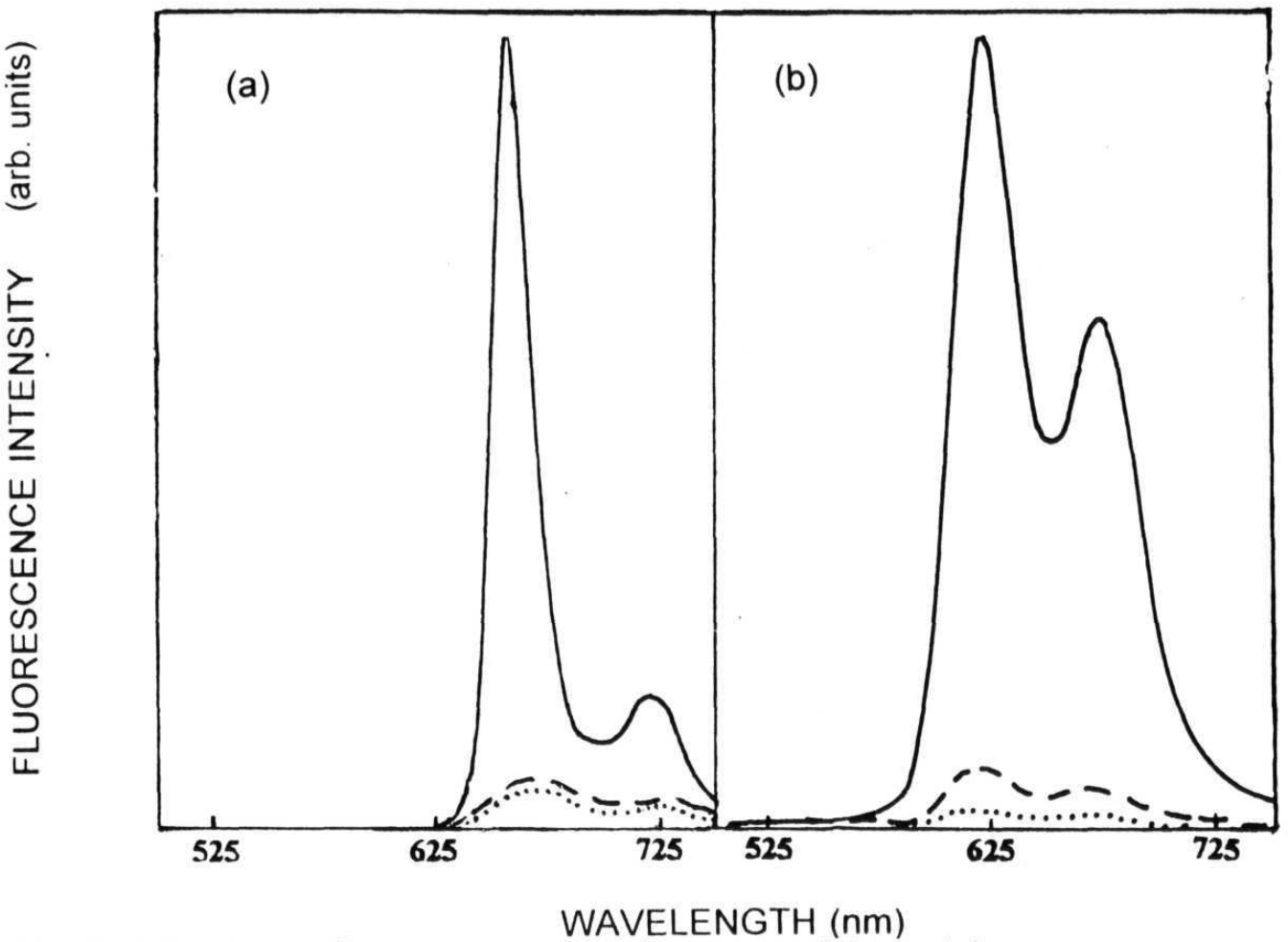

Fig. 5.14. Steady state fluorescence spectra of **3a** (-----) and **4** (.....)along with their precursors (a) $1(OH)_2$ (——) and (b) **2** (——) in CH_2Cl_2.

Table 5.5 Fluorescence data in various solvents

λ_{exc} (nm) = Compound	toluene		CH_2Cl_2		DMF		ΔG^a (1) (eV)	ΔG^b (2) (eV)
	405	445	405	445	405	445		
	λ_{em}, nm (ϕ)							
$1(OH)_2$		620, 669 (0.115)		625, 675 (0.120)		630, 680 (0.120)		
2	656, 721 (0.110)		655, 717 (0.110)		655, 718 (0.120)			
ZnTPP	598, 646 (0.032)		604, 650 (0.036)		607, 659 (0.033)	614, 659		
3a	617, 657, 716 (0.018)	618, 669 (0.020)	617, 655, 720 (0.005)	620, 671 (0.008)	620, 657, 722 (0.004)	621, 670 (0.002)	-0.42	-0.55
3f	618, 664 (0.017)	619, 668 (0.032)	620, 660 (0.003)	621, 670 (0.005)	621, 655 (0.004)	622, 672 (0.016)	-0.85	-0.85
3g		624, 673 (0.028)		634, 684 (0.010)		636, 684 (0.009)		
4	615, 656, 720 (0.003)	620, 666 (0.002)	616, 654, 717 (0.005)	620, 671 (0.006)	616, 656m, 718 (0.003)	625, 656 (0.002)	-0.42	-0.55

[a] Free energy change values for equn. 5.1 [b] Free energy change values for equn. 5.2

inspection of the data given in this Table reveals that all of these arrays show quenching of fluorescence when excited at wavelengths corresponding to absorption by the central P(V) porphyrin (445 nm) as well as by the axial porphyrin subunits (405 nm).

Various radiative and non-radiative intramolecular processes can be conceived to participate in the excited state decay of these novel, hybrid-type, donor-acceptor systems. Among these, electronic energy transfer (EET) from the central P(V) porphyrin to the axial free-base porphyrin as well as photoinduced electron transfer (PET) between the free-base/Zn(II) and the P(V) porphyrin seem to be more probable as revealed by the thermodynamic considerations based on the redox potential and singlet state energy data. These criteria indicate the possibility of a PET from the axial porphyrins to the central porphyrin by the following two pathways.

$$^{1}(\text{axial porphyrin})^{*} \rightarrow \text{central porphyrin} \qquad (5.1)$$

$$\text{axial porphyrin} \rightarrow {}^{1}(\text{central porphyrin})^{*} \qquad (5.2)$$

The free-energy changes for reactions 5.1 and 5.2 that can, in principle, occur in trimers **3a, 3f** and **4** are given in Table 5.5.

Collection of emission from **3a** and **4** (λ_{ex} = 720 nm) and from **3f** (λ_{ex} = 650 nm) gave the corresponding excitation spectra. These spectra showed negligible contribution (< ca. 4%) arising from the P(V)

porphyrin subunit and, this fact provides support for the absence of any intramolecular EET in these systems. It appears, based on the free-energy change values given in Table 5.5, that the efficiency of PET from the singlet axial porphyrin to the ground state central porphyrin and that from the ground state axial porphyrin to the singlet manifold of the central porphyrin both seem to be feasible processes (equns.5.1 and 5.2). Thus, the low ϕ values obtained upon excitation of **3a**, **3f** and **4** can be interpreted in terms of the participation of PET reactions 5.1 and 5.2 in each case. The dependence of ϕ values on the polarity of the solvent (see Table 5.5) also corroborate the participation of a PET reaction in the excited state decay of these hybrid arrays.

In the case of **3g**, excitation of this trimer at 445 nm results in quenching of emission with respect to the corresponding precursor. However, all the subunits being the same chromophores, selective excitation of the individual chromophores was not possible. Shimidzu and co-workers have earlier observed fluorescence quenching in 'wheel-and-axle' type phosphorus porphyrin dimers in which the porphyrin units are connected *via* the central phosphorus atom by ether bridges.[5] This observation coupled with diminished lifetimes of the dimers, in comparison with the monomers, in polar solvents led them to suggest that besides internal conversion and inter-system crossing, there exists an alternative non-radiative decay channel through a charge transfer state. It is possible that participation of such a charge transfer state in the excited state decay of **3g** is responsible for the fluorescence quenching observed for this trimer.

5.4 Summary:

In summary, a series of new, 'axial-bonding' type trimeric porphyrin arrays and a 'branched chain' type heptameric array have been synthesized and fully characterized by various spectroscopic methods. The UV-vis. data reveal that the spectrum of each trimer is more or less similar to the spectrum resulting from a combination (1:2 mole/mole ratio of P(V) porphyrin and free-base/metalloporphyrin) of the corresponding individual precursors. The ^{1}H NMR data suggest that the pyrrole-β, bridging phenyl and the central imino protons of the two axial porphyrins in these trimers simultaneously experience the shielding effect due to the central porphyrin and deshielding effect due to the axial porphyrins. Cyclic voltammetric data suggest that the redox potential values of the trimers are in the same range as those of the corresponding individual constituent monomeric porphyrins. All these observations indicate that there exists a symmetric but, a non-parallel disposition of the two axial porphyrins with respect to plane of the central porphyrin thus conferring a unique architectural identity for these arrays. While the ESR spectral parameters of the paramagnetic trimers were found to be close to those of corresponding monomeric paramagnetic monomers, the fluorescence due to the diamagnetic trimers were found to be quenched in comparison with the corresponding unlinked monomeric porphyrins. The low ϕ values obtained upon excitation of the diamagnetic trimers have been interpreted in terms of the participation of PET reactions. Finally, the properties of

the heptamer **4** are found to be close to those exhibited by its lower homologe **3a**.

5.5 References

1. For recent examples, see (and also references therein): (a) Sessler, J. L.; Capuano, V. L.; Harriman, A. *J. Am. Chem. Soc.* **1993**, 115, 4577. (b) Chambron, J. -C.; Harriman, A.; Heitz, V.; Sauvage, J. -P. *J. Am. Chem. Soc.* **1993**, 115, 7419. (c) Lin, V. S.-Y.; DiMango, S. G.; Therien, M. J. *Science* **1994**, 264, 1105. (d) Lindsey, J. S.; Prathapan, S.; Johnson, T. E.; Wagner, R. W. *Tetrahedron* **1994**, 50, 8941. (e) Anderson, S.; Anderson, H. L.; Bashall, A.; McPartlin, M.; Sanders, J. K. M. *Angew. Chem., Int. Ed. Engl.* **1995**, 34, 1096 (f) Ichihara, K.; Naruta, Y. *Chem. Lett.* **1995**, 631. (g) Higuchi, H.; Shimizu, K.; Ojima, J.; Sugiura, K.; Sakata, Y. *Tetrahedron Lett.* **1995**, 36, 5359. (h) Osuka, A.; Tanabe, N.; Nakajima, S.; Maruyama, K. *J. Chem. Soc., Perkin Trans. 2* **1996**, 199. (i) Reimers, J. R.; Lu, T.X.; Crossely, M. J.; Hush, N. S. *Chem. Phys. Lett.* **1996**, 256, 353 (j) Officer, D. L.; Burrell, A. K.; Reed, D. C. W. *J. Chem. Soc. Chem., Commun.* **1996**, 1657. (k) Wagner, R. W.; Johnson, T. E.; Lindsey, J. S. *J. Am. Chem. Soc.* **1996**, 118, 11166.

2. Representative Reviews: (a) Wasielewski, M. R. *Chem. Rev.* **1992**, 92, 435. (b) Gust, D.; Moore, T. A.; Moore, A. L. *Acc. Chem. Res.* **1993**, 26, 198. (c) Anderson, S.; Anderson, H. L.; Sanders, J. K. M. *Acc. Chem. Res.* **1993**, 26, 469. (d) van Nostrum, C. F.; Nolte, R. J. M. *J. Chem. Soc., Chem. Commun.* **1996**, 2385.
3. (a) Marks, T. J. *Angew. Chem., Int. Ed. Engl.* 1990, 29, 857. (b) Hanack, M.; Deger, S.; Lange, A. *Coord. Chem. Rev.* **1988**, 83, 115.
4. Anderson, H. L.; Hunter, C. A.; Mesh, M. N.; Sanders, J. K. M. *J. Am. Chem. Soc.* **1990**, 112, 5780 (b) Fleischer, E. B.; Schachter, A. M. *Inorg. Chem.* **1991**, 30, 3763. (c) Anderson, H. L. *Inorg. Chem.* **1994**, 33, 972. (d) Hunter, C. A. *Chem. Soc. Rev.* **1994**, 101. (e) Drain, C. M.; Lehn, J. -M. *J. Chem. Soc., Chem. Commun.* **1994**, 2313.
5. Segawa, H.; Kunimoto, K.; Susumu, K.; Taniguchi, M.; Shimidzu, T. *J. Am. Chem. Soc.* **1994**, 116, 11193. (b) Susumu, K.; Kunimoto, K.; Segawa, H.; Shimidzu, T. *J. Phys. Chem.* **1995**, 99, 29. (c) Susumu, K.; Segawa, H.; Shimidzu, T. *Chem. Lett.* **1995**, 929.
6. Kimura, A.; Funatsu, K.; Imamura, T.; Kido, H.; Sasaki, Y. *Chem. Lett.* **1995**, 207. (b). Funatsu, K; Kimura, A.; Imamura, T.; Ichimura, A.; Sasaki, Y. *Inorg. Chem.* **1997**, 36, 1625.
7. Barbour, T.; Belcher, W. J.; Brothers, P. J.; Rickard, C. E. F.; Ware, D. C. *Inorg. Chem.*, 1992, 31, 746.
8. Kasha, M. *Pure Appl. Chem.*, **1965**, 11, 317.
9. (a) Tran-Thi, T. H.; Lipskier, J. F.; Maillard, P.; Momenteau, M.; Lopez-Castillo, J. -M.; Jay-Gerrin, J. P. *J. Phys. Chem.*,**1992**, 96,

1073. (b) Lin, V. S. -Y.; DiMagno, S. G.; Therien, M. J. *Science* **1994**, 264, 1105. (c) Gouterman, M.; Holten, D.; Lieberman, E. *Chem. Phys.* **1977**, 25, 139. (d) Selensky, R.; Holten, D.; Windsor, M. W.; Paine III, J. B.; Dolphin, D. *Chem. Phys.* **1981**, 60, 33.(e) Osuka, A.; Maruyama, K. *J. Am. Chem. Soc.* **1988**, 110, 4454. (f) Hunter, C. A.; Sanders, J. K. M.; Stone, A. J. *Chem. Phys.* **1989**, 133, 395.

10. Abraham, R. J.; Bedford, G. R.; McNeillie, D.; Wright, D. *Org. Magn. Reson.* 1980, 14, 418.
11. *Multinuclear NMR* ; Mason, J., Ed.; Plenum Press: New York, **1987**; p369.
12. Nicholson, R. S.; Shain, I. *Anal. Chem* **1964**, 36, 706.
13. (a) Marrese, C. A.; Carrano, C. J.; *J. Chem. Soc., Chem. Commun.* **1982**, 1279. (b)Marrese, C. A.; Carrano, C. J. *Inorg. Chem.* **1984**, 23, 3961.
14. (a) Wasielewski, M. R.; Niemczyk, M. P. *J. Am. Chem. Soc.* **1984**, 106, 5043. (b) Murov, S.; L. *Handbook of Photochemistry* Marcel Dekker, Inc.: New York, 1973.

CHAPTER 6

Conclusions

Photochemically active donor-acceptor (D-A) systems based on variously substituted monomeric- and oligomeric porphyrin species are of current interest because of their immense utility in research related to both biological and abiological chemistry. Over the last two decades, a great variety of porphyrins bearing electron donor/acceptor groups at their peripheral (P_1 and P_2) or axial (A) (see Fig. 6.1) positions have been synthesized and their photochemical activity investigated. Literature on recently reported systems that bear relevance to biomimetic photosynthesis and molecule-based optoelectronics have been reviewed in chapter 1. Results obtained during the present research that deals with the design, synthesis and photochemical properties of D-A systems derived from 'axial' and/or 'peripheral' site substitution of free-base, metallo- and metalloid porphyrins are reported in chapters 3, 4 and 5.

6. 1 Peripherally substituted porphyrins

Initial attempts to build D-A systems relied on the time-tested, well-established methods involving manipulation at the porphyrin pyrrole-β and/or *meso* positions. Thus, spectroscopic and electrochemical

studies were first carried out on the free-base, copper(II) and zinc(II)

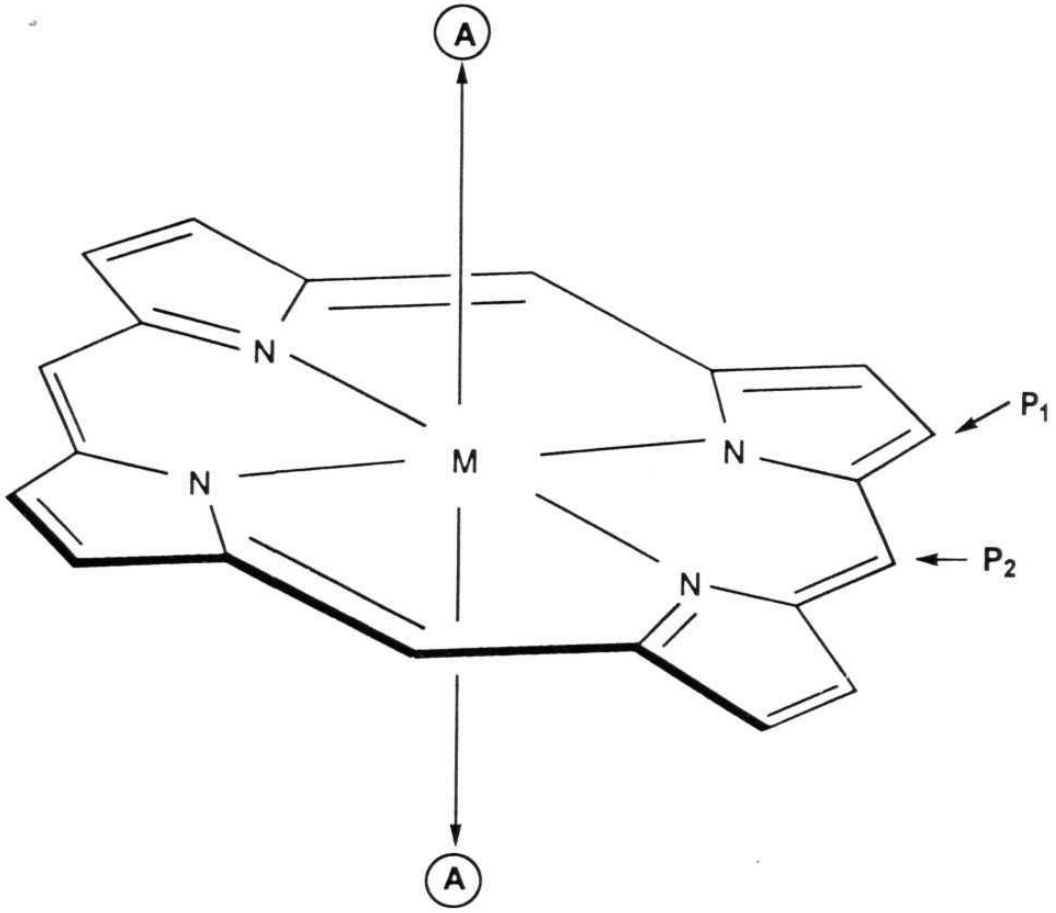

Fig. 6.1

derivatives of 2-nitro-substituted 5,10,15,20-tetra(aryl)porphyrins (aryl = phenyl, 2-naphthyl or diphenylpyrazolyl), chapter 3. The results indicate that the substitution of a nitro group at the pyrrole-β position of the three tetra(aryl) porphyrins investigated in this study has a profound influence on their spectral properties and electronic structures. Red shifts and broadening of the optical absorption bands, downfield shifts of both the pyrrole-β and imino proton NMR peaks and decrements in the reduction

potentials have been observed for these nitroporphyrins, in comparison with the corresponding spectral or electrochemical parameters for the unsubstituted parent porphyrins. These spectral changes were found to be not so sensitive to the type of the aryl group at the *meso* position. In addition, the ESR spectral data of copper(II) derivatives of the nitroporphyrins were found to be indistinguishable from the data for the unsubstituted analogues. This latter observation suggests that the effect due to the nitro group substitution does not 'reach' the metal center in these systems. All these features of the nitroporphyrins have been interpreted in terms of a perturbation of the frontier orbitals of the porphyrin π-ring system by the directly attached nitro group. The excited state properties of these nitroporphyrins are also interesting. Solvent-dependent fluorescence spectral data of the free-base and zinc(II) derivatives of the nitroporphyrins have been analyzed in terms of twisted intramolecular charge transfer in these complexes.

6.2 Axially substituted porphyrins

Unlike the case with the D-A systems described in chapter 3 wherein the porphyrin peripheral positions were utilized for linking the donor/acceptor groups, the axial positions of the resident metalloid ion in the porphyrin have been employed to link the donor/acceptor groups for the systems described in chapters 4 and 5. Phosphorus(V) (P(V)) porphyrin has been specifically chosen here for effecting the 'axial-bonding' between the donor and the acceptor subunits because of its (i)

ability to undergo facile axial substitution reactions and (ii) well-known photochemical and electrochemical activity. In this regard, it should be noted that the majority of non-transition metal and metalloid porphyrins have been reported to show strong luminescence[1] as against the transition metal porphyrins most of which, being paramagnetic, are relatively less luminescent. In addition, P(V) porphyrins are one of the easiest-to-reduce among the various metallo/metalloid porphyrins known to date.[2]

In the beginning, organic π-donor/π-acceptor subunits were linked at the axial sites of a P(V) porphyrin. In chapter 4, design, characterization and photochemical activity of six aryloxo derivatives of phosphorus(V) porphyrins of the type $[(TpTP)P(OR)_2]^+$ where TpTP is the dianion of *meso*- 5,10,15,20 tetratolylporphyrin and OR is an axial aryloxo ligand ('formally' π-donor/π-acceptor) have been described. These new type of D-A systems were fully characterized by FAB-mass, UV-vis, fluorescence, infrared, and nuclear magnetic resonance (^1H and ^{31}P) spectroscopies and cyclic voltammetric methods. The ^1H NMR data as analyzed by the ring-current model was particularly useful in establishing the vertical disposition of donor and acceptor subunits in these compounds. Cyclic voltammetric studies reveal that each porphyrin undergoes two successive one-electron reductions with the site of electron transfer being the porphyrin ring and not the metalloid center. The singlet state properties of these D-A systems, as probed by the fluorescence spectroscopy in various solvents, have been discussed in light of a PET reaction of the type

$$P(V)P^{*} \text{ -- } OR \quad \rightarrow \quad P(V)P^{-} \text{ -- } (OR)^{+} \qquad ..(6.1)$$

where P(V)P* - OR represents singlet excited state of the aryloxo P(V) porphyrins and $P(V)P^{-}$ - OR^{+}, the charge separated species. It is interesting that even the formally π-acceptor type nitroaryloxy species act as donor moieties in these compounds; this fact is consistent with the ease of reduction of the P(V) porphyrins.

After gaining some experience in the chemistry, electrochemistry and photochemistry of relatively less known, axially-substituted P(V) porphyrins, attention was diverted to the synthesis of porphyrin arrays by utilizing the axial bonding capability of P(V) porphyrin. Porphyrin arrays are particularly attractive species for incorporation into supramolecular assemblies that are useful in the fabrication of photosynthetic model systems, molecular electronic devices, molecular catalysts etc. A great variety of homologous porphyrin arrays have been reported so far but, relatively less attention seems to have been paid towards the construction of the functionally-active, hybrid systems. In addition, barring only a few exceptions, all of the hither-to reported porphyrin arrays have been obtained *via* cumbersome and often, low-yielding organic synthesis protocols which involve manipulation at either the pyrrole-β or the *meso*-phenyl position/s of the monomers. In the present study (chapter 5), a new 'building-block' approach, which is based on simple 'inorganic' reactions

such as axial bond formation of main-group element containing porphyrins and insertion of metal/metalloid ions into porphyrin cavities has been employed to readily furnish hybrid-type multiporphyrin arrays. The highlights of this study are: (i) modular synthesis of a series of P(V porphyrin-based, 'axial-bonding' type hybrid trimers and a 'branched-chain', heptameric array and (ii) demonstration of a facile and pre-determined modulation of the redox and photophysical properties of these soluble arrays.

The UV-vis. data revealed that the spectrum of each trimer is more or less similar to the spectrum resulting from a combination (1:2 mole/mole ratio of P(V) porphyrin and free-base/metalloporphyrin) of the corresponding individual precursors. This is unlike the case with the 'face-to-face' porphyrins, porphyrin aggregates or the wheel-and-axle type porphyrins[3] wherein the shifts in the λ_{max} values and reductions in the ε values have been reported. The ^{1}H NMR (1D and 2D) data suggest that the pyrrole-β, bridging phenyl and the central imino protons of the two axial porphyrins in these trimers simultaneously experience the shielding effect due to the central porphyrin and deshielding effect due to the axial porphyrins. Cyclic voltammetric data suggest that the redox potential values of the trimers are in the same range as those of the corresponding individual constituent monomeric porphyrins. All these observations indicate that there exists a symmetric but, a non-parallel

disposition of the two axial porphyrins with respect to plane of the central porphyrin thus conferring a unique architectural identity for these arrays. While the ESR spectral parameters of the paramagnetic trimers were found to be close to those of corresponding monomeric paramagnetic monomers, the fluorescence due to the diamagnetic trimers were found to be quenched in comparison with the corresponding unlinked monomeric porphyrins. The low ϕ values obtained upon excitation of the diamagnetic trimers have been interpreted in terms of the participation of PET reactions (equns. 6.2 and 6.3).

$$(CP)^*\text{-}(AP) \rightarrow (CP)^{-}\text{-}(AP)^{+} \quad ..(6.2)$$

$$(CP)\text{-}(AP)^* \rightarrow (CP)^{-}\text{-}(AP)^{+} \quad ..(6.3)$$

where CP is the central P(V) porphyrin and AP is the axial porphyrin. Finally, the properties of the heptamer are found to be close to those exhibited by the corresponding lower trimeric homologue.

A vast body of literature dealing with PET from the porphyrin to an appended electron acceptor is available but, only a few studies have examined electron transfer to a porphyrin from an attached donor.[4-6] Secondly, studies on PET reactions involving porphyrin excited states and axially ligated organic/organometallic electron donors or acceptors are scarce in the current literature.[7-14] In this sense, the aryloxo P(V) porphyrins investigated in chapters 4 and 5 can be considered as the rarely encountered and newly emerging examples of porphyrin-based D-A (in

fact, D_2-A triads) compounds in which the axial sites of a porphyrin, rather than its meso-phenyl or the pyrrole-β position, have been utilized for covalently linking the donor moiety. The results obtained in this study also testify the powerful oxidizing ability of the excited states of P(V) porphyrins and further suggest that the porphyrin derivatives investigated here are well suited as components of porphyrin-based supramolecular arrays.

6.3 Future scope

Notwithstanding the fact that the present study has been helpful, to some extent, in providing new directions to the construction of biomimetic D-A systems, an in-depth analysis of the various chapters described in various chapters of this thesis suggests that a lot remains to be done. For example, more elaborate photophysical experiments involving the time-resolved absorption and fluorescence techniques can be carried out to learn more about the mechanistic details of the PET reactions occurring in these D-A systems. Axial-bonding type, D-A systems based-on P(V) porphyrins having rigid spacers can be built and the intricacies involved in the PET reactions occurring in them can be compared with those of systems described in chapters 4 and 5. The experience gained in this study while working on various D-A systems can be advantageously used for the construction of triads/arrays of the type D-A_1-A_2, D_1-A-D_2 etc. Axial-bonding type D-A systems having solubility in aqueous environments can also be prepared.

The results described in chapter 4 and 5 also provide some insight into the design aspects of new, architecturally more-appealing supramolecular arrays. For example, it should be possible to utilize different main-group element (e.g. Ge(IV), Sn(IV) or Al(III)) containing porphyrins as the basal scaffolding units and free-base-, metallo- or metalloid-porphyrins as the axial donor/acceptor subunits for the fabrication of systems with varying spectral, redox and photophysical properties. It should also be possible to extend this 'building-block' approach and construct higher, branched-chain oligomers. In this regard, it can be noted that a sequence involving the peripheral and axial substitution reactions can be attempted to construct 'dimeric trimers' of the type shown in Fig 6.2. Hybrids of the type shown in Fig. 6. 3 can be readily generated by controlled metallation reaction of the trimers such as **3a** of chapter 5. It appears that the modular approach employed here which involves the 'metalloid porphyrin preparation, axial-bond formation and selective metal ion insertion' sequence is, by far, the only method that can readily provide such 'truly' hybrid-trimeric species. Finally, a combination of covalent and non- covalent axial bonding capabilities of various metalloid-/metallo- porphyrins is expected to generate 'stair-case' porphyrins of the type shown in Fig. 6.4.

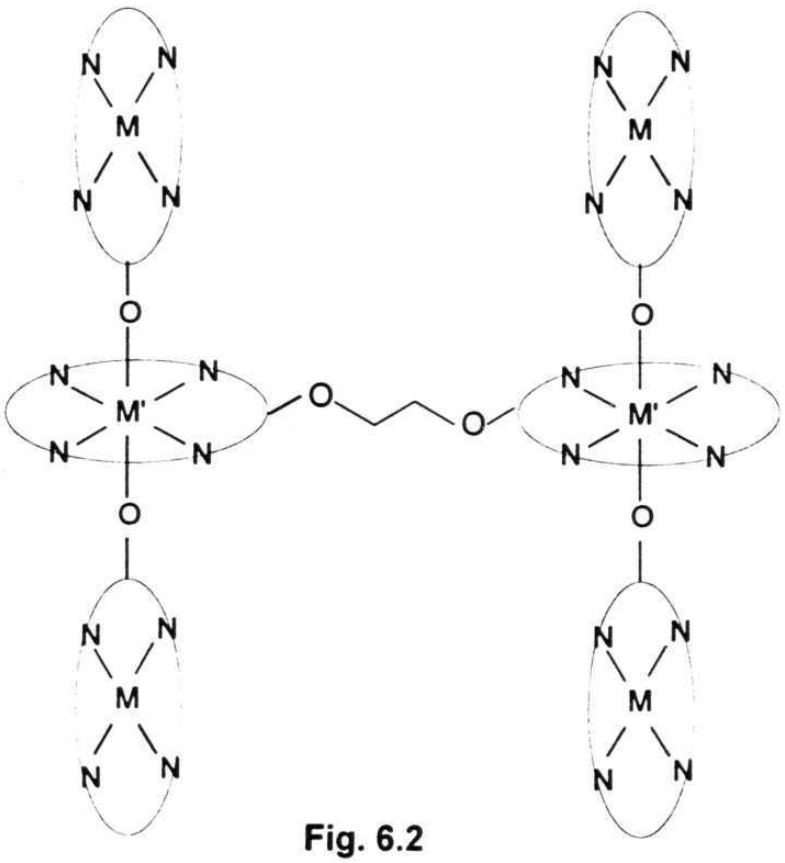

Fig. 6.2

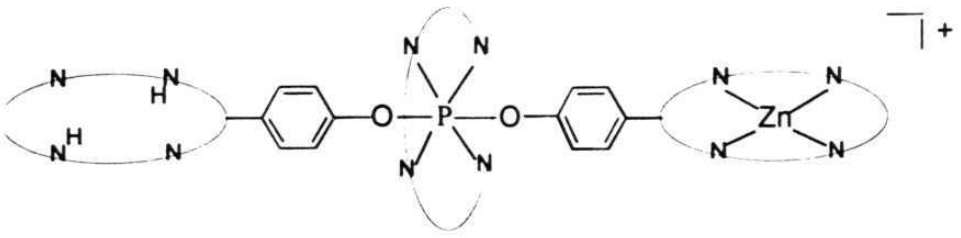

Fig. 6.3

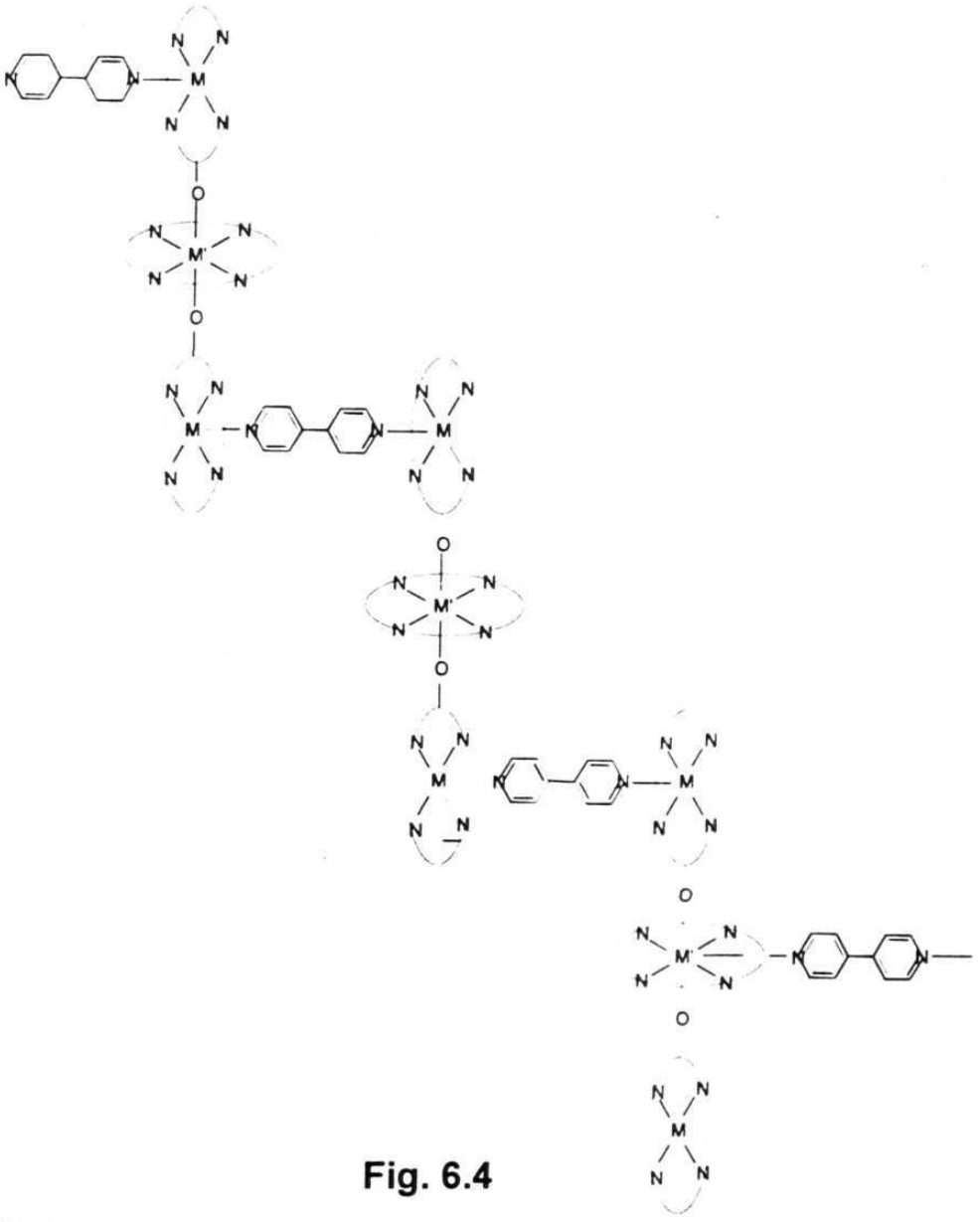

Fig. 6.4

6.4 References

1. Sayer, P.; Gouterman, M.; Connell, C. R. *Acc. Chem. Res.* **1982**, *15*, 73

2. Liu, Y. H.; Benassy, M. -F.; Chojnacki, S.; D'Souza, F.; Barbour, T.; Belcher, J. W.; Brothers, P. J.; Kadish, K. M. *Inorg. Chem.* **1994**, 33, 4480.

3. Segawa, H.; Kunimoto, K.; Susumu, K.; Taniguchi, M.; Shimidzu, T. *J. Am. Chem. Soc.* **1994**, 116, 11193.

4. Harriman, A; Hoise, R. *J. Photochem.* **1981**, 15, 163.

5. Wasielewski, M. R.; Gaines, G. L., III; O'Neil, M. P.; Svec, W. A.; Niemczyk, M. P. *J. Am. Chem. Soc.* **1990**, 112, 4559.

6. Loppnow, G. R.; Melamed, D.; Hamilton, A. D.; Spiro, T. G. *J. Phys. Chem.* **1993**, 97, 8957 (and references therein).

7. Kimura, A.; Funatsu, K.; Imamura, T.; Kido, H.; Sasaki, Y. *Chemistry Lett.* **1995**, 207.

8. Crouch, A. M.; Sharma, D. K.; Langford, C. H. *J. Chem. Soc., Chem. Commun.* **1988**, 307.

9. Maiya, B. G.; Barbe, J. -M.; Kadish, K. M. *Inorg. Chem.* **1989**, 28, 2524.

10. Zakrzewski, J.; Giannotti, C. Coord. *Chem. Rev.* **1995**, 140, 169.

11. Segawa, H.; Kunimoto, K.; Susumu, K.; Taniguchi, M.;Shimidzu, T. *J. Am. Chem. Soc.* **1994**, 116, 11193

12. Susumu, K.; Kunimoto, K.; Segawa, H.; Shimidzu, T. *J. Phys. Chem.* **1995**,99, 29..

13. Susumu, K.; Segawa, H.; Shimidzu, T. *Chemistry Lett.* **1995**, 929.

14. Saito, T.; Kitamura, M.; Tanaka, M.; Morimoto, M.; Segawa, H; Shimidzu, T. *Nucleosides & Nucleotides* **1995**, 13, 1607.

APPENDIX I

List of Publications

1. Rao, T. A.; Maiya, B. G. 'Spectroscopic, Redox and Emission Properties of 2-Nitro-Substituted Free Base- and Metallo-Tetra-aryl Porphyrins' *Polyhedron* **1994**, 13, 1863.
2. Rao, T. A.; Maiya, B. G. 'Axial-bonding Type Hybrid Porphyrin Trimers: Design, Synthesis and Modulation of Redox and Photophysical Properties. *J. Chem. Soc., Chem. Commun.* **1995**, 939.
3. Rao, T. A.; Maiya, B. G. 'Aryloxo Derivatives of Phosphorus(V) Porphyrins. Synthesis, Spectroscopy, Electrochemistry and Singlet State Properties. *Inorg. Chem.* **1996**, 35, 4829.
4. Giribabu, L.; Rao, T. A.; Maiya, B. G. 'Axial-bonding Type Hybrid Porphyrin Arrays' *Angew. Chem., Int. Ed. Engl.* (Communicated)